AN EFFICIENT APPROACH FOR DYNAMIC STABILITY ANALYSIS OF POWER SYSTEMS - INCLUDING LOAD EFFECTS

AN EFFICIENT APPROACH FOR DYNAMIC STABILITY ANALYSIS OF POWER SYSTEMS - INCLUDING LOAD EFFECTS

By

Hussain Magdy Zein El-Din, M.Sc.

A Thesis

Submitted to the School of Graduate Studies

in Partial Fulfilment of the Requirements

for the Degree

Doctor of Philosophy

McMaster University

September, 1977

DOCTOR OF PHILOSOPHY (1977)
(Electrical Engineering)

McMaster University
Hamilton, Ontario

TITLE: AN EFFICIENT APPROACH FOR DYNAMIC STABILITY ANALYSIS OF POWER SYSTEMS - INCLUDING LOAD EFFECTS

AUTHOR: Hussain Magdy Zein El-Din
B.Sc. (Cairo University, Egypt)
M.Sc. (Cairo University, Egypt)

SUPERVISOR: Dr. R.T.H. Alden

NUMBER OF PAGES: xvi, 193

SCOPE AND CONTENTS:

Dynamic (small) signal stability of multimachine power systems is considered. Efficient techniques for modeling and analysing this class of stability are developed.

System dynamics are analysed using eigenvalue methods. Eigenvalue sensitivity techniques are developed and employed for stability predictions. The relationships between different mode dynamics and components in the system are investigated.

These computational techniques are applied to a number of practical problems - in particular situations involving insufficient damping torques due to system composite loads and control interactions, subsynchronous resonance and dynamic induction motor loads.

ABSTRACT

This thesis describes an efficient approach for modeling and analysing small signal (dynamic) stability of balanced interconnected power systems. Systems are modeled into the state-space form where a partitioning technique is used to systematically reduce system equations into that form. Consequently, eigenvalue and eigenvalue sensitivity methods are used for dynamic stability prediction.

The formulation technique allows the inclusion of nonlinear and dynamic load representation and network and shaft dynamics in addition to detailed generator, turbine-governor and excitation system simulations currently being used by industry. The partitioning approach eliminates the need for storing large blocks of null elements. It also preserves the identity of various sub-systems. Consequently, this approach is particularly economical in studies involving system modification updating.

An algorithm is developed to calculate eigenvalue second-order sensitivities with respect to system control and design parameters. The sensitivities are obtained in terms of the eigenvalues and eigenvectors of the base case coefficient matrix. It is shown that the inclusion of the second-order terms in an overall sensitivity package does not add any computational complexity.

Eigenvalue first and second-order sensitivities are combined with an inverse iteration technique in an efficient algorithm for tracking possible movement of any sensitive subset of system eigenvalues due to parameter changes. The method is applicable in situations where a relatively small number of eigenvalues are critical in describing system dynamic stability. The efficiency of this algorithm over the repeated eigenvalue method is demonstrated.

These concepts and techniques are applied to a number of practical problems currently receiving attention in the power industry. In particular situations involving insufficient damping torque due to interaction between turbine-generator and network dynamics, turbine-generator and stabilization control, and the effect of static excitation and induction motor loads are analysed.

The interactions between system composite loads and excitation-stabilization control loops are examined on a reasonably general basis. It is shown that load characteristics have a considerable effect on system stability. It is also shown that there are specific situations where the choice of the load model can make a difference in stability prediction. In particular, at light generation levels the use of a power system stabilizer with a constant power local load leads to a prediction of instability while stability is predicted for a constant impedance load model.

ACKNOWLEDGEMENT

First I would like to express my sincere appreciation to my supervisor, Dr. R.T.H. Alden, for having made this work a pleasurable exchange of information. My special thanks go to Dr. N.K. Sinha for helpful advice, encouragement, and discussions. Appreciation is also due to Dr. D.S. Weaver for his interest in the work.

Special thanks are also due to Dr. P.C. Chakravarti for informal discussions - especially concerning mathematical aspects of the research. Very useful discussions, both on mathematical techniques and physical interpretations, with my friend Dr. P.J. Nolan are acknowledged. I would like also to thank Professor C.D. diCenzo for helpful discussions and encouragement.

I am also grateful to my associates, A. Maksoud and W. Ishak for their useful discussions.

Appreciation is expressed to the National Research Council of Canada and McMaster University for their financial support.

I would like to sincerely thank Ms. N. Sine, Miss Pat Dillon and Mrs. Betty Petro in the Word Processing Centre, for their typing and cheerful cooperation in preparing this manuscript.

LIST OF PRINCIPAL SYMBOLS

STATE SPACE MODEL FOR THE OVERALL SYSTEM

$\underset{\sim}{f},\underset{\sim}{g},\underset{\sim}{h},\underset{\sim}{K}$	Vector functions
A,B,C,D	Matrices for the state-space description
ns,nv,m	Number of states, algebraic variables and inputs
$\underset{\sim}{x}$, $\underset{\sim}{y}$, $\underset{\sim}{u}$	Vectors of states, algebraic variables and inputs,
P,Q,R,S,E	Matrices associated with the PQR method
I, O	Identity and null matrices
GXS,AO,GS, VC,VP,QA, QC,RB,RD	Submatrices associated with the PQR partitioning method

GENERATING UNIT MODEL

$\underset{\sim}{\psi}_i$	Vector of total fluxes of the stator and rotor circuits of the i^{th} machine
$\underset{\sim}{i}_{mi}$	Vector of currents in the stator and rotor circuits of the i^{th} machine
$\underset{\sim}{v}_{mi}$	Vector of terminal voltage components referred to the i^{th} machine reference frame
$\underset{\sim}{i}_{Mi}$	Stator current components for the ith machine referred to the internal reference frame
e_{fdi}	Field voltage of the i^{th} machine
R	Diagonal matrix of stator and rotor circuit resistances
X_i	The i^{th} machine internal reactance matrix
T_e	Machine electrical torque

P_o	Machine output power
δ_i	Rotor angle of the i^{th} machine referred to the reference frame
ωi	Rotor angular speed of the i^{th} machine
ω_o	Synchronous angular frequency
P, Q	Active and reactive power
E'_q	Voltage proportional to direct axis flux linkages
H	Inertial time constant
D	Dampling coefficient

NETWORK SYSTEM MODEL

R, X_e, X_c	Resistance, inductive and capacitive reactances of a transmission line
Y, Y_B	Nodal admittance and YBUS matrices
I, I_C	Series and shunt capacitive currents
$\underset{\sim}{i}_N$	Vector of network current components referred to the generalized reference frame
$\underset{\sim}{v}_N$	Vector of network voltage components referred to the generalized reference frame
n	Number of generating units in the system
T	Network transformation matrix
G	Real network admittance matrix
$\underset{\sim}{i}_{NI}$, $\underset{\sim}{v}_{NI}$	Vectors of current and voltage components of an infinite bus referred to the generalized reference frame

EXCITATION SYSTEM MODELS

$\underset{\sim}{x}_e$	States associated with exciter
e_{fd}	Field voltage

e_v	Voltage sensor output
τ_v	Voltage sensor time constant
$e_{ref.}$	Reference voltage

Static Exciter-Stabilizer

$\tau_e, \tau_Q, \tau_a, \tau_x$	Time constants associated with exciter, wash-out and lead lag circuit
K_e, K_Q	Exciter and stabilizer
e_a, e_b	Velocity and acceleration components of stabilizing signal
e_s	Stabilizing signal

Type 1 Rotating Exciter

τ_A, τ_E, τ_F	Time constants associated with amplifier, exciter and stabilizing loop
K_A, K_F	Exciter and stabilizing loop gains
e_A	Amplifier output voltage
e_x	Stabilizer output voltage

TURBINE-GOVERNOR

$\underset{\sim}{x}_g$	States associated with turbine governor
P_c	Control power
P_m	Output mechanical power

Steam Unit

τ_3	Speed sensor time constant
K_g	Speed sensor gain
τ_4	Turbine time constant

Hydro Unit

τ_1	Speed relay time constant
K	Speed relay gain
τ_3	Servomotor time constant
τ_5, τ_w	Time constants associated with turbine

Mechanical Shaft System

M_i	Inertia of the i^{th} lumped mass element
S_{ij}	Stiffness between i^{th} and j^{th} lumped masses
D_i	Damping coefficient between i^{th} lumped mass and synchronous reference frame

LOAD MODELS

Dynamic Induction Motors

X_s, X_r, X_{sr}	Stator, rotor and mutual inductive reactances
r_s, r_r	Stator and rotor resistances
$i_{sD}, i_{sQ}, i_{rD}, i_{rQ}$	Stator and rotor currents in D-Q axes
H_m	Motor inertial time constant (sec.)
v_{sD}, v_{sQ}	Terminal voltage in D-Q axes

Static Loads

P_L, Q_L	Load active and reactive power
c_o, c_1, ... c_n	Proportionality constants
K_p, K_q	Power-voltage sensitivity coefficients
Y_L	Static linear admittance

EIGENVALUES AND EIGENVALUE SENSITIVITIES

λ	System eigenvalue
$\hat{\lambda}$, μ	Estimated eigenvalues
$\dot{\lambda}_n$	Normalized first-order eigenvalue sensitivity
$\ddot{\lambda}_n$	Normalized second-order eigenvalue sensitivity
ξ, η	System parameters
$\underset{\sim}{z}$, $\underset{\sim}{v}$	Eigenvectors of the [A] matrix and its transpose
α_{ij}, β_{ij}	ns-space vector polynomial coefficients
W_s	Eigenvector current estimate in the inverse iteration process
w_s	The element of W_s with the largest magnitude
$\underset{\sim}{X}_o$	Eigenvector initial estimate
$\underset{\sim}{\epsilon}$, $\underset{\sim}{\delta}$	ns-dimensional error vectors
L, U	Lower and upper triangular matrices
$\underset{\sim}{b}$	ns-dimensional vector associated with solution of matrix equation

MISCELLANEOUS

Δ	Prescript denoting incremental change
$\cdot$	Superscript denoting differentiation with respect to time
$\sim$	Subscript denoting vector quantity
t	Superscript denoting matrix or vector transpose
-1	Superscript denoting matrix inverse

o	Subscript denoting equilibrium value
D, Q	Subscripts denoting direct and quadrature axis quantities (generalized frame)
S	Laplace operator
Units:	All time constants (including inertial time constants) in seconds, all angles in radians. Other quantities are in per unit (p.u.)

TABLE OF CONTENTS

LIST OF FIGURES

LIST OF TABLES

Chapter 1

INTRODUCTION

1.1 Dynamical Properties of Power Systems

Present day interconnected power systems are typical examples of large scale complex multivariable systems. They generally comprise a large number of dynamic units (synchronous generators and dynamic loads such as synchronous and induction motors). The generated electrical energy is transmitted over an interconnecting network which supplies, in turn, the demanded power to load centres. The system loads may be dynamic or static in nature. Much of the complexity arises from the fact that in the analysis of any one segment of the system the whole interconnected system should be considered.

The study of system dynamics around the steady-state, and under transient, conditions is of primary interest to power system engineers. Dynamics of power systems covers a wide spectrum of phenomena: electrical, electromechanical and thermomechanical in nature [1]. The problems and effects involved in power system dynamic studies have been always associated with the phenomenon of power system stability. This concerns the question of whether or not a system remains in synchronism after a credible disturbance

[1].

In recent years, due to the increase in system size and the tendency to operate systems near their stability limits, emphasis has been placed on the design of additional control loops for the synchronous machines. Consequently, it is of paramount importance to study the effect of different system components and parameters on system stability. Generally, it is not only required to know whether a system is stable or not, but it is also very important to evaluate the system performance or the quality of stability.

Dynamic problems in power systems have been classified [1] under the major categories of:

(1) Electrical machine and system dynamics

(2) System governing and generation controls

(3) Prime-mover energy supply system dynamics and controls.

Usually, the second class of dynamics last for many minutes whereas the third class of dynamics last for several seconds to a few minutes. Hence, for the analysis of system dynamics included in these two classes the network and machine electrical transients can be neglected.

The first class of dynamics is the most involved in stability studies being performed by electrical utilities. It is related to machine and system dynamics, and hence the

interaction between machines, excitation systems, turbine-governors, and system loads should be considered. Usually, the simulated dynamics in this class result in relatively large equivalent systems. This requires, in turn, efficient modeling and analysis techniques. Furthermore, these techniques should render simple ways of appropriate interpretation of the results. Concurrent with these requirements is the need for good understanding of the fundamentals and the physics involved in system interactions.

A variety of field tests in a number of utilities have recently demonstrated the importance of accurate modeling of loads in system stability studies [1]-[4]. This is becoming of particular importance with the trend towards sophisticated representation of system controls.

This thesis is mainly concerned with the aspects of modeling and analysing the first class of dynamics. The emphasis is on the establishment of an efficient computational analysis approach. This approach is used to develop the basic concepts related to the interaction between system loads and excitation control.

1.2 Transient and Dynamic Stability

Power system stability is usually divided into two main categories. These are transient and dynamic stability. Dynamic stability is concerned with the behaviour of the system following a "small perturbation" around a steady-state operating condition. On the other hand, transient stability is concerned with the behaviour of the system following a "major or large disturbance".

Major disturbances can arise as a result of a variety of abnormal conditions such as short circuit faults, the outage of major generation, etc. In this case the differential equations describing the dynamic performance of the system are fundamentally nonlinear due mainly to the sinusoidal nature of the torque-load angle relationships. Nonlinearities are also due to magnetic saturation, control limits, the sinusoidal transformation of reference frames, and nonlinear load characteristics. The system behaviour after a major disturbance is a function of the nature of the fault and the system properties.

Until recently, utilities were only concerned with the transient stability aspect and it was considered that a transiently stable system was sure to be dynamically stable [5]. This is no longer the case for present day systems. The use of high response fast static exciters, while improving transient stability properties, deteriorates

dynamic stability by introducing negative damping [6]. Another reason for an increasing tendency towards concern for dynamic stability is the decreased strength of transmission systems relative to the size of generating stations [5].

In dynamic stability studies the nonlinear equations describing system performance can be linearized around the chosen operating point. This facilitates the use of linear system theory and the application of modern control theory concepts.

Throughout this thesis attention will be limited to dynamic stability aspects since the interactions involved in the problems under investigation can be adequately studied using the linearized analysis approach. However, it should be noted that the inherent approximations, and therefore the limitations, in this analysis are taken into consideration. It is also understood that it is essential to complement the linear analysis by performing transient stability studies for the overall evaluation of power system stability. The subject of transient stability analysis is outside the scope of this thesis. A number of excellent references on the subject are [7]-[12].

1.3 Dynamic Stability: Operation and Design Studies

Small signal stability studies are very important in

the operation of interconnected power systems. This kind of analysis can predict different instability modes in the system. One example is monotonic instability caused primarily by a lack of synchronizing torque. This is a situation typical of a machine working at, or above, the dynamic stability limit [6], [13]. Other instability problems might arise due to a lack of damping of the synchronous machine torque-load angle loop [5], [6] or of the mechanical shaft modes [14], [15].

The use of different types of excitation systems and stabilizing signals has made it essential to study the effect of different parameters and components in the system on the damping of different system modes [16]. The effect of voltage regulator characteristics on dynamic stability has long been studied [17]. The effect of excitation systems on the dynamic stability limit has also been analysed [18]. Recently, the effect of static exciters on dynamic stability has been explored and the philosophy of power system stabilizer design has been established [6]. The general concepts in [6] have been extended in [19], to include the effect of another commonly used type of exciter under different operating conditions, and in [20] where a two-machine situation has been considered. Practical experience in the area of static excitation and power system stabilizers has been pioneered by implementation in the

Ontario Hydro system [18], [21], [22].

The subject of subsynchronous resonance is of current interest. This phenomenon can result in negative damping and hence instability of the mechanical shaft modes. Shaft damage due to this effect has been recorded in a series compensated system [14]. Shaft instability can also occur due to the use of a speed sensitive power system stabilizer [15]. A general discussion on series capacitor compensation is in [23] and a number of analysis papers on the phenomenon of subsynchronous resonance and related problems have recently appeared [24]-[32].

The modeling and effect of load characteristics is one of the most important aspects currently being studied [4]. The importance of load effects on system stability has long been recognized [33]. Recently, the IEEE Computer Analysis Power Systems Working Group (CAPS) documented the need for improved load representation in stability analysis programs [2]. There are two different aspects related to the load problem. One is the development of realistic models that can represent the actual behaviour of loads. The second is the analysis of load effects on system stability through the investigation of the interaction with other system components.

Two different approaches have been followed in the development of load models. The first examines the system

data to determine the most appropriate model to use in subsequent studies [2], [3], [34]. The second constructs the load model by analysing and combining the simulated characteristics of each individual component in a composite load [35]-[38].

System loads can be represented as either static or dynamic elements according to their inherent characteristics. While static representation of loads as nonlinear functions of load bus voltage has been recommended in references [2], [3], and [35], dynamic representations have been emphasized in some specific situations [2], [34]. Dynamic modeling is necessary in the case of large industrial loads including large induction and synchronous motors. These motors can have significant inertial time constants as compared to the system generation. The subject of induction motor representation in stability studies has been treated in [39], [40]. More recently, the equivalence of induction motor groups has been studied [41], [42]. A recent state of the art paper has been presented by Concordia [4].

Nonlinear static load models have been used in different ways to assess the effect of load characteristics on transient and dynamic stability [11], [43], [44]. Induction motor load effects on system stability have also been analysed [45]-[47].

It was mentioned in Section 1.2 that the damping of different modes related to system dynamical response can be destroyed as a result of system component interaction. Consequently, different stabilization schemes have been proposed in order to maintain satisfactory dynamic operation. Each stabilization loop design is dependent on the aspect of stability intended to be improved. Generally, it is of great importance to investigate the possibility of any conflicting effects on other aspects of stability. For example, the use of static exciters is beneficial in improving transient stability properties. However, they can destroy inherent machine damping and hence cause dynamic instability [6]. On the other side the incorporation of a power system stabilizer designed to improve dynamic stability properties can provide adverse effects on transient stability properties [48]. The possibility of exciting shaft instability modes due to the use of a power system stabilizer with a thermal unit is also known [15].

The design of a power system stabilizer for dynamic stability improvement has been achieved using a variety of methods. Among these methods, the damping and synchronizing torque concepts have been used most successfully [6], [15], [21]. The successful use of the root locus technique has also been reported [49]. Practical considerations for power system stabilizing signals have been documented in [21].

Optimal control theory has been applied in a variety of ways to improve dynamic stability [50]-[53]. Design procedures of suboptimal controllers, using low-order system models, have also been considered [54]-[57]. These control theory techniques have generally considered single machine - infinite bus problems though multimachine examples have also been studied [58].

1.4 Dynamic Stability Evaluation

The differential and algebraic equations describing the performance of a power system are basically nonlinear. System performance can be described by a set of first-order differential equations [59], [60]

$$\begin{aligned} \underset{\sim}{\dot{x}} &= \underset{\sim}{f}(\underset{\sim}{x}) + \underset{\sim}{g}(\underset{\sim}{u}) \\ \underset{\sim}{y} &= \underset{\sim}{h}(\underset{\sim}{x}) + \underset{\sim}{k}(\underset{\sim}{u}) \end{aligned} \tag{1.1}$$

where x, u, and y are vectors of state, input, and algebraic variables of order n, m and r respectively and $\underset{\sim}{f}$, $\underset{\sim}{g}$, $\underset{\sim}{h}$ and $\underset{\sim}{k}$ are vector functions [61].

When dealing with small disturbance stability of a system, equation (1.1) can be expressed in terms of deviations from the equilibrium point. If the disturbance is small enough, second-order and higher-order terms are negligible in a Taylor series expansion. The equations therefore take on the linear form:

$$\Delta \underset{\sim}{x} = [A]\ \Delta \underset{\sim}{x} + [B]\ \Delta \underset{\sim}{u}$$

$$\Delta \underset{\sim}{y} = [C]\ \Delta \underset{\sim}{x} + [D]\ \Delta \underset{\sim}{u} \qquad (1.2)$$

[A], [B], [C] and [D] are real constant matrices with appropriate dimensions. The entries of these matrices are functions of all the system parameters as well as the steady-state operating conditions. The state-space form, equation (1.2), is convenient for the application of modern control theory concepts [62], [63].

After the system equations are formulated in the state-space form, system stability can be analysed using different approaches. The most straightforward method is the direct integration of the system differential equations. However, numerical integration is not an efficient tool to determine system dynamic stability. An alternative and economical approach is to apply modern control theory techniques.

Thus, evaluation of the dynamic stability of a power system involves two related aspects. First is the use of a formulation which reduces the system equations into state-space form. Second is the use of an appropriate analysis technique to assess system stability.

It should be noted, at this stage, that modeling, and formulation and analysis techniques are highly dependent upon the problem under investigation. This has been

strongly emphasized in [1] and the relation between modeling precision and the various aspects of stability being studied has been discussed in the literature [13], [64].

1.4.1 Formulation Approaches

The application of modern control theory techniques to the analysis of power system dynamics requires the manipulation of system equations into state-space form. For small problems such as a single machine connected to an infinite bus, the number of differential and algebraic equations describing the system performance is relatively small. The reduction of these equations into state-space form is rather simple and can be performed by hand. However, for interconnected systems the situation is different and it is of primary importance to use a systematic reduction technique.

The formulation of a state-space model for multi-machine systems has been a subject of interest since the early work of Enns et al [65] and Laughton [66].

Enns et al suggested a systematic formulation technique. The system linearized differential and algebraic equations are arranged in the following form:

$$[P]\begin{bmatrix} \dot{\underset{\sim}{x}} \\ \\ \underset{\sim}{y} \end{bmatrix} = [Q]\ \underset{\sim}{x} + [R]\ \underset{\sim}{u} \qquad (1.3)$$

where the state, algebraic, and input vectors $\underset{\sim}{x}$, $\underset{\sim}{y}$ and $\underset{\sim}{u}$ are considered now as the vectors of perturbations from the steady-state equilibrium point and are of the same dimensions as those of equation (1.2). [P], [Q], and [R] are real constant matrices of compatible dimensions with $\underset{\sim}{x}$, $\underset{\sim}{y}$ and $\underset{\sim}{u}$. These matrices are functions of the system structure and the steady-state operating conditions. Equation (1.3) is then premultiplied by the inverse of the [P] matrix. Consequently, the state-space form is obtained by appropriate partitioning.

The approach by Enns et al has been extended in later work [60], [67] where the method was termed by Anderson the PQR method. Nolan et al have used the PQR method with a sensitivity analysis technique [68] and then modified the method to allow the inclusion of network and shaft dynamics [69].

Alternatively, Laughton [66] recommended a matrix build up technique to formulate the system coefficient matrix [A] from the subsystem models.

This approach has been extended by Undrill [70] with emphasis on the efficiency that results by avoiding large blocks of null elements. The proposed method in Chapter 2 combines the organizational simplicity of the PQR technique with the efficiency of submatrix build up.

In all the above formulation techniques, the state

grouping approach is an important feature of each method. The two possibilities are [61]:

(1) Type grouping, i.e., all states associated with the same process in each machine are grouped together, e.g., the grouping of rotor angles of all machines, rotor speeds of all machines, etc.

(2) Generator grouping, i.e., all states associated with a particular dynamic unit are grouped together.

The first approach has been adopted in [5], [66], [70], [71] whereas the second appoach has been used in [61], [67], [72], [73]. The second scheme is simpler than the first, especially for the general case with different degrees of generator modeling, and also for system updating. The generator grouping approach has been used by the author in [72], [73] with a specific ordering technique for system variables. This technique results in a considerable saving of computation time and improved flexibility for subsequent stability analysis.

The advantages of this method over others, in stability studies of interest, are demonstrated in Chapter 2.

The procedures adopted for formulating the linearized state-space equation of a power system in these methods are basically similar. They begin with the nonlinear differential and algebraic equations of each subsystem

model, linearize the equations about an operating condition, then formulate the overall system equation. The steady-state equilibrium condition of the overall system is usually obtained using a load flow routine [74].

Recently, an approach has been recommended [75] to construct the state matrix equation of the linearized system from a nonlinear time simulation program which models the system. This approach is specifically useful if it is desired to examine both system transient and dynamic stability under several operating conditions. However, it suffers from computational difficulties in the analysis of system dynamic stability under different parameter settings.

The simulation of an integrated power system and the subsequent analysis of its behaviour requires a fundamental understanding of each individual subsystem model and its dynamic characteristics. Fortunately, each of these subsystems has been in itself a subject of extensive study. The models describing the subsystems considered in this thesis are briefly reviewed in Appendix A. The modeling concepts and dynamic properties have been described in detail in the following references:

(1) Synchronous Machines [8], [60], [76]-[80]

(2) Excitation Systems [81]-[83]

(3) Turbine-Governors, Boilers [84]-[89]

(4) Mechanical Shaft Systems [23], [26], [90], [91]

(5) Transmission Networks [92]-[94]

(6) Induction Motors [39], [40].

1.4.2 Analysis Techniques

As was mentioned earlier, the numerical integration of the system differential equations is a straightforward method for determining stability. This method is very effective in studying the transient stability of power systems since it easily admits the inclusion of the effect of nonlinearities inherent in the system behaviour. More importantly, it is flexible enough to accommodate system changes during transients such as circuit breaker and under-voltage relay operation, etc. However, for dynamic stability evaluation it is not economical to perform numerical integration. Since this thesis is concerned with dynamic stability, the subject of numerical integration is considered to be outside our scope. A number of excellent references on the subject are [8], [10], [95]-[97].

Alternatively, many of the linear control theory techniques have been successfully applied to analyse power system dynamics. These include Routh-Hurwitz [17], Nyquist [98]-[100], and root locus [49], [101]. The concepts of damping and synchronizing torques, based on a frequency response technique, have been applied in the analysis of synchronous machines [102]-[104] and the study of excitation

systems and load parameter effects [6], [19], [44]. These concepts have also been used to design power system stabilizing signals [15], [21]. Although damping and synchronizing torque techniques are valuable in building up the basic concepts related to system parameter and component effects, they are restricted to the analysis of small systems. An example is a single machine connected to an infinite bus.

Among all these methods, eigenvalue techniques have received widespread application in the analysis of power system dynamics [105]-[107]. The methods of finding the eigenvalues of a linear system are well established in the literature [108], [109], and are in use in most computer centres [110]. Methods for calculating eigenvectors or mode-shapes are also available [108], [111].

The efficiency of eigenvalue analysis techniques has further been enhanced by the application of eigenvalue sensitivities (with respect to variable parameters) [69], [72], [112], [113]. First-order eigenvalue sensitivity expressions have been derived by a number of different methods [108], [114], [115]. The application of these expressions concerned a variety of problems. Eigenvalue sensitivity analysis has been applied in numerical analysis [108], [114], perturbation theory [108] and in linear systems theory [112], [115]. The advantages of using first-

order sensitivities have been complemented by the development and application of second-order sensitivities to different studies of power system dynamics [116]-[118].

In dynamic stability studies, it is of interest to investigate the effect of different parameter settings on dynamic stability. Usually, under certain parameter changes only a small subset of the whole eigenvalue pattern would be sensitive and exibit considerable movement due to parameter variation. This situation has been considered in a recent publication [119] which summarizes a technique to track the movement of only this small sensitive subset. In some other cases, it might be of interest to study the stability of a small subsystem including the effect of the whole system interactions. This situation has been recently considered in [120] where a diakoptic approach has been recommended.

Eigenvalue and eigenvalue sensitivity techniques have also been used in design procedures for synchronous machine controllers [121], [122].

1.5 Objectives of This Thesis

The main effort in this thesis is directed toward the establishment of an efficient computational approach to evaluate the dynamic stability of an interconnected power system. This approach is divided into two specific sections. First is the development of a technique to

manipulate the system linearized equations into the state-space form. The formulation allows ease of updating system parameters in subsequent stability studies. Second is the development of an eigenvalue tracking technique in which only a critical subset of eigenvalues is tracked over a practical range of parameter variation.

This computational approach is applied to the analysis of a variety of practical problems in dynamic stability. One important concern currently receiving a good deal of attention is the analysis of load effects on system stability. Instead of applying the eigenvalue tracking approach directly to study load effects for specific systems, an attempt is made to analyse interactions between system loads and the excitation-stabilization subsystem on a reasonably general basis. In order to reach quite general conclusions regarding these interactions, the simple concepts of damping and synchronizing torques are followed. However, the validity of using this simple approach is justified by applying the eigenvalue tracking approach to specific situations where load effects are expected to be critical in system stability predictions.

The objectives of this thesis can be stated as follows:

1.5.1 Theoretical Development

(1) To develop an efficient state-space formulation for a power system comprising an arbitrary number of generating units. The formulation is to be flexible in order to accommodate the modeling aspects of machine controllers, network transients, and load effects.

(2) To develop new appropriate expressions for second-order eigenvalue sensitivities with respect to system parameters.

(3) To use the techniques developed in (1) and (2) in an efficient algorithm for the purpose of evaluating the dynamic stability of interconnected power systems. This algorithm is to be appropriately designed to compute a critical system eigenvalue/eigenvector subset over a wide range of parameter settings. The proposed algorithm is particularly useful at the system planning stage where it is the practice to analyse the effect of different control and design parameter settings on system stability.

1.5.2 Application

To apply the above techniques to dynamic stability studies of practical systems. Special attention will be devoted to developing the basic concepts associated with the

interaction of composite loads with different characteristics and machine static excitation and stabilization control. This phenomenon will be illustrated by considering small perturbations around a wide range of operating conditions. Other studies include subsynchronous resonance instabilities and the effect of different components and parameters on these instabilities. Also the stability of modes corresponding to the torque-angle performance in a multimachine system are studied.

1.6 Thesis Structure

In Chapter 2 the formulation of the linearized state-space model for a multimachine system is outlined. The development and use of first and second-order eigenvalue sensitivities are considered in Chapter 3. The overall approach of tracking sensitive eigenvalues of a system with varying parameters is constructed in Chapter 4. Chapter 5 is devoted to the analysis of possible interactions between system composite loads and synchronous machine excitation-stabilization control.

The formulation and analysis techniques developed in Chapters 2-4 and the concepts regarding load effects developed in Chapter 5 are applied to three specific studies in Chapter 6. The first concerns the instability of a lightly loaded hydro-unit supplying a composite local load.

The second examines the effect of different system parameters and components on subsynchronous resonance modes. The third study illustrates the use of the overall tracking approach in the evaluation of multimachine dynamic stability. In Chapter 7 the main conclusions of the thesis are summarized and the specific contributions of the research and suggestions for future work are outlined.

Chapter 2

STATE-SPACE FORMULATION OF INTEGRATED POWER SYSTEMS

2.1 Introduction

This Chapter presents the development of an efficient technique to formulate a small signal multimachine model in the normal state-space form. Once the equations are obtained in this form, the eigenvalues of the system coefficient matrix can be calculated and examined to obtain information on the system dynamic performance. The state-space form is also convenient for most control studies where modern control theory can be applied.

Methods for formulating multimachine dynamic models from the system differential and algebraic equations have been proposed by Enns et al [65] and Laughton [66]. These in turn have been extended by Anderson [67] and Undrill [70]. The approach proposed in [65] and [67] has tended to concentrate on a systematic formulation of the original differential and algebraic equations for the system in the PQR form, equation (1.3). On the other hand, the procedure recommended in [66] and [70] is a technique for building up the system coefficient matrix from submatrices representing system segments and thus avoiding large blocks of null elements. The formulation described in this chapter

combines the organizational simplicity of the PQR technique with the efficiency of submatrix build up while retaining the identity between submatrices and system components. This allows greater flexibility and convenience in varying parameters and system structure in control studies.

In all of these methods for formulating a dynamic multimachine model, system loads have been modeled as constant impedance elements, which is not true in many practical situations. Also network dynamics have been neglected to avoid very high order systems. Reference [69] describes a procedure to include the effect of network and shaft dynamics in subsynchronous resonance studies. This procedure follows the approach of Enns et al [65] in building up the system coefficient matrix. The formulation presented here, while preserving efficiency is flexible enough to include network dynamics in systems with medium length tie lines. Furthermore, the procedure can be adapted to include the effects of dynamic and nonlinear static loads.

In Section 2.2 the system equations are given and the vector grouping and ordering technique is described. The state-space coefficient matrices are derived in Section 2.3.

The practical advantages of using this technique over others in dynamic stability analysis of integrated power systems is presented in Section 2.4.

Section 2.5 documents the procedure of including the network dynamics whereas in Section 2.6 the incorporation of loads with different characteristics in the overall formulation is described.

The important aspects in the overall approach of formulating a multimachine dynamic model are summarized in Section 2.7.

2.2 Formulation

In dynamic (small signal) stability studies of power systems, it is useful to manipulate the linearized differential and algebraic equation sets describing the performance of the system into the state-space form:

$$\begin{aligned} \dot{\underset{\sim}{x}} &= [A]\underset{\sim}{x} + [B]\underset{\sim}{u} \\ \underset{\sim}{y} &= [C]\underset{\sim}{x} + [D]\underset{\sim}{u} \end{aligned} \tag{2.1}$$

In general, it is difficult to write the equations directly in the above form. Alternatively, they can be written in a straightforward manner as in equation (1.3) as:

$$[P]\begin{bmatrix} \dot{\underset{\sim}{x}} \\ \\ \underset{\sim}{y} \end{bmatrix} = [Q]\ \underset{\sim}{x} + [R]\ \underset{\sim}{u} \tag{2.2}$$

If the [P] matrix is arbitrarily constructed then equation (2.1) can be obtained by a standard matrix inversion routine. On a large system the inversion time is

relatively long and has to be performed every time a parameter setting is changed. The formulation developed in this thesis is based on the ordering of the state, algebraic and output variables of each individual machine in such a way as to set up the [P] matrix in quasi block diagonal form to avoid the inversion of a large matrix. This enhances the computational efficiency of the inversion time initially and for most parameters eliminates the need for any further inversion of the [P] matrix in the eigenvalue analysis.

An interconnected power system is usually constructed with three major components; these are:

1. Synchronous generators; each unit is usually equipped with two main controllers, the exciter and governor control.
2. Three-phase transmission network; this is represented by a linear, multiport, lumped-parameter electrical network.
3. Electrical loads; these may be dynamic or static. The majority of the dynamic loads are synchronous or asynchronous motors. Static loads may be considered as linear or nonlinear components depending on their inherent characteristics.

Figure (2.1) shows a simplified diagram of the basic system considered.

2.2.1 Individual Generating Unit Model

A general model based on Park's equations for each single synchronous machine is adequately documented in the literature and has been formulated in many recent papers [60], [76] - [80]. The excitation and governor schemes are described in two IEEE committee reports [81], [85]. In the formulation of the overall system model, each subsystem model is taken directly from the appropriate references. These models with their state-space representation are documented in Appendix A.

The equations of a model based on linear approximation around an appropriate operating condition are, for the i^{th} unit, written as:

$$\Delta \dot{\underset{\sim}{\psi}}_i - \omega_o [R]\ \Delta \underset{\sim}{i}_{mi} - \omega_o [L]\ \Delta \underset{\sim}{v}_{mi} = \omega_o [IF]\ \Delta \underset{\sim}{\psi}_i + [IC] \begin{bmatrix} \Delta\omega_i \\ \Delta e_{fdi} \end{bmatrix} \tag{2.3}$$

where:

ψ_i ≡ vector of total fluxes of the stator and rotor circuits of the i^{th} machine

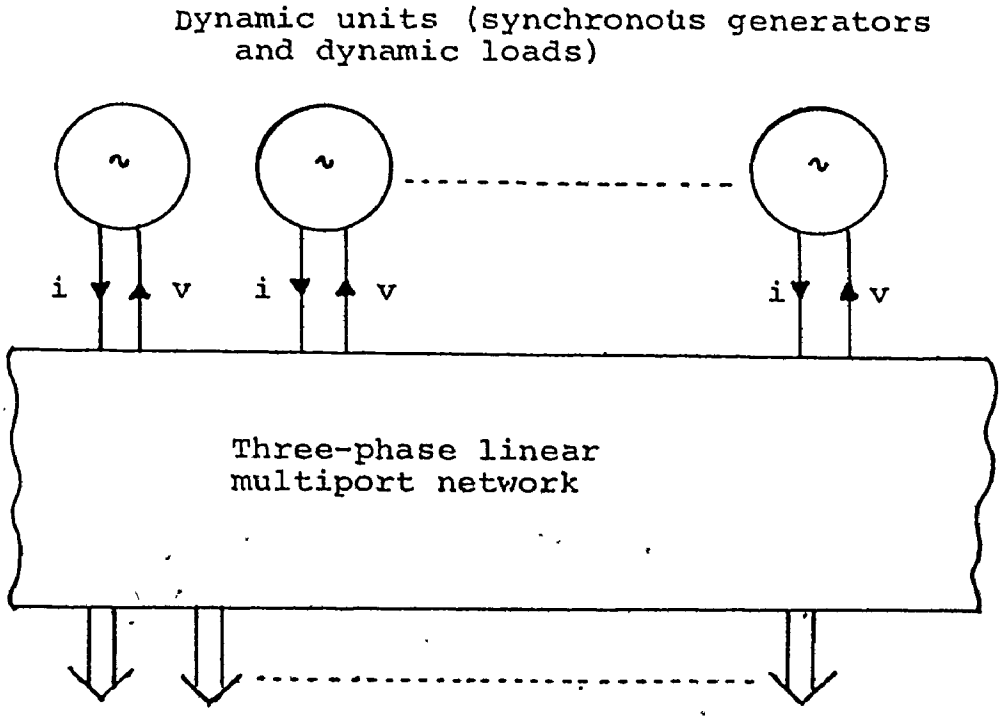

Figure 2.1 Interconnected Power System Structure

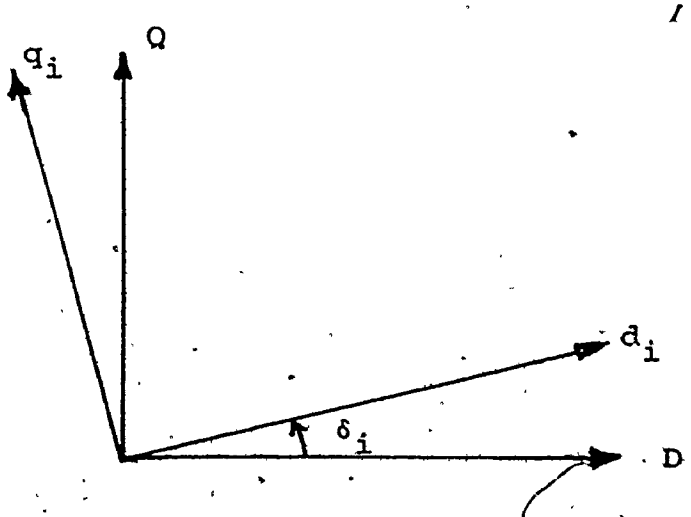

Figure 2.2 Machine (d_i,q_i) and Generalized Reference (D,Q) Frames

i_{mi} ≡ vector of currents in the stator and rotor circuits of the i^{th} machine

v_{mi} ≡ vector of terminal voltage components referred to the i^{th} machine reference frame

ω_i ≡ rotor angular speed of the i^{th} machine (elec. rad./sec)

e_{fdi} ≡ field voltage of the i^{th} machine

ω_o ≡ the synchronous angular speed (elec. rad/sec.)

[R] ≡ diagonal matrix of stator and rotor circuit resistances.

[L], [IF], [IC] matrices of compatible order containing values of steady-state variables.

The structure of the matrices in equation (2.3) are given in Appendix A.

The state-space form of the governor and excitation controls, as in Appendix A, for the i^{th} machine can be written as:

$$\underset{\sim}{X}_{gi} - [CN]\,\Delta\omega_i = [Q_{gi}]\,\underset{\sim}{X}_{gi} + [B_{gi}]\,\underset{\sim}{u}_{gi} \qquad (2.4)$$

$$\underset{\sim}{X}_{ei} - [TV]\,\Delta v_{ti} = [Q_{ei}]\,\underset{\sim}{X}_{ei} + [B_{ei}]\,\underset{\sim}{u}_{ei} \qquad (2.5)$$

The algebraic and output equations are:

$$\underset{\sim}{\Delta\psi}_i = [X_i]\,\underset{\sim}{\Delta i}_{mi} \qquad (2.6)$$

$$\Delta v_{ti} = [VC]\,\underset{\sim}{\Delta v}_{mi} \qquad (2.7)$$

$$\Delta P_{oi} = [CI]\,\underset{\sim}{\Delta v}_{mi} + [VI]\,\underset{\sim}{\Delta i}_{Mi} \qquad (2.8)$$

$$\Delta T_{ei} = [CI]\ \Delta \underset{\sim}{\psi}_i + [SI]\ \Delta \underset{\sim}{i}_{Mi} \qquad (2.9)$$

The coefficient matrices in equations (2.4) to (2.9) are given as explicit functions of the initial conditions and system parameters in Appendix A. The notation of system variables is also given.

2.2.2 Formulation of Network Equations

The equations of each individual machine, as described in Appendix A, are expressed with reference to two perpendicular axis (d,q) which rotate in synchronism with the machine rotor. In order to establish the relationship between the internal quantities of the different machines in the system, a reference frame (D,Q) which rotates at the angular frequency of the steady state network current is considered. The relationship between internal machine reference frames (d_i, q_i) and the general network reference frame (D,Q), at steady state, is illustrated in Figure (2.2).

Thus, one can refer individual machine quantities to the general reference frame as:

$$\begin{bmatrix} v_{di} \\ v_{qi} \end{bmatrix} = \begin{bmatrix} \cos \delta_i & \sin \delta_i \\ -\sin \delta_i & \cos \delta_i \end{bmatrix} \begin{bmatrix} v_{Di} \\ v_{Qi} \end{bmatrix} \qquad (2.10)$$

or symbolically as:

$$\underset{\sim}{v}_{mi} = [T_{ii}]\ \underset{\sim}{v}_{Ni}$$

Considering all the units connected to the network

$$\underset{\sim}{v}_m = \begin{bmatrix} T_{11} & & & 0 \\ & T_{22} & & \\ & & \ddots & \\ 0 & & & T_{nn} \end{bmatrix} \underset{\sim}{v}_N \qquad (2.11)$$

or simply

$$\underset{\sim}{v}_m = [T]\ \underset{\sim}{v}_N$$

For small perturbations in the system, equation (2.11) can be linearized around the operating condition. This yields:

$$\Delta\underset{\sim}{v}_m = [T]_o\ \Delta\underset{\sim}{v}_N = \begin{bmatrix} v_{q1} & 0 & \cdots & 0 \\ -v_{d1} & 0 & \cdots & 0 \\ 0 & v_{q2} & & \\ \vdots & -v_{d2} & & \\ \vdots & \vdots & & \\ \vdots & 0 & \cdots & v_{qn} \\ 0 & 0 & & -v_{dn} \end{bmatrix} \begin{bmatrix} \Delta\delta_1 \\ \Delta\delta_2 \\ \vdots \\ \Delta\delta_n \end{bmatrix}$$

The network is assumed to be completely described by the nodal admittance matrix equation [92]:

$$\underset{\sim}{I} = [Y]\ \underset{\sim}{v}_N \qquad (2.13)$$

For the present approach, all the linear static loads are incorporated in the [Y] matrix as constant admittances. This is achieved by eliminating all the nongenerator buses that supply only linear static loads. The construction of the [Y] matrix from the bus admittance matrix, which is usually formulated in load flow studies, is developed in Appendix B.

Let us consider for the time being that system loads can be represented by constant impedances, i.e., they are static and linear. Loads with different characteristics will be considered in Section 2.6. Under this assumption the [Y] matrix is complex and of an order equal to the number of the system generator buses n. It is necessary in this formulation to separate the n complex equations (2.13) into 2n real equations as proposed by Taylor [92]. Hence we obtain:

$$\begin{bmatrix} i_{D1} \\ i_{Q1} \\ \vdots \\ i_{Dn} \\ i_{Qn} \end{bmatrix} = \begin{bmatrix} g_{11} & -b_{11} & \cdots & g_{1n} & -b_{1n} \\ b_{11} & g_{11} & & b_{1n} & g_{1n} \\ \vdots & \vdots & & \vdots & \vdots \\ & & & g_{nn} & -b_{nn} \\ & & & b_{nn} & g_{nn} \end{bmatrix} \begin{bmatrix} v_{D1} \\ v_{Q1} \\ \vdots \\ v_{Dn} \\ v_{Qn} \end{bmatrix} \qquad (2.14)$$

Equation (2.14) can be written symbolically as:

$$\underset{\sim}{i}_N = [G]\ \underset{\sim}{v}_N$$

The power invariance theorem of Kron [93] requires that:

$$\underset{\sim}{i}_N = [T]^t \underset{\sim}{i}_M \tag{2.15}$$

where $[T]^t$ is the transpose of the matrix $[T]$. It can also be proved that:

$$\{[T]^t\}^{-1} = [T], \quad \text{and} \quad [T]^t = [T]^{-1} \tag{2.16}$$

therefore

$$\underset{\sim}{i}_M = [T]\ [G]\ \underset{\sim}{v}_N \tag{2.17}$$

or

$$[T]^t\ \underset{\sim}{i}_M = [G]\ \underset{\sim}{v}_N \tag{2.18}$$

Equation (2.18) can be linearized for small perturbations, considering a constant nodal admittance matrix, as:

$$[T]^t\ \Delta\underset{\sim}{i}_M - [G]\ \Delta\underset{\sim}{v}_N = \begin{bmatrix} i_{Q1} & 0 & \cdots & 0 \\ -i_{D1} & 0 & \cdots & 0 \\ 0 & i_{Q2} & & 0 \\ 0 & -i_{D2} & & 0 \\ \vdots & & & \vdots \\ & & & -i_{Qn} \\ 0 & & & -i_{Dn} \end{bmatrix} \begin{bmatrix} \Delta\delta_1 \\ \Delta\delta_2 \\ \vdots \\ \Delta\delta_n \\ \\ \\ \end{bmatrix} \tag{2.19}$$

2.2.3 Inclusion of an Infinite Bus

An infinite bus is considered to have constant voltage and frequency; hence, if the system has an infinite bus, equation (2.14) is re-formulated in the form:

$$\begin{bmatrix} i_{NI} \\ \hline \underset{\sim}{i}_N \end{bmatrix} = [G] \begin{bmatrix} v_{NI} \\ \hline \underset{\sim}{v}_N \end{bmatrix} \tag{2.20}$$

Also the infinite bus transformation matrix is

$$[T_I] = \begin{bmatrix} 1 & 0 \\ 0 & 1 \end{bmatrix} \tag{2.21}$$

Noting that:

$$\Delta \underset{\sim}{v}_{NI} = \underset{\sim}{0} \tag{2.22}$$

and if Δi_{NI} is the change in the infinite bus current, equation (2.20) can be perturbed to obtain:

$$\left[\begin{array}{c|c} [T_I] & 0 \\ \hline 0 & [T]_o^t \end{array}\right] \left[\begin{array}{c} \Delta \underset{\sim}{i}_{NI} \\ \hline \Delta \underset{\sim}{i}_N \end{array}\right] - \left[\begin{array}{c} GI \\ \hline G \end{array}\right] \Delta v_N = \begin{bmatrix} 0 & 0 \ldots & 0 \\ 0 & 0 \ldots & 0 \\ i_{Q1} & & 0 \\ -i_{D1} & & 0 \\ \vdots & & \vdots \\ 0 & & i_{Qn} \\ 0 & & -i_{Dn} \end{bmatrix} \begin{bmatrix} \Delta\delta_1 \\ \Delta\delta_2 \\ \vdots \\ \Delta\delta_n \end{bmatrix} \tag{2.23}$$

If the system does not include an infinite bus, equation (2.19) replaces equation (2.23) and the time invariant reference for the rotor angles is lost. This can be accounted for by allowing a synchronously rotating reference frame that will contribute a zero eigenvalue for the [A] matrix. Undrill [70] used an alternative approach whereby one angle, and hence state, is eliminated by using one machine rotor as a rotating reference frame. Useful comments on the latter approach have been made in reference [61]. It is important to notice that the applicability of the proposed formulation is not affected in either case.

2.2.4 Ordering of the System Vectors

The state variable vector for each individual machine can be easily constructed from the perturbed values of the internal flux linkages, relative rotor position and speed, governor and exciter state variables. The state variable vector for the i^{th} generating unit is:

$$\underset{\sim}{x}_i = [\Delta\underset{\sim}{\psi}_i^t, \Delta\delta_i, \Delta\omega_i, \underset{\sim}{x}_{gi}^t, \underset{\sim}{x}_{ei}^t]^t \qquad (2.24)$$

The state variable vector of the whole system is then constructed from all of the individual vectors of each machine as:

$$\underset{\sim}{x} = [\underset{\sim}{x}_1^t, \underset{\sim}{x}_2^t, \ldots, \underset{\sim}{x}_n^t]^t \qquad (2.25)$$

The algebraic and output vectors are constructed from the algebraic and output variables of each individual machine as:

$$\underset{\sim}{y} = \Delta[\underset{\sim}{i}_{m1}^t, \underset{\sim}{i}_{m2}^t, \ldots, \underset{\sim}{i}_{mn}^t, \underset{\sim}{v}_{m1}^t, \underset{\sim}{v}_{m2}^t, \ldots, \underset{\sim}{v}_{mn}^t, v_{t1}, v_{t2}, \ldots$$

$$\ldots, v_{tn}, T_{e1}, T_{e2}, \ldots, T_{en}, \ldots, i_{DI}, i_{QI}, \underset{\sim}{v}_N^t]^t$$

The input vector, $\underset{\sim}{u}$, can be constructed simply from the input vectors of each machine as:

$$\underset{\sim}{u} = [\underset{\sim}{u}_1^t, \underset{\sim}{u}_2^t, \ldots, \underset{\sim}{u}_n^t]^t \qquad (2.27)$$

2.3 State-Space Formulation

The [P], [Q] and [R] matrices of equation (2.2) can now be simply constructed. The [P] matrix is partitioned as:

$$[P] = \left[\begin{array}{c|c} I & AO \\ \hline 0 & GXS \end{array}\right] \begin{matrix} ns \\ nv \end{matrix} \qquad (2.28)$$

where ns and nv are the number of state and algebraic variables respectively. [I] is an identity matrix, [0] a null matrix, and [AO] is very sparse. The matrix [GXS] is of particular interest since it has to be inverted. A two machine structure example is given in Figure (2.3). It is itself partitioned as:

$$[GXS] = \left[\begin{array}{c|c} X & 0 \\ \hline VP & GS \end{array}\right] \qquad (2.29)$$

Both the [X] and [GS] matrices are further partitioned, to reduce the inversion computation time as follows:

$$[X] = \left[\begin{array}{c|c|c|c} X_1 & & & 0 \\ \hline & X_2 & & \\ \hline & & \ddots & \\ \hline 0 & & & X_n \end{array}\right] \text{ and } [GS] = \left[\begin{array}{c|c|c|c} I & 0 & 0 & -T \\ \hline VC & I & 0 & 0 \\ \hline 0 & 0 & I & -GI \\ \hline 0 & 0 & 0 & \lambda-G \end{array}\right] \qquad (2.30)$$

Thus, only a fraction of the [P] matrix has in fact to be inverted. The $[X_i]$ are the reactance matrices, one per machine, and [G] is the real network admittance matrix.

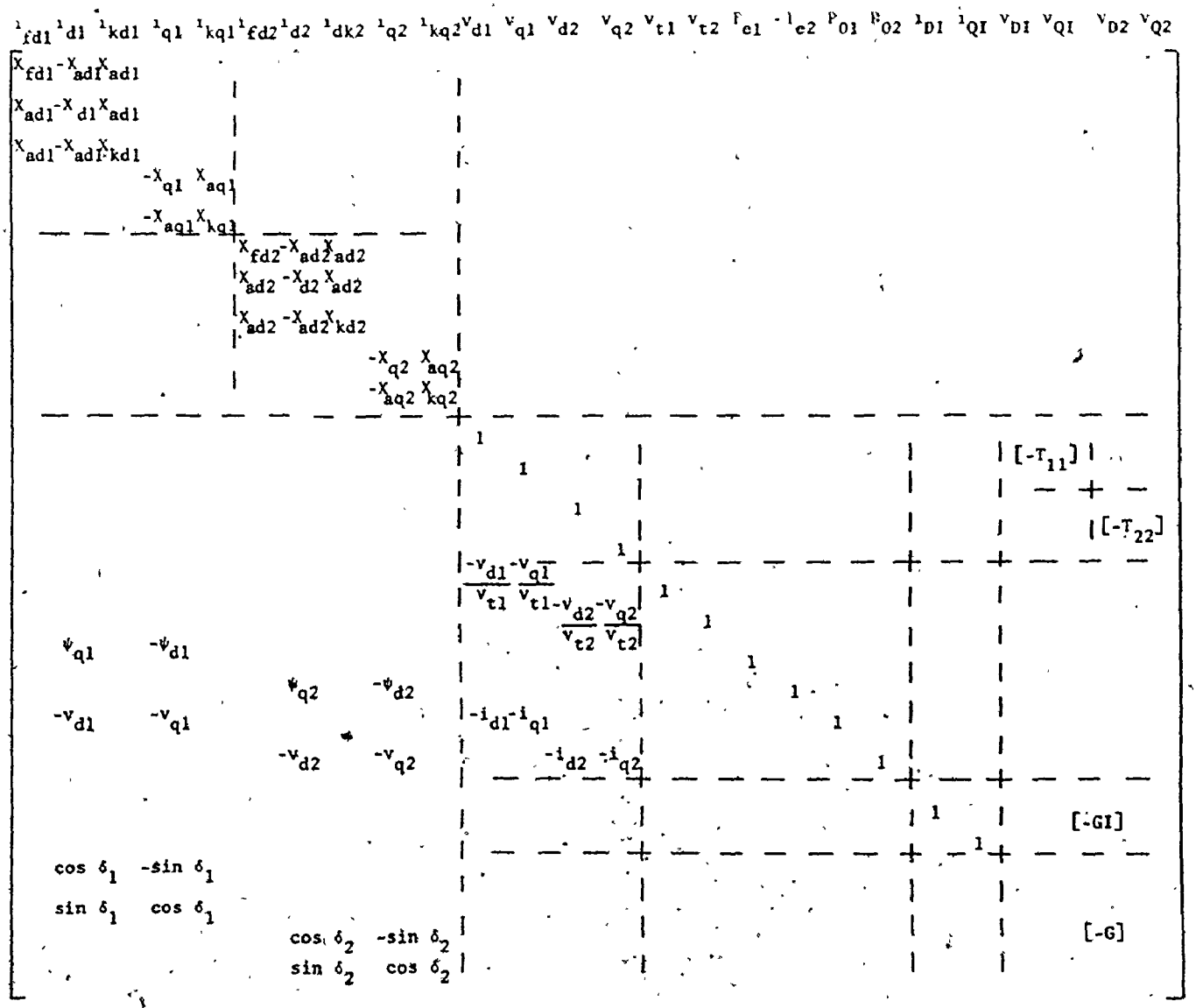

Figure 2.3 GXS Matrix for Two Machine System

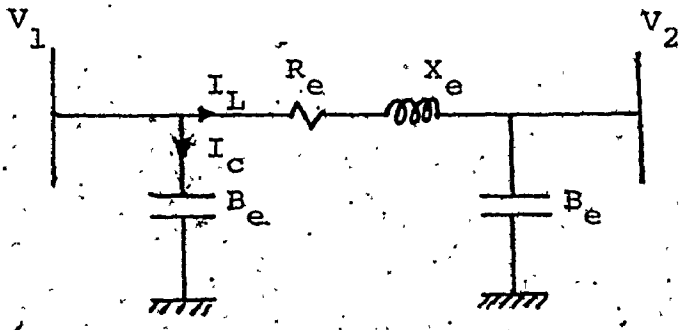

Figure 2.4 Medium Tie-Line Model

Performing the inversion by partitioning we obtain:

$$[GXS]^{-1} = \left[\begin{array}{c|c} [X]^{-1} & 0 \\ \hline -[GS]\ [VP]\ [X]^{-1} & [GS]^{-1} \end{array}\right] \tag{2.31}$$

where

$$[GS]^{-1} = \left[\begin{array}{c|c|c|c} I & 0 & 0 & [T]\ [-G]^{-1} \\ \hline -[VC] & I & 0 & [VC]\ [T]\ [-G]^{-1} \\ \hline 0 & 0 & I & [GI]\ [-G]^{-1} \\ \hline 0 & 0 & 0 & [-G]^{-1} \end{array}\right] \tag{2.32}$$

and hence

$$[P]^{-1} = \left[\begin{array}{c|c} I & -[AO]\ [GXS]^{-1} \\ \hline 0 & [GXS]^{-1} \end{array}\right] \tag{2.33}$$

The [Q] and [R] matrices are partitioned as:

$$[Q] = \left[\begin{array}{c} QA \\ \hline QC \end{array}\right] \begin{array}{l} ns \\ nv \end{array}, \quad [R] = \left[\begin{array}{c} RB \\ \hline RD \end{array}\right] \begin{array}{l} ns \\ nv \end{array} \tag{2.34}$$

and the coefficient matrices of equation (2.1) are then obtained as:

$$\begin{aligned} [A] &= [QA] - [AO]\ [C] \\ [B] &= [RB] \\ [C] &= [GXS]^{-1}\ [QC] \\ [D] &= [GXS]^{-1}\ [RD] \end{aligned} \tag{2.35}$$

2.4 Use of The Formulation in Dynamic Stability Studies

The use of this technique results in a linearized state variable model for a multimachine power system in which each generator can be simulated to any degree of

complexity desired. Consequently, one may represent a certain segment of a power system explicitly while representing another in much less detail. Undrill [70] recommended a procedure for computing a multimachine model which represented each generator with the same degree of complexity and required a matrix inversion of order 11n. On the other hand, the formulation recommended by Anderson et al [67] requires the inversion of n matrices of order 15 to produce the same model. The procedure developed here requires only the inversion of n machine reactance matrices, of order 5 or less, and the real network matrix, [G], of order 2n. The inversion of this last matrix is not required if the network impedance matrix is developed instead of the admittance matrix. This reduction in computation gives significant savings in computer time for a moderately large power system, since the matrix inversion accounts for a reasonably large portion of the solution time. Knowing that the inversion time is proportional to the cube of the matrix order [108], the difference between the family of methods can be easily predicted.

The saving in computation time is even more significant if one wishes to evaluate the effect of changing control parameters on the overall system stability. An example of this situation is an eigenvalue plot to determine the effect of changing regulator gain. Under these

conditions the method in reference [70] would still require the inversion of an $11n^{th}$-order matrix while the method presented in reference [67] will require the inversion of one 15^{th}-order matrix (if all parameters undergoing change belong to one machine). In the method recommended here, the [A] matrix is composed of two matrices as in equation (2.34). Most of the significant parameters that are likely to be changed do not appear in the second matrix and are likely to appear as simple explicit functions in the [QA] matrix. Hence, in the majority of cases of parameter updating and stability evaluation no further matrix inversion is needed at all, only simple division or multiplication of elements in the corresponding rows of the matrix [QA].

It has been shown in [72], and it will also be demonstrated in the next two chapters, that this property of the [A] matrix is particularly useful if eigenvalue sensitivity techniques are applied in the analysis of power system dynamics.

Alternatively, if an analysis is required for a variety of generation conditions, there is no need for additional matrix inversion. It is only required to re-run the load flow program and change the appropriate elements in the [AQ], [GXS] and [QC] matrices.

2.5 Inclusion of Network Transients

The amount of detail in the overall system model is highly dependent on the kind of problem under investigation [13], [64]. For example, if one is concerned about the stability of the dominant modes corresponding to slow rotor oscillations, the inclusion of network transients is practically insignificant and one would favour ignoring them to avoid very large system orders. Whereas if the study is directed toward the analysis of subsynchronous resonance the consistant inclusion of network and stator transients [13] is necessary to predict the right interactions. The inclusion of network transients in multimachine formulations for dynamic stability studies has been considered in [69] and [73].

Considering the medium tie-line model depicted in Figure (2.4), the linearized two axis dynamic equations of the network referred to a synchronously rotating frame (D,Q) are taken directly from [61] as:

$$\begin{bmatrix} \Delta i_{Dc1} \\ \Delta i_{Qc1} \end{bmatrix} = \begin{bmatrix} 0 & -B_e \\ B_e & 0 \end{bmatrix} \begin{bmatrix} \Delta v_{D1} \\ \Delta v_{Q1} \end{bmatrix} + \frac{B_e}{\omega_o} \begin{bmatrix} \Delta \dot{v}_{D1} \\ \Delta \dot{v}_{Q1} \end{bmatrix} \qquad (2.36)$$

and

$$\begin{bmatrix} {}^{\Delta}i_D \\ {}^{\Delta}i_Q \end{bmatrix} = \omega_o \begin{bmatrix} \frac{1}{x_e} & 0 \\ 0 & \frac{1}{x_e} \end{bmatrix} \begin{bmatrix} \Delta v_{D1} - \Delta v_{D2} \\ \Delta v_{Q1} - \Delta v_{Q2} \end{bmatrix} - \begin{bmatrix} \frac{\omega_o R_e}{x_e} & -\omega_o \\ \omega_o & \frac{\omega_o R_e}{x_e} \end{bmatrix} \begin{bmatrix} \Delta i_D \\ \Delta i_Q \end{bmatrix} \tag{2.37}$$

Consequently, to account for network transients, the state vector in (2.25) should be extended to include the tie-line states:

$$x = {}^{\Delta}[v_{D1},\ v_{Q1},\ v_{D2},\ v_{Q2},\ i_D,\ i_Q]^t$$

and in the output variable vector (2.26), the network voltage components $[{}^{\Delta}v_D,\ {}^{\Delta}v_Q]$ should be replaced by the shunt capacitor current components $[{}^{\Delta}i_{DC},\ {}^{\Delta}i_{QC}]$. These changes will result in further diagonalization of the [P] matrix and eliminate the need for inverting the real network matrix [G].

In the proposed procedure, a medium tie-line model is considered for the transmission lines in the network. A practical difficulty arises in the inclusion of the feeder and transformer connected directly to the machine terminals. Here the choice of current in the series inductance as a state is inconsistent with the choice of stator flux linkage in the machine. This can be resolved in one of three ways: (1) include the external series inductance with the stator leakage inductance; (2) use stator current instead of stator flux linkage as the state [61]; and (3) add a shunt path at

the machine terminals representing the capacitance to ground that might otherwise have been omitted.

2.6 Inclusion of Nonlinear and Dynamic Loads

In power system studies, loads can be represented in different ways according to their inherent dynamics and characteristics. In the past, due to the lack of knowledge about load behaviour it was traditional to represent the loads as shunt lumped impedances at the different load buses. In Chapter 5 a variety of load models are considered and their effects on the overall system performance are also analysed. In this section the procedure of including loads, with different characteristics, in the overall formulation of the integrated system is described.

2.6.1 Inclusion of Nonlinear Composite Loads

Composite loads can be represented by a static model where load power is considered as an exponential function of load bus terminal voltage. The equations describing this model are stated in Chapter 5 as:

$$P_\ell = C_1 \, v_t^{K_p}$$
$$Q_\ell = C_2 \, v_t^{K_q} \qquad (2.38)$$

where K_p and K_q are the load indices, C_1 and C_2 are constants determined from field measurements. Considering small perturbations, the linearized version of equation (2.38) can be obtained as in Appendix C as:

$$\begin{bmatrix} \Delta P_\ell \\ \Delta Q_\ell \end{bmatrix} = \begin{bmatrix} \frac{P_\ell K_p}{V_t} \\ \frac{Q_\ell K_q}{V_t} \end{bmatrix} \Delta V_t = \begin{bmatrix} i_{D\ell} & i_{Q\ell} \\ -i_{Q\ell} & i_{D\ell} \end{bmatrix} \begin{bmatrix} \Delta V_D \\ \Delta V_Q \end{bmatrix} + \begin{bmatrix} V_D & V_Q \\ V_Q & -V_D \end{bmatrix} \begin{bmatrix} \Delta i_{D\ell} \\ \Delta i_{Q\ell} \end{bmatrix} \tag{2.39}$$

Using the relationship between the pertubations in the terminal voltage and the direct and quadrature components of the voltage in Section C2.1 we obtain:

$$\begin{bmatrix} V_D & V_Q \\ V_Q & -V_D \end{bmatrix} \begin{bmatrix} \Delta i_{D\ell} \\ \Delta i_{Q\ell} \end{bmatrix} = \begin{bmatrix} \left(\frac{P_\ell K_p V_D}{V_t^2} - i_{D\ell}\right) & \left(\frac{P_\ell K_p V_Q}{V_t^2} - i_{Q\ell}\right) \\ \left(\frac{Q_\ell K_q V_D}{V_t^2} + i_{Q\ell}\right) & \left(\frac{Q_\ell K_q V_Q}{V_t^2} - i_{D\ell}\right) \end{bmatrix} \begin{bmatrix} \Delta V_D \\ \Delta V_Q \end{bmatrix} \tag{2.40}$$

and hence to account for static nonlinear loads, the output variable vector in (2.26) should be extended to include the components of the load current $[\Delta i_{D\ell}, \Delta i_{Q\ell}]$.

In the build up procedure of the nodal admittance matrix, considering nonlinear loads, the size and construction of the matrix is different depending on the type of bus at which the loads are grouped. If the loads are grouped at a generator bus, the current components of the load can be

subtracted from the generator current components. The net current is equal to the sum of all currents leaving the bus through all the transmission lines connected to the same bus. Consequently, the order of the [Y] matrix is unchanged. On the other hand, if loads are grouped at a separate load bus the voltage of this bus should be retained in constructing the [Y] matrix. This matrix now has an order which is greater than n by the number of nongenerator nonlinear load buses in the system.

Thus, in the overall formulation of the system model, the inclusion of each group of nonlinear loads results in a further inversion of only a (2x2), matrix. In addition, the order of the [G] matrix may be increased by 2.

2.6.2 Inclusion of Dynamic Loads

Synchronous motor loads in a system can be described by the same model as the generator except that the governor effects are neglected and the shaft system is modified to account for mechanical load dynamics.

Induction motor groups with significant inertial time constants can be simulated by one or more dynamically equivalent units at a high voltage bus. It will be shown in Chapter 5 that the equations for each equivalent unit can be represented in the form:

$$v = [R]\ i + \frac{1}{\omega_o}\ [X]\ \dot{i} + [G_o]\ i \tag{2.41}$$

$$\frac{2H_m}{\omega_o}\ \dot{\omega}_r + D\ \omega_r + T_m = T_e \tag{2.42}$$

$$T_e = X_{sr}\ (i_{rD}\ i_{sQ} - i_{rQ}\ i_{sD}) \tag{2.43}$$

The structure of the matrices in equation (2.41) and the notation of the variables in equations (2.41) - (2.43) are given in Section 5.2.

Thus, for systems including induction motor groups, the nodal admittance matrix can be constructed by following the procedure described in Section 2.6. It is apparent from equations (2.41) - (2.43) that the proposed partitioning approach to invert the [P] matrix requires the inversion of a reactance matrix for each induction motor group. Each reactance matrix is usually of order 4 or less.

2.7 Summary

A procedure has been derived in this chapter to formulate the linearized equations of a multimachine system in state-space form. The basic PQR technique has been used which is ideally suited for the systematic assembly of equations for a realistic power system. It allows flexibility of representation for different system portions while retaining a simplicity of form that is an important feature in assembling a complicated analysis program.

Careful consideration of the system structure with a special ordering of system variables results in an efficient formulation that reduces significantly both the initial time to compute the coefficient matrices [A], [B], [C] and [D] and in certain cases eliminates the need for additional matrix inversion in subsequent analysis.

An important feature of this formulation is the flexibility to include or neglect the effect of network transients and system loads with different characteristics.

The proposed partitioning approach is economical with regard to storage requirements in that large null sections of the [P] matrix are never stored. An added convenience is the fact that the system inputs remain explicit throughout the manipulations.

Chapter 3

EIGENVALUE SENSITIVITIES APPLIED TO POWER SYSTEM DYNAMICS

3.1 Introduction

In dynamic stability studies of large interconnected power systems described in the state-space form (2.1) the evaluation of system performance under a variety of operating conditions is necessary in both planning and operation. Dynamic stability prediction of such systems is a direct function of the system coefficient matrix eigenvalues. Eigenvalue techniques are receiving widespread application in the analysis of power system dynamics [5], [70], [105] - [107].

Normally, it is required to locate the system eigenvalues for certain operating conditions and, in addition, it is necessary to examine the possible movement of the critical subset under changes in system control and design parameters around the chosen base condition. This can generally be achieved by either eigenvalue recalculation for different parameter settings or by employing eignevalue sensitivities around the base case. The second approach is much more efficient and convenient, especially for relatively large systems.

In this chapter analytical expressions are developed

for first and second-order eigenvalue sensitivity coefficients with respect to general system parameters. Different expressions for first-order coefficients have been derived by a number of different methods [108], [114], [115] and have been applied to a variety of problems as indicated in Chapter 1.

Expressions for second-order eigenvalue sensitivity coefficients are given in [108], [115]. These expressions have been developed in terms of system matrix entries rather than system parameters, and it is very difficult to reexpress their formulations as each element of the system matrix can be a complex function of more than one parameter and more than one element can be a function of a particular system parameter. For use in physical systems we require the sensitivities in terms of the system parameters. This has been done for first-order sensitivities by Faddeev and Faddeeva [114] and is extended in Section 3.3 for second-order terms.

The sensitivity expressions, as developed here, are particularly suitable for systems with distinct eigenvalues, which is usually the case for large physical systems.

Section 3.2 discusses the importance of employing first-order sensitivity in the analysis of power system dynamics. The limitations of using only the first-order terms are also discussed. In Section 3.3 the actual

eigenvalue sensitivity expressions are developed. Then, the system matrix derivatives with respect to system parameters are derived in a very straightforward manner.

The use of eigenvalue sensitivities is illustrated in Section 3.4 through their application to two specific examples of simplified second and fourth-order systems. The efficiency and convenience of the eigenvalue sensitivity approach is further illustrated by applying the method to systems with higher orders in Chapter 6 of this thesis.

The practical limitations of the method as applied to the analysis of power system dynamics are discussed in Section 3.5.

A general discussion of the method is presented in Section 3.6.

3.2 First-Order Sensitivity

The eigenvalues of the system coefficient matrix [A] are indicative of the system dynamic stability. These eigenvalues are, in general, functions of all control and design parameters in the system. A change in any of these parameters affects the system performance, and hence, causes a shift in the whole eigenvalue pattern.

An estimated value $\hat{\lambda}_i$ of a specific eigenvalue λ_i due to a change $\Delta\xi$ in a certain parameter ξ can be obtained using Taylor series expansion around the base value λ_{io} as

follows:

$$\hat{\lambda}_i = \lambda_{io} + \left.\frac{\partial \lambda_i}{\partial \xi}\right|_{\xi_o} (\Delta\xi) + \frac{1}{2}\left.\frac{\partial^2 \lambda_i}{\partial \xi^2}\right|_{\xi_o} (\Delta\xi)^2 + \ldots \quad (3.1)$$

provided that there is no correlation between the control parameters, which is true in most practical situations.

In equation (3.1) the term

$$\left.\frac{\partial \lambda_i}{\partial \xi}\right|_{\xi_o}$$

is defined as the first-order sensitivity coefficient of the eigenvalue λ_i with respect to the parameter ξ at ξ_o. If the estimation process is terminated after the second term, the estimation is a first-order approximation and it is only valid for small parameter changes. Consequently, a low sensitivity value can not be taken, in general, as an indication that larger variation in the parameter will continue to have a small effect on system stability [116].

Eigenvalue first-order sensitivity analysis has been applied in [68], [69], [72], [112], [113]. These studies have presented a variety of results that demonstrate the advantages of employing eigenvalue sensitivities in:

1. Identifying different system modes.
2. Choosing appropriate model precision.
3. Estimating the required accuracy of field measurements for system simulation studies.

The expression for the first-order sensitivity coefficient with respect to a general system parameter is derived in Section 3.3 as a step in the overall derivation of second-order coefficients.

3.3 Second-Order Sensitivity

The second-order partial derivative

$$\left.\frac{\partial^2 \lambda_i}{\partial \xi^2}\right|_{\xi_o}$$

in equation (3.1) is called the second-order sensitivity coefficient of the eigenvalue λ_i with respect to the system parameter ξ. The use of a second-order term in equation (3.1) tends to improve the accuracy of the sensitivity analysis [117] and therefore results in the following advantages:

1. The sensitivity calculation is valid over a wider range of parameter variation.
2. Fewer eigenvalue computations need to be performed. This implies that the accuracy of tracking eigenvalue movement over a relatively wide parameter variation can be improved for the same total computation cost and thus forms a good basis for optimal parameter selection.

The analytical expressions of the second-order

sensitivity coefficients are derived, in this section, in terms of the eigenvalues and normal and transposed eigenvectors at the base condition.

3.3.1 Mathematical Development

The eigenvalues λ_i and eigenvectors $\underset{\sim}{z}_i$ of the coefficient matrix [A] of equation (2.1) satisfy the equation:

$$[A]\ \underset{\sim}{z}_i = \lambda_i\ \underset{\sim}{z}_i,\ i = 1, 2, \ldots, n_s \qquad (3.2)$$

and $\underset{\sim}{z}_i$ is non-trivial if λ_i is a root of the determintal equation:

$$|A - I\lambda| = 0 \qquad (3.3)$$

Differentiating equation (3.2) with respect to a general system parameter ξ we obtain:

$$[A]\ \frac{\partial \underset{\sim}{z}_i}{\partial \xi} + \frac{\partial [A]}{\partial \xi}\ \underset{\sim}{z}_i = \lambda_i\ \frac{\partial \underset{\sim}{z}_i}{\partial \xi} + \frac{\partial \lambda_i}{\partial \xi}\ \underset{\sim}{z}_i \qquad (3.4)$$

The transposed matrix $[A]^t$ has the same set of eigenvalues as the matrix [A] but a different set of eigenvectors $\underset{\sim}{v}_i$ [108]. Post-multiplying equation (3.4) by $\underset{\sim}{v}_i^t$ and cancelling out equal terms:

$$\frac{\partial \lambda_i}{\partial \xi} = \left(\frac{\partial [A]}{\partial \xi} \underset{\sim}{z}_i, \underset{\sim}{v}_i\right) / \left(\underset{\sim}{z}_i, \underset{\sim}{v}_i\right) \tag{3.5}$$

where $(\underset{\sim}{f}, \underset{\sim}{g})$ signifies the inner product of $\underset{\sim}{f}$ and $\underset{\sim}{g}$.

Differentiating equation (3.4) once again with respect to another system parameter η yields:

$$[A] \frac{\partial^2 \underset{\sim}{z}_i}{\partial \xi \partial \eta} + \frac{\partial [A]}{\partial \eta} \frac{\partial \underset{\sim}{z}_i}{\partial \xi} + \frac{\partial [A]}{\partial \xi} \frac{\partial \underset{\sim}{z}_i}{\partial \eta} + \frac{\partial^2 [A]}{\partial \xi \partial \eta} \underset{\sim}{z}_i$$

$$= \lambda_i \frac{\partial^2 \underset{\sim}{z}_i}{\partial \xi \partial \eta} + \frac{\partial \lambda_i}{\partial \eta} \frac{\partial \underset{\sim}{z}_i}{\partial \xi} + \frac{\partial^2 \lambda_i}{\partial \xi \partial \eta} \underset{\sim}{z}_i + \frac{\partial \lambda_i}{\partial \xi} \frac{\partial \underset{\sim}{z}_i}{\partial \eta} \tag{3.6}$$

Post-multiplying equation (3.6) by $\underset{\sim}{v}_i^t$ and cancelling out equal terms further yields:

$$\left(\frac{\partial^2 [A]}{\partial \xi \partial \eta} \underset{\sim}{z}_i, \underset{\sim}{v}_i\right) + \left(\frac{\partial [A]}{\partial \eta} \frac{\partial \underset{\sim}{z}_i}{\partial \xi}, \underset{\sim}{v}_i\right) + \left(\frac{\partial A}{\partial \xi} \frac{\partial \underset{\sim}{z}_i}{\partial \eta}, \underset{\sim}{v}_i\right)$$

$$= \left(\frac{\partial^2 \lambda_i}{\partial \xi \partial \eta} \underset{\sim}{z}_i, \underset{\sim}{v}_i\right) + \frac{\partial \lambda_i}{\partial \eta} \left(\frac{\partial \underset{\sim}{z}_i}{\partial \xi}, \underset{\sim}{v}_i\right) + \frac{\partial \lambda_i}{\partial \xi} \left(\frac{\partial \underset{\sim}{z}_i}{\partial \eta}, \underset{\sim}{v}_i\right) \tag{3.7}$$

We assume throughout that all the eigenvalues are distinct, so that there are ns independent eigenvectors $\underset{\sim}{z}_i$, $i = 1, 2, \ldots, ns$, and any arbitrary ns-space vector can be expressed as a linear combination of all eigenvectors. Consequently, the partial derivative (sensitivity) of all system eigenvectors with respect to a system parameter can be expressed as a linear function of all eigenvectors at the base case as follows:

$$\frac{\partial z_i}{\partial \xi} = \sum_{j=1}^{ns} \alpha_{ij} \, z_j$$

$$\frac{\partial z_i}{\partial \eta} = \sum_{j=1}^{ns} \beta_{ij} \, z_j \qquad (3.8)$$

where α_{ij} and β_{ij} are taken directly from reference [114] as:

$$\alpha_{ij} = \left(\frac{\partial [A]}{\partial \xi} z_i, v_j\right) / (z_j, v_j)(\lambda_i - \lambda_j) \qquad (3.9)$$

$$\beta_{ij} = \left(\frac{\partial [A]}{\partial \eta} z_i, v_j\right) / (z_j, v_j)(\lambda_i - \lambda_j) \qquad (3.10)$$

It is clear from equations (3.9) and (3.10) that α_{ii} and β_{ii} are undefined, but terms including them will cancel out. Substituting equations (3.9) and (3.10) in equation (3.7) we obtain:

$$\left(\frac{\partial^2 [A]}{\partial \xi \partial \eta} z_i, v_i\right) + \left(\frac{\partial [A]}{\partial \eta} \sum_{\substack{j=1 \\ j \neq i}}^{ns} \alpha_{ij} \, z_j, v_i\right)$$

$$+ \left(\frac{\partial [A]}{\partial \eta} \alpha_{ii} \, z_i, v_i\right) + \left(\frac{\partial [A]}{\partial \xi} \sum_{\substack{j=1 \\ j \neq i}}^{ns} \beta_{ij} \, z_j, v_i\right)$$

$$+ \left(\frac{\partial [A]}{\partial \xi} \beta_{ii} \, z_i, v_i\right)$$

$$= \left(\frac{\partial^2 \lambda_i}{\partial \xi \partial \eta} z_i, v_i\right) + \left(\frac{\partial \lambda_i}{\partial \eta} \sum_{\substack{j=1 \\ j \neq i}}^{ns} \alpha_{ij} \, z_j, v_i\right) + \frac{\partial \lambda_i}{\partial \eta} (\alpha_{ii} \, z_i, v_i)$$

$$+ \frac{\partial \lambda_i}{\partial \xi} \left(\sum_{\substack{j=1 \\ j \neq i}}^{ns} \beta_{ij} \, z_j, v_i\right) + \frac{\partial \lambda_i}{\partial \xi} (\beta_{ii} \, z_i, v_i) \qquad (3.11)$$

using the fact that:

$$(\underset{\sim}{z}_i, \underset{\sim}{v}_j) = 0 \quad \text{for all } i \neq j$$

therefore

$$\frac{\partial^2 \lambda_i}{\partial \xi \partial \eta} = \left\{ \left(\frac{\partial^2 [A]}{\partial \xi \partial \eta} \underset{\sim}{z}_i, \underset{\sim}{v}_i \right) + \left(\frac{\partial [A]}{\partial \xi} \sum_{\substack{j=1 \\ j \neq i}}^{ns} \beta_{ij} \underset{\sim}{z}_j , \underset{\sim}{v}_i \right) + \left(\frac{\partial [A]}{\partial \eta} \sum_{\substack{j=1 \\ j \neq i}}^{ns} \alpha_{ij} \underset{\sim}{z}_j , \underset{\sim}{v}_i \right) \right\} / (\underset{\sim}{z}_i, \underset{\sim}{v}_i) \qquad (3.12)$$

and hence:

$$\frac{\partial^2 \lambda_i}{\partial \xi^2} = \frac{\left(\frac{\partial^2 [A]}{\partial \xi^2} \underset{\sim}{z}_i, \underset{\sim}{v}_i \right) + 2 \left(\frac{\partial [A]}{\partial \xi} \sum_{\substack{j=1 \\ j \neq i}}^{ns} \alpha_{ij} \underset{\sim}{z}_j , \underset{\sim}{v}_i \right)}{(\underset{\sim}{z}_i, \underset{\sim}{v}_i)} \qquad (3.13)$$

Equation (3.13) gives the second-order sensitivity coefficient with respect to different control parameters under the assumption that they are uncorrelated whereas equation (3.12) allows any two parameters to be correlated. The expressions for second-order sensitivity as given in equations (3.12) and (3.13) do not add any significant computational complexity. The only additional computation required over the first-order calculation is that of the second-order derivative of the system matrix [A] and the coefficients α_{ij} and β_{ij}. The system eigenvalues and the normal and transposed eigenvectors have to be computed for the first-order calculation in any case and these

computations take the largest proportion of the time. Hence for a practical system the increase in computation time to include the second-order term is insignificant.

3.3.2 Computation of System Matrix Derivatives

It was shown in Chapter 2 that in dynamic stability studies, the set of linearized differential and algebraic equations describing the system performance are systematically manipulated into the PQR form as in equation (2.2). If this equation is pre-multiplied by $[P]^{-1}$, one obtains:

$$\begin{bmatrix} \dot{\underset{\sim}{x}} \\ \\ \underset{\sim}{y} \end{bmatrix} = [S]\ \underset{\sim}{x} + [E]\ \underset{\sim}{u} \tag{3.14}$$

where:

$$[S] = [P]^{-1}\ [Q] = \left[\begin{array}{c} A \\ \hline C \end{array}\right],\quad [E] = [P]^{-1}\ [R] = \left[\begin{array}{c} B \\ \hline D \end{array}\right] \tag{3.15}$$

It is clear from the derivation of the state-space matrices that the [A] matrix is the result of matrix manipulations including inverses and products of constituent matrices. Therefore, the relationship between the individual elements of the [A] matrix and system parameters is usually highly complicated.

The technique described in the previous chapter formulates the [A] matrix from the addition of two matrices.

One of them contains most of the control and design parameters in the system as simple explicit functions. This facilitates the direct calculation of the [A] matrix derivatives.

On the other hand, if it is required to compute eigenvalue sensitivities with respect to parameters that appear in the matrix [P], the technique used by Nolan et al [68] for calculating matrix first-order derivatives can be extended to calculate the second-order matrix derivatives as follows.

Differentiating equation (3.15) with respect to the parameter ξ.

$$\frac{\partial [S]}{\partial \xi} = \frac{\partial}{\partial \xi} \{ [P]^{-1} [Q] \} = [P]^{-1} \frac{\partial [Q]}{\partial \xi} + \frac{\partial [P]^{-1}}{\partial \xi} [Q] \qquad (3.16)$$

Using the definition of the matrix inverse:

$$[P] [P]^{-1} = [I]$$

where [I] is the unit matrix, we obtain:

$$\frac{\partial [P]^{-1}}{\partial \xi} = - [P]^{-1} \frac{\partial [P]}{\partial \xi} [P]^{-1} \qquad (3.17)$$

and hence if

$$\frac{\partial [Q]}{\partial \xi} = [0]$$

therefore

$$\frac{\partial [S]}{\partial \xi} = - [P]^{-1} \frac{\partial [P]}{\partial \xi} [S] \qquad (3.18)$$

then $\partial[A]/\partial\xi$ is the matrix containing the ns-top rows of $\partial[S]/\partial\xi$.

Differentiating equation (3.18) gives:

$$\frac{\partial^2[S]}{\partial\xi^2} = -[P]^{-1}\left\{\frac{\partial^2[P]}{\partial\xi^2}\cdot[S] + 2\,\frac{\partial[P]}{\partial\xi}\,\frac{\partial[S]}{\partial\xi}\right\} \qquad (3.19)$$

Again $\partial^2[A]/\partial\xi^2$ is the matrix containing the ns-top rows of the matrix $\partial^2[S]/\partial\xi^2$.

The matrices $[P]$, $\partial[A]/\partial\xi^2$ and $\partial^2[A]/\partial\xi^2$ are very sparse so that sparse matrix techniques can be employed to overcome storage problems that might arise with very large systems.

3.4 Use of Eigenvalue Sensitivities in the Analysis of Power Systems

The use of eigenvalue sensitivities in the analysis of synchronous machine dynamics is illustrated in this section by considering two simplified systems. The first example is a simplified second-order system representing the performance of the main torque-angle loop of a synchronous machine connected to an infinite bus. The second example examines the effect of static exciter parameters on the stability of a synchronous machine connected to an infinite bus where the machine is represented by a simplified third-order model.

3.4.1 Simplified Second-Order Example

In small perturbation studies of a synchronous machine and at a certain frequency of oscillation, the machine braking torque can be analysed into two components [6]: the damping component in phase with the machine rotor speed deviation ($\Delta\omega$), and the synchronizing component in phase with the rotor angle deviation ($\Delta\delta$). Hence, the system can be described by the block diagram in Figure (3.1). The two roots of this system are:

$$\lambda_{1,2} = \frac{-\omega_o D}{4H} \pm j\,\omega_d,\quad \omega_d = \left(\frac{\omega_o K_s}{2H} - \frac{\omega_o^2 D^2}{16H^2}\right)^{1/2} \qquad (3.20)$$

where ω_o is the angular synchronous speed.

It is desirable to introduce a damping torque component without affecting the synchronizing torque component [6]. In another words, to increase the damping coefficient D keeping the synchronizing coefficient K_s or the natural frequency of oscillation, practically constant.

The analytical expressions for the first and second-order sensitivities of the system roots with respect to the damping coefficient D can be obtained directly from equation (3.20) as:

$$\frac{\partial\lambda_1}{\partial D} = -\frac{\omega_o}{4H} - j\,\frac{\omega_o^2 D}{16H^2}(\omega_d)^{-1} \qquad (3.21)$$

and

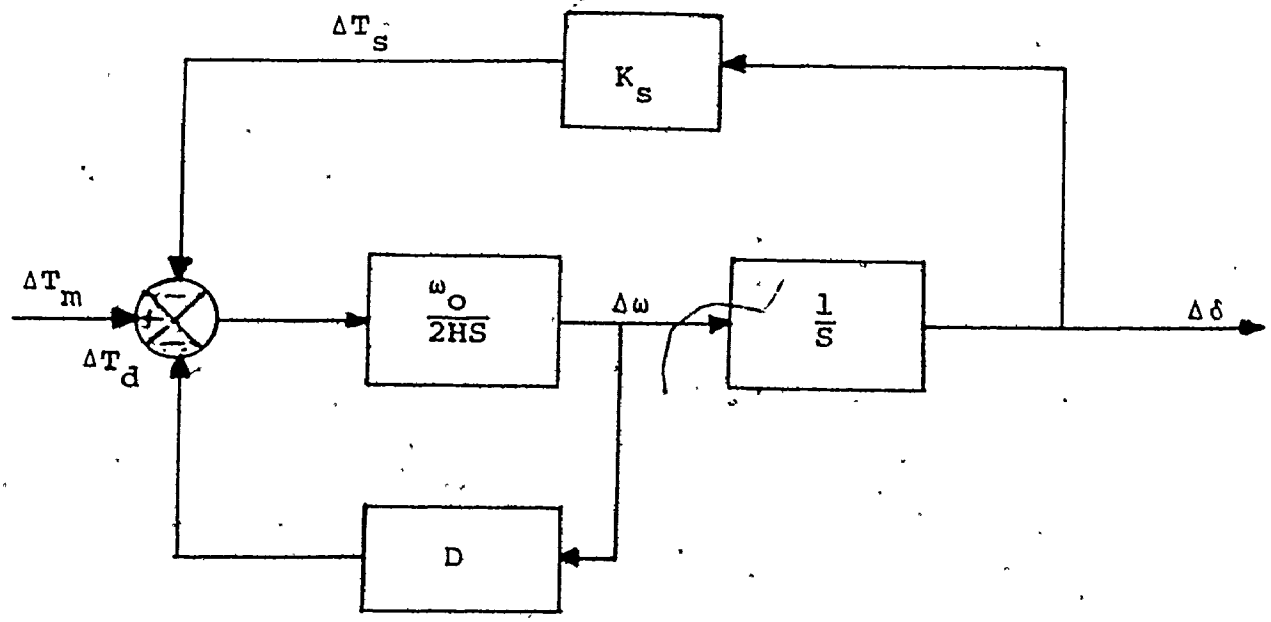

Figure 3.1 Second-Order System Block Diagram

ω_o = 377. rad/sec., H = 4.29 sec.

K_s = 2.0 , D = .16

Table 3.1 Eigenvalue and Eigenvalue Sensitivities For Second-Order System

$\lambda_{1,2}$	$(\dot{\lambda}_{1,2})_n$	$(\ddot{\lambda}_{1,2})_n$
$-3.55 \pm j8.8$	$-3.55 \mp j1.42$	$0.0 \mp j.82$

$$\frac{\partial^2 \lambda_1}{\partial D^2} = 0.0 + j \frac{\omega_o^4 D^2}{256H^4} (\omega_d)^{-3} + \frac{\omega_o^2}{16H^2} (\omega_d)^{-1} \qquad (3.22)$$

Typical values of parameters for a hydraulic machine are shown in Figure (3.1). These values are taken directly from reference [72]. Hence, the corresponding eigenvalues and their normalized sensitivities are obtained and stated in Table (3.1). The sensitivities are normalized in the sense that they give directly the shift in the eigenvalue due to a unit change in the corresponding parameter. The estimated shift is, of course, a second-order approximation. For example, if $\dot{\lambda}_{ni}$ and $\ddot{\lambda}_{ni}$ are the normalized sensitivities of the eigenvalue λ_i with respect to D, the estimated eigenvalue for a 50% increase over the base value of D is

$$\lambda_i = \lambda_{io} + (.5)\, \dot{\lambda}_{ni} + (.5)^2\, \ddot{\lambda}_{ni} \qquad (3.23)$$

First and second-order estimates of the imaginary part of the complex pair of eigenvalues are plotted in Figure (3.2) together with a plot of the directly computed values over a wide range of damping coefficient.

The amount of damping, in the mode considered is adequate if the equivalent second-order damping ratio lies between .2 and .5 which corresponds respectively to values of .086 and .23 for the damping coefficient D. Under the prescribed range of the damping ratio variation, the corresponding change in the frequency of oscillation is

relatively small and the assumption of a constant synchronizing coefficient is valid. It can also be seen from Figure (3.2) that second-order approximation is fairly good, especially in the practical range of the damping torque coefficient variation.

3.4.2 Simplified Single Machine-Infinite Bus With Static Exciter

In this example, eigenvalue and eigenvalue sensitivity techniques are employed to examine the effect of static exciter parameters on the dynamic stability of a steam unit connected to an infinite bus through a transmission line. A single line diagram of the system is shown in Figure (3.3). The system data are obtained directly from reference [6]. Under small perturbations, the system can be represented by the simple block diagram shown in Figure (3.4). This model neglects the effect of damper windings, stator resistance, flux derivatives and governor action. The block diagram model, in spite of its simplicity, has been used by many authors [6], [19] to analyse and design machine excitation systems under a variety of conditions. The block diagram coefficients (K_1 - K_6) are functions of the machine and tie line parameters and the system operating conditions. The values of these coefficients, as obtained

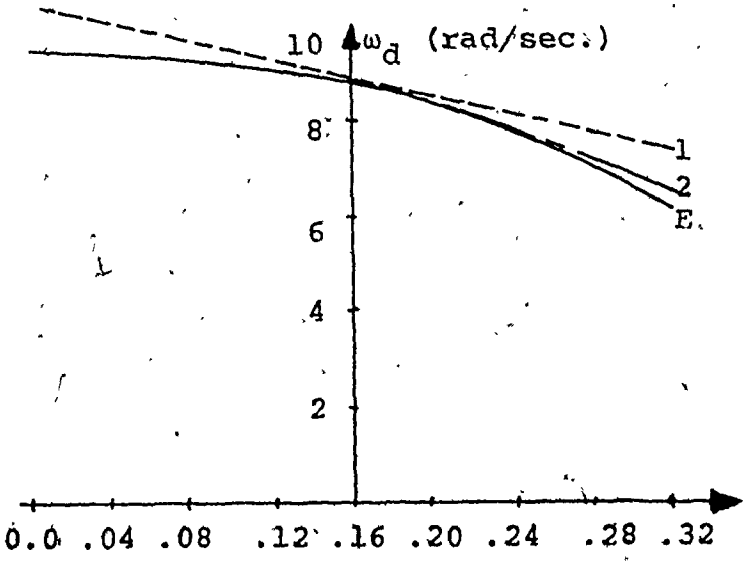

Figure 3.2 ω_d vs the Damping Coefficient D

------ 1st-Order Estimate

—— - —— 2nd-Order Estimate

——— Exact value

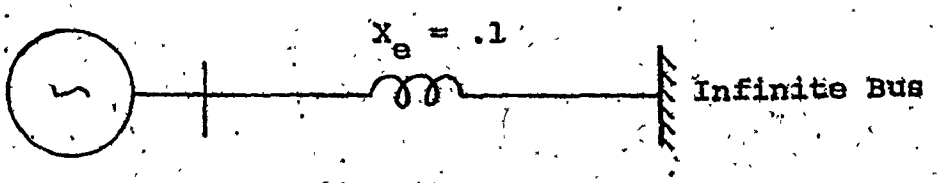

Figure 3.3 Single Machine-Infinite Bus Configuration

$H = 1.5$ sec. , $X_d = 1.6$, $X'_d = .32$

$X_q = 1.55$, $T'_{do} = 6$ sec.

$P_G = 1.0$, $Q_G = .5$ p.u.

in [6], are given in Figure (3.4).

The system equations are arranged in state-space form and system eigenvalues as well as their sensitivities with respect to exciter gain (K_e) and time constant (τ_e) are listed in Table (3.2).

Eigenvalue sensitivities are then used to obtain estimates for the movement of system eigenvalues around the base case. These estimates as compared to the exact movement are illustrated in Figures (3.5) and (3.6). It is apparent from these figures that, in general, the second-order estimates are significantly better than the first-order estimates, and are never worse. This is specifically true for up to a 100% change in the parameters considered.

3.5 Practical Limitations

It has been stated at the beginning of this Chapter that the eigenvalue sensitivity expressions, as developed, are only valid for systems of non-repeated eigenvalues. This is usually true for large power systems. However, if identical eigenvalues occur, the base case parameters can be modified slightly so that the method can be applied. Eigenvalue first and second-order sensitivities have been calculated for relatively large power systems [117], [119] and no difficulty has been experienced in obtaining the sensitivity coefficients, even though some of the eigen-

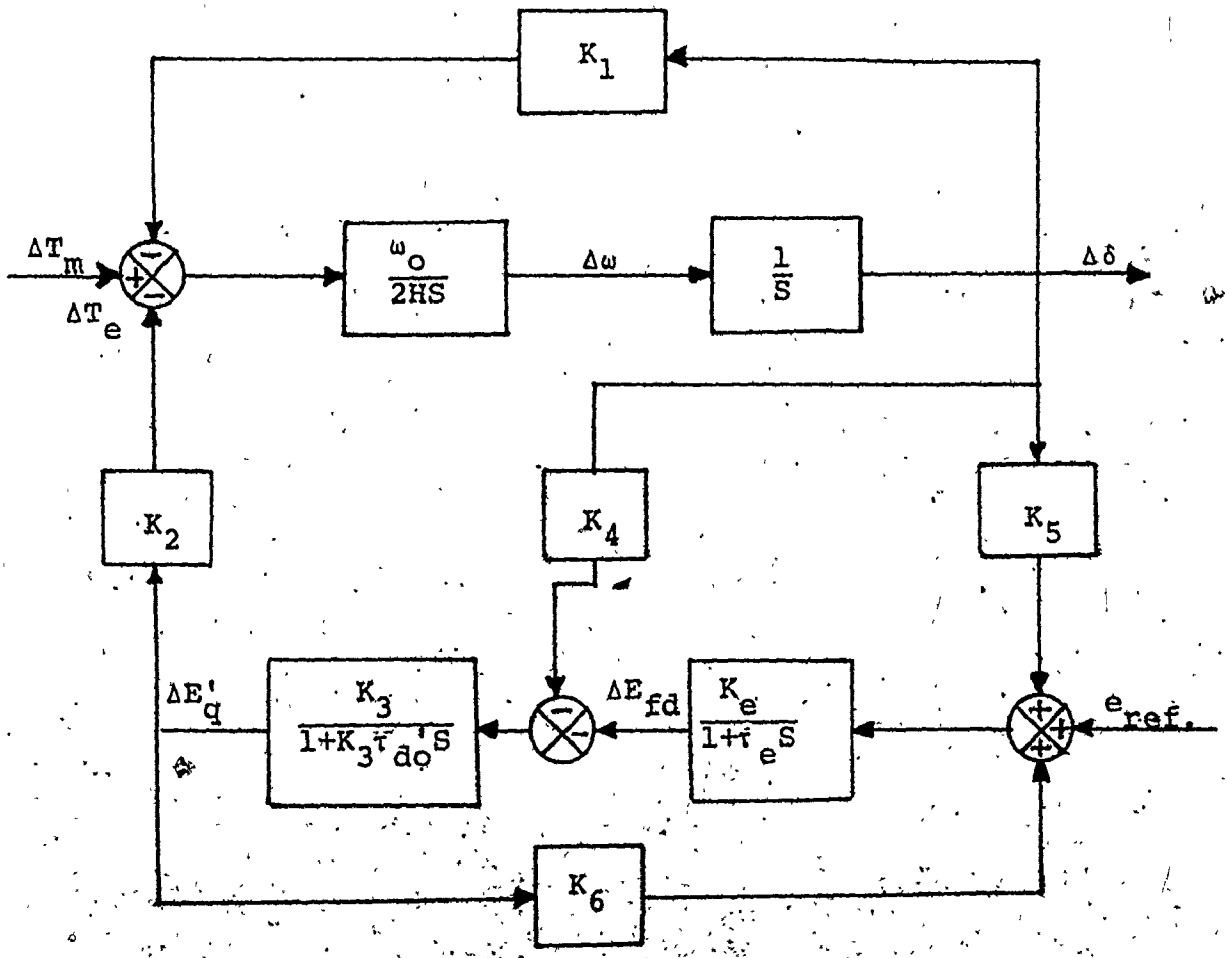

Figure 3.4 : Block Diagram Representation of Single Machine-Infinite Bus

$K_1 = 1.01$, $K_2 = 1.149$, $1/K_3 = 2.78$

$K_4 = 1.47$, $K_5 = -.097$, $K_6 = .419$

$K_e = 25$, $T_e = .05$ sec.

Table 3.2 Eigenvalue and Eigenvalue Normalized Sensitivities For 4th-Order System

n	λ	K_e		τ_e	
		$\lambda_n^{\cdot}$	$\lambda_n^{\cdot\cdot}$	$\lambda_n^{\cdot}$	$\lambda_n^{\cdot\cdot}$
1	-2.724	-2.923	-.484	-.461	-.175
2	-17.851	2.482	.443	20.619	-19.779
3	.056±j11.170	.220∓j.063	.020±j.036	-.079∓j.078	-.023±j.052

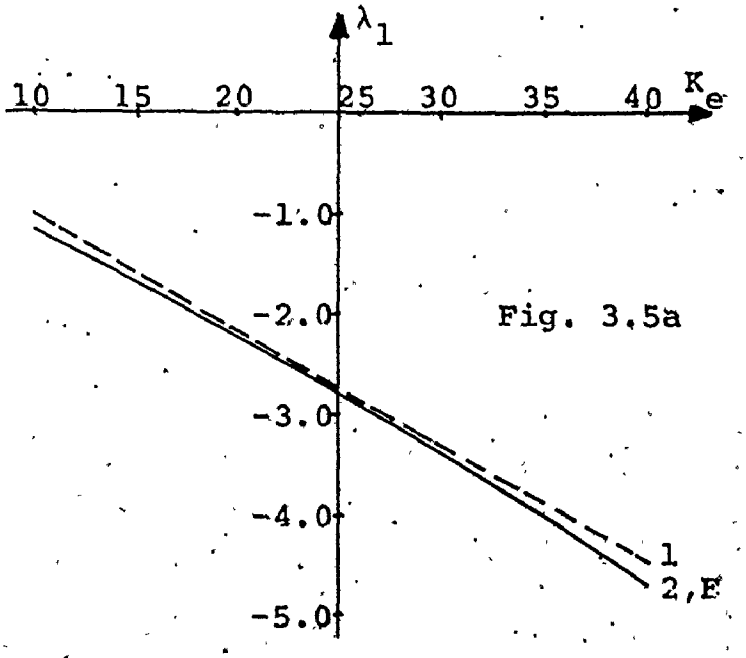

Fig. 3.5a

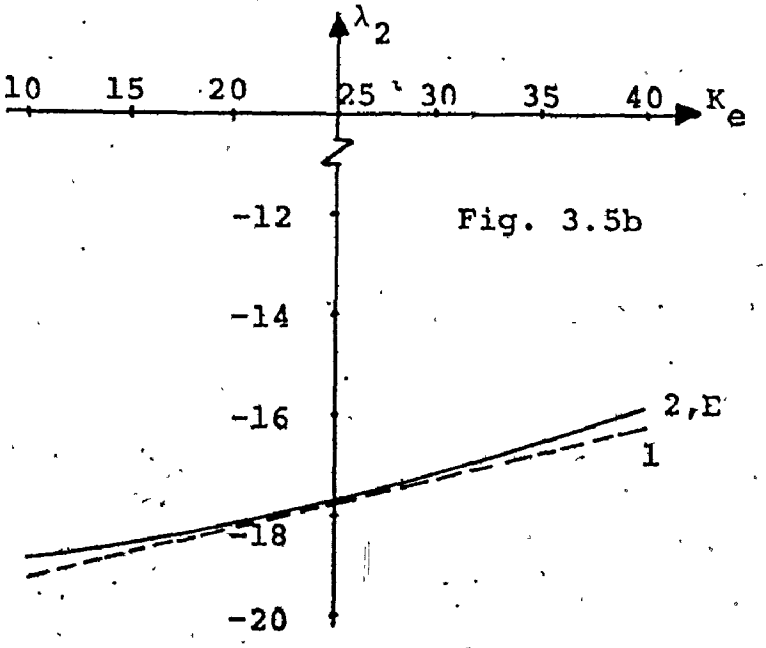

Fig. 3.5b

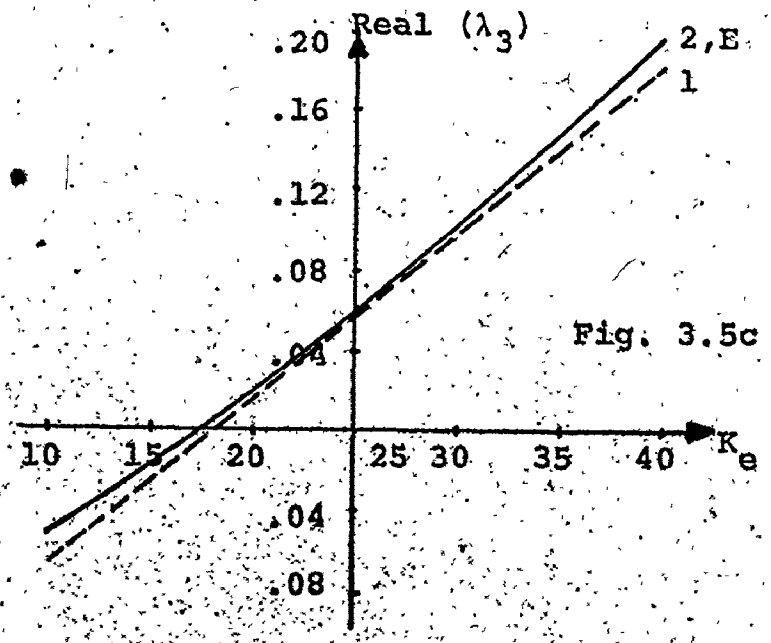

Fig. 3.5c

Figure 3.5 Eigenvalue Movement vs Machine Exciter Gain K_e

--------1st-Order Estimate

————2nd-Order Estimate

————Exact value

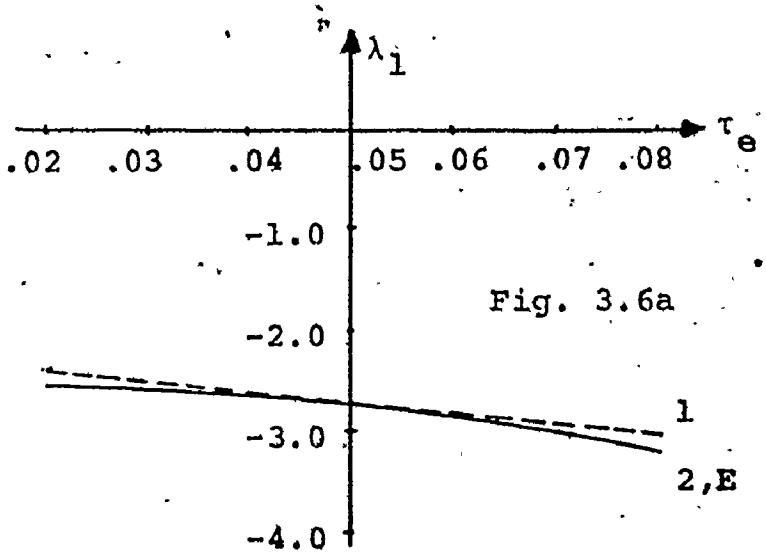

Fig. 3.6a

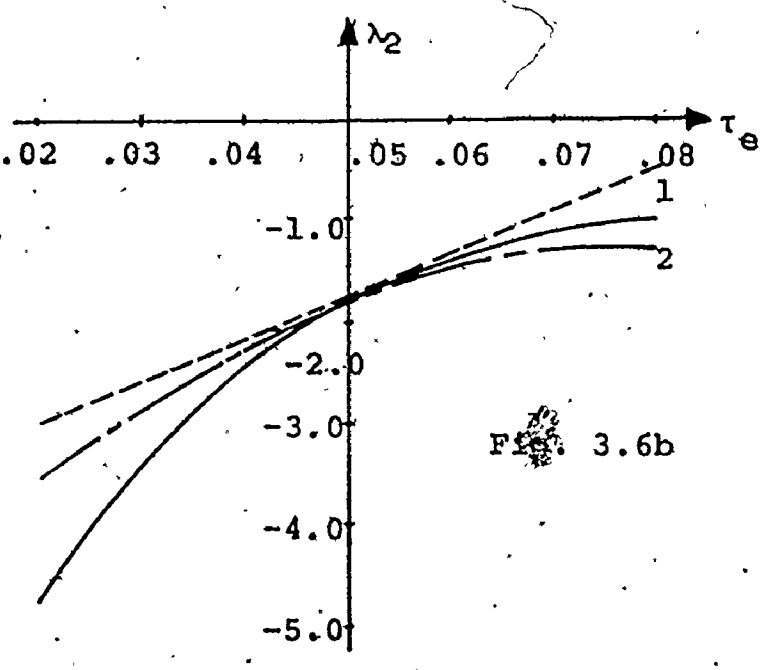

Fig. 3.6b

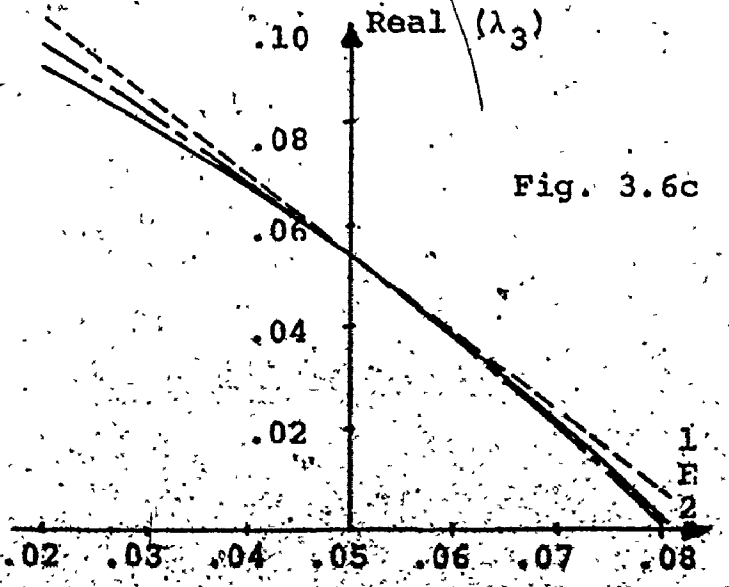

Fig. 3.6c

Figure 3.6: Eigenvalue Movement vs Machine Exciter Time Constant τ_e

——————1st-Order Estimate

——————2nd-Order Estimate

——————Exact Value

values were very close, since the difference was in the second decimal place for base eigenvalues of magnitudes in the order of ten [119].

The eigenvalue sensitivity approach can be used to examine the critical roots and then to adjust the design parameters in such a way as to achieve stability improvement. Recalling the sensitivity expressions, it can be noticed that they are functions of the base values. Therefore, the sensitivities will change as a consequence of any parameter change. Consequently, the design procedure reduces to a step by step optimization search so that the process is repeated and after a few iterations the most convenient parameter setting can be chosen. The process should also be repeated over a practical range of operating conditions.

This approach is very convenient for relatively large systems, especially if interactive computation is used, since it provides the engineer with a good feel for the effect of different parameter selection on the stability of the different loops in the system. However, the choice of the appropriate set of parameters (using the sensitivity approach) should be justified by examining the large disturbance performance of the system so that the effect of nonlinearities can be taken into consideration.

The employment of the eigenvalue sensitivity

techniques is efficient in the analysis of large scale power system dynamics. It is important to realize however, that there is always a limit to the order of systems that can be handled by this method. This limit depends on ,the size of the available memory of the computer under use. However, a relatively large portion of the matrices involved in the eigenvalue sensitivity computation are extremely sparse so that the limit on system order can be extended by employing sparse-matrix techniques.

3.6 Summary

The development and use of first and second-order eigenvalue sensitivities have been presented. The eigenvalue sensitivity coefficients are given in terms of system parameters rather than system matrix entries. This allows greater flexibility and convenience in the analysis of large scale power systems, especially, with the use of interactive computation.

Two simplified examples have been considered to illustrate the applicability of the method. The inclusion of second-order terms in an eigenvalue sensitivity package is recommended since the additional computation cost is relatively small compared to the improvement in efficiency of the sensitivity package and its attendent use in eigenvalue analysis.

Chapter 4

EIGENVALUE ESTIMATION AND TRACKING

4.1 Introduction

In the previous chapter it was stated that dynamic stability evaluation of interconnected power systems through eigenvalue location and movement is attractive because it is far more efficient than the alternative of time integration to predict system time response. In the analysis of such large systems, one is usually interested in tracking the movement of a small number of eigenvalues under specific parameter variation. This small subset can, generally, include eigenvalues with different magnitudes spread all over the complete eigenvalue pattern.

In the literature one can find a method like the Power method [108], [109] that provides a well established algorithm to find selected eigenvalues in the upper or lower range of the whole eigenvalue pattern. Unfortunately, this method is only useful if it is required to compute the few largest or smallest eigenvalues of a general matrix, but not any of the middle ones. Hence, the application of the Power method is limited to some particular problems [109] and it is not suitable for our purpose. On the other hand, it is

inefficient to recompute the complete set of eigenvalues for every parameter selection, especially with relatively large systems and many parameter changes.

As an alternative approach, this Chapter describes a highly efficient computer based procedure for determining system dynamic stability as a function of system parameters. The method is particularly applicable in situations where a relatively small number of the system eigenvalues are known to be critical in describing stability. A full set of eigenvalues and eigenvectors is determined once, as a base case, then the movement of these critical eigenvalues is tracked over relatively wide parameter variations without the need to recompute the whole set of eigenvalues or eigenvectors. The new values are estimated using first and second-order eigenvalue sensitivity terms followed by an iterative technique to refine the estimate.

The expressions developed for the eigenvalue sensitivity terms in the previous Chapter form the basis for the proposed method. The inverse iteration method developed by Wilkinson [108] and the modification developed by Van Ness [111] were primarily concerned with finding of system eigenvectors. These eigenvectors are insensitive to small errors in the corresponding eigenvalues. This method is used here to find accurate eigenvalues with the corresponding eigenvectors for different parameter settings.

Section 4.2 describes the estimation procedure of the eigenvalue movement and outlines the overall "tracking" approach. In Section 4.3 the procedure of refining the estimates of eigenvalue movement is developed. The procedure is divided into two steps: first to calculate an accurate eigenvector using the inverse iteration technique, and second to use this eigenvector to obtain an accurate value for the corresponding eigenvalue.

The use of the method is discussed in Section 4.4. Real and complex eigenvalues are considered and the computational aspects associated with both situations are studied. The convergence properties of the method under practical situations are considered. Finally the computational efficiency of the proposed approach as compared with the repeated eigenvalue approach is discussed.

The practical limitations of the method as applied to the analysis of power system dynamic stability are discussed in Section 4.5.

A summary of the overall approach and its practical use is presented in Section 4.6.

4.2 Eigenvalue Tracking Approach

In this method the first and second-order sensitivities of the system eigenvalues with respect to a specific parameter are computed at a certain base condition. Then,

the corresponding second-order approximation μ_i due to a change $\Delta\xi$ in a system parameter ξ is obtained using Taylor series expansion around the base condition as:

$$\mu_i = \lambda_{io} + \frac{\partial \lambda_i}{\partial \xi}_{\xi_o} (\Delta\xi) + \frac{1}{2} \frac{\partial^2 \lambda_i}{\partial \xi^2}_{\xi_o} (\Delta\xi)^2 \qquad (4.1)$$

Examining the results obtained for the examples studied in Section 3.4 and for further systems analysed in Chapter 6, it can be seen that second-order estimates are satisfactory for relatively wide parameter changes (up to 50% change in a system parameter on both sides of the base value). For a wider change in the parameter, or where the second-order approximation is inaccurate, the inverse iteration technique is used to converge to the exact eigenvector and the corresponding eigenvalue with the estimated values as the starting guess.

Thus, the tracking approach for the movement of the eigenvalues of interest can be summarized in the following steps:

1. Compute the system eigenvalues, and the normal and transposed eigenvectors at the base condition.
2. Compute first and second-order sensitivities of the eigenvalues with respect to system parameters of interest.
3. Considering a specific parameter, identify the subset of sensitive eigenvalues and choose the one(s) to be

tracked over different settings of the parameter.

4. Estimate the new eigenvalue location due to a specific change in the parameter (using Taylor series expansion and first and second-order sensitivity terms at the base case).

5. If an accurate value for the eigenvalue of interest is required at the new parameter setting, the estimated value can be used with the updated system matrix to compute the exact value (using the inverse iteration technique).

Usually, at the beginning of the tracking, second-order approximation is obtained followed by inverse iteration and eigenvalue computation at the lower and upper limits of the parameter settings. If the difference between the estimated and the exact eigenvalues is relatively large, the operation should be repeated at some point closer to the base value until there is no significant difference. Hence, all the closer points to the base value are obtained using only second-order estimates.

4.3 Refinement of Estimation

The error in the estimated value of a specific eigenvalue shift due to a parameter change ($\Delta\xi$), using equation (4.1), is proportional to $(\Delta\xi)^3$. Consequently, μ_i is a good approximation to the exact value, especially for a

relatively small per unit change in the parameter ξ. If a more accurate value is desired, the eigenvalue estimation μ_i can be refined using the inverse iteration method to find the exact eigenvector. This eigenvector can then be used to find the corresponding accurate eigenvalue under the new parameter setting.

4.3.1 The Inverse Iteration Method

The basic inverse iteration method, as developed by Wilkinson [108], is described by the following two equations:

$$[A - \mu_i I]\, \underset{\sim}{W}_{s+1} = \underset{\sim}{x}_s \qquad (4.2)$$

$$\underset{\sim}{X}_{s+1} = \frac{\underset{\sim}{W}_{s+1}}{\max(w_{s+1})} \qquad (4.3)$$

where:

μ_i = the estimated value of λ_i

$\max(w_{s+1})$ = the element of $\underset{\sim}{W}_{s+1}$ with the largest magnitude

$\underset{\sim}{X}_o$ = the initial value of $\underset{\sim}{X}$

$\underset{\sim}{X}_{s+1}$ = the current estimate of the desired eigenvector corresponding to λ_i

The iteration process is terminated when no further significant improvement can be achieved in $\underset{\sim}{X}$. To prove the convergence of the method, first consider the iterative scheme as in equation (4.2) without applying the normalization process in equation (4.3).

$$\underset{\sim}{W}_{s+1} = [A - \mu_i I]^{-1} \underset{\sim}{X}_s \tag{4.4}$$

For systems with non-repeated eigenvalues, the arbitrary vector $\underset{\sim}{X}_o$ can be expressed as a linear combination of the system eigenvectors as in equation (3.8) so that:

$$\underset{\sim}{X}_o = \sum_{r=1}^{ns} \alpha_r \underset{\sim}{z}_r \tag{4.5}$$

Expanding equation (4.4) we obtain:

$$\underset{\sim}{W}_{s+1} = [A - \mu_i I]^{-1} \underset{\sim}{X}_s = \{[A - \mu_i I]^{-1}\}^2 \underset{\sim}{X}_{s-1}$$

$$= \ldots\ldots\ldots = \{[A - \mu_i I]^{-1}\}^{(s+1)} \underset{\sim}{X}_o \tag{4.6}$$

Combining equations (4.5) and (4.6) yields:

$$\underset{\sim}{W}_{s+1} = \sum_{r=1}^{ns} \alpha_r (\lambda_r - \mu_i)^{-(s+1)} \underset{\sim}{z}_r \tag{4.7}$$

or

$$\underset{\sim}{W}_{s+1} = \frac{\alpha_i \underset{\sim}{z}_i}{(\lambda_i - \mu_i)^{s+1}} + \sum_{\substack{r=1 \\ \neq i}}^{ns} \frac{\alpha_r \underset{\sim}{z}_r}{(\lambda_r - \mu_i)^{s+1}} \tag{4.8}$$

If μ_i is a good estimate to λ_i so that the factor $(\lambda_i - \mu_i)$ is smaller in magnitude than any other factor $(\lambda_r - \mu_i)$, and if α_i is not zero, the process will ultimately reduce to:

$$\underset{\sim}{W}_{s+1} = \frac{\alpha_i \underset{\sim}{z}_i}{(\lambda_i - \mu_i)^{(s+1)}} + \underset{\sim}{\epsilon}^{(s+1)} \qquad (4.9)$$

where $\underset{\sim}{\epsilon}^{(s+1)}$ is a vector with very small components compared to the corresponding components of $\underset{\sim}{W}_{s+1}$.

The difference between the estimated and the exact eigenvalues is usually small. Therefore, each successive vector in the iteration process is normalized, as in equation (4.3), in order to keep numbers within range. Since any eigenvector can be divided or multiplied by an arbitrary constant and still be an eigenvector, the normalization process as described earlier does not, basically, affect the convergence of the method.

4.3.2 Calculation of Correct Eigenvalues

Examining equation (4.8), it can be seen that the computed eigenvector does not depend on the error in the estimation of the corresponding eigenvalue. It is also apparent that the eigenvector can be obtained as accurately as necessary depending on the chosen error allowance to terminate the iterative process. Thus, the calculated eigenvector can be used in either one of the following two methods to obtain the correct eigenvalue.

1. Rayliegh Quotient: This method gives the desired eigenvalue in terms of the updated system coefficient matrix [A] and the corresponding correct eigenvector $\underset{\sim}{z}_i$ as:

$$\lambda_i = \frac{\underset{\sim}{z}_i^t [A] \underset{\sim}{z}_i}{\underset{\sim}{z}_i^t \underset{\sim}{z}_i} \qquad (4.10)$$

2. Residual Correction: Recalling equation (4.8), the dominant term on the right corresponds finally to the value $(\lambda_i - \mu_i)$. This quantity is ultimately the ratio of the components of the vector $\underset{\sim}{W}_s$ to those of $\underset{\sim}{W}_{s+1}$. In the normalization process the element of the eigenvector current estimate with the largest magnitude is set to unity at every iteration. Hence, after the process converges to the correct eigenvector, the reciprocal of the largest component is the current estimate of $(\lambda_i - \mu_i)$ and thus, the desired eigenvalue is obtained as:

$$\lambda_i = \mu_i + 1/\max(w_{s+1}) \qquad (4.11)$$

Both methods have been used and the results obtained in Section 6.4 are in agreement with the direct repeated eigenvalue computations.

4.4 Use of The Method

The use of the inverse iteration method involves the iterative solution of the set of linear equations (4.2). In practice, it is inefficient to solve this set of equations by inverting the matrix $[A - \mu_i I]$, but better to solve successively with the same left-hand side matrix but with different right-hand sides. This can be achieved by

performing LU-factorization [108] of the matrix $[A - \mu_i I]$.

4.4.1 Real Eigenvalues

In tracking the movement of a real eigenvalue the estimate μ_i is also real and the iterative solution of equation (4.2) involves the LU-factorization of the real matrix $[A - \mu_i I]$. A standard Gaussian elimination method with row interchange is used. This process can be described as in [108] and [111] as follows:

$$[K]\ [A - \mu_i I] = [L]\ [U] \qquad (4.12)$$

where [K] is a matrix containing information about the row interchange. This matrix is never stored, but the information contained in [K] is kept in a table. [L] is a lower triangular matrix with all diagonal elements equal to unity, and [U] is an upper triangular matrix.

Forward and backward substitution is then used to solve for $\underset{\sim}{W}_{s+1}$ as in [111]. The solution is described by the following two equations:

$$[L]\ \underset{\sim}{b} = [K]\ \underset{\sim}{X} \qquad (4.13)$$

$$[U]\ \underset{\sim}{W}_{s+1} = \underset{\sim}{b} \qquad (4.14)$$

where $\underline{b}$ is an ns-dimentional vector.

The basic criterion for convergence is that the estimated eigenvalue μ_i is closer to the exact eigenvalue λ_i than any other eigenvalue λ_j. As the estimate μ_i approaches the exact value λ_i, the matrix $[A - \mu_i I]$ becomes ill-conditioned. This matrix is singular under the limiting case of μ_i identical to λ_i and hence, the last diagonal element in the [U] matrix will be zero [111].

Actually, this situation seldom occurs with the use of the "tracking" approach since our estimate μ_i is only a second-order approximation of λ_i in addition to the effect of round-off errors involved in the computational procedure. If the corresponding eigenvector is needed, as well, the zero element in the [U] matrix can be taken as a very small number, such as 2^{-t} in a t-digit decimal computer, and we proceed in the solution as described before. This has been suggested in [109] and has been successfully used in [111].

4.4.2 Complex Eigenvalues

If the eigenvalues of interest are complex, the tracking method, as outlined in the previous section, is still valid. However, some difficulties will arise such that the storage requirement will be doubled and also the computation time will increase because of the complex arithmetic operations involved. Wilkinson [108] has

proposed four different methods to overcome these difficulties. His fourth method has been used by Van Ness [111] and it will be used here as well.

Let μ_i be replaced by $(\alpha + j\,\beta)$, $\underset{\sim}{X}$ be $\underset{\sim}{Q} + j\underset{\sim}{R}$ and $\underset{\sim}{W}$ be $\underset{\sim}{M} + j\underset{\sim}{N}$. Solving for the real and imaginary parts of equation (4.2) gives:

$$[(A - \alpha I)^2 + \beta^2 I]\, \underset{\sim}{N}_{s+1} = \beta\, \underset{\sim}{Q}_s + [A - \alpha I]\, \underset{\sim}{R}_s \qquad (4.15)$$

$$-\beta\, \underset{\sim}{M}_{s+1} + [A - \alpha I]\, \underset{\sim}{N}_{s+1} = \underset{\sim}{R}_s \qquad (4.16)$$

Consequently, the iterative solution in this case involves the LU-factorization of the left hand matrix of equation (4.15) which has the same order as [A] following the squaring of the matrix $[A - \alpha I]$. The iteration requires the squaring of the matrix [A] only once. The solution is performed for equation (4.15) in the same way as for equation (4.2) in the real case. Then $\underset{\sim}{N}_{s+1}$ is used to obtain $\underset{\sim}{M}_{s+1}$ from equation (4.16).

If the eigenvalue is complex and the estimate is very close to the exact eigenvalue, more than one diagonal element in the [U] matrix can be very small or zero. In this case, these elements can be replaced by small numbers as described in 4.4.1 in order to obtain the desired eigenvectors.

4.4.3 Convergence Properties

The rate of convergence to the correct solution depends partly on the constants α_r in equation (4.8), but more effectively on the ratio of the factor $|\lambda_i - \mu_i|$ for the desired eigenvalue λ_i to each other factor for the remaining system eigenvalues. The smaller these ratios are, the faster will be the convergence.

The rate of convergence depends as well on the ratio $|\alpha_i/(\lambda_i - \mu_i)|$. If α_i is very small, the convergence will slow down. The limiting case is when α_i is zero, and the solution does not converge to the required eigenvector. In practice, we work with a fixed number of figures, and successive vectors are rounded, so that instead of producing exactly X_{s+1} from X_s we produce $X_{s+1} + \delta$ [109], where δ is a vector formed from the rounding errors. If this vector contains a non-zero multiple of z_i its effect will grow in later iterations and will ultimately be the dominant part of the vector. An example of this situation with detailed discussion is presented in reference [109].

In all the systems studied in preparing this thesis, the initial vector has been constantly chosen as one and no convergence problem has been experienced [119]. The method usually converges after three or four iterations.

The tracking approach is particularly useful for systems having well separated eigenvalues of interest. If

the eigenvalues being tracked are close, the convergence rate will be relatively slow since the first interfering root will be significantly close to the desired eigenvalue. It can also be noted that one should be careful in choosing the step size of the parameter change, since it is essential to have good estimates for the eigenvalue movement to start with, so that the method converges to the correct eigenvalue. This may require the computation of first-order sensitivity in an intermediate step. On the other hand, the repeated eigenvalue approach can provide the correct solution every time. However, apart from the expense, it will leave us with an identification problem since it will be very difficult to keep track of which eigenvalue is which unless the eigenvalue computations are repeated for very small incremental parameter changes. The tracking approach does not suffer from the identification problem since the calculation of the corresponding eigenvector and eigenvalue sensitivities provides useful information about incremental eigenvalue movement under specific parameter variations.

4.4 Comparison of the Computation Cost

Normally, when plotting eigenvalue movement, the complete set of eigenvalues and eigenvectors is obtained at an appropriate operating condition and first-order

sensitivities are obtained to aid in the choice of the appropriate step size of parameter change. Then, eigenvalue computation of the complete set can be repeated over a specified range of parameter variation. Unfortunately, using this method, the required computational time is prohibitive, especially for large systems.

A widely used algorithm for obtaining the eigenvalues of a general real matrix is the so called QR algorithm [108]. Using this algorithm, the system coefficient matrix [A] is first reduced to upper Hessenberg form by means of similarity transformations [108]. This reduction process (using the Householder method) involves approximately 5/3 ns^3 arithmetic operations [108] for a matrix of order ns. Each arithmetic operation equals one multiplication and one addition. The QR double step method [108] is a numerically stable technique to obtain all the eigenvalues (real and complex) for a real matrix. This technique uses an iterative process where each step of iteration involves $8ns^2$ arithmetic operations. The number of the required operations to obtain the whole system eigenvalues depends on the accuracy desired in the computed eigenvalues. For all program runs performed during the preparation of this thesis, it has been noticed that the time required for matrix reduction to upper Hessenberg form is relatively small compared to the computation time for all eigenvalues.

In other words, the iterative process in the QR method takes the majority of the computation time.

Table 4.1 Typical Execution Times of Eigenvalues and Eigenvectors

Matrix Order "n"	Time to compute Eigenvalues (sec.)	Time to compute Eigenvalue/eigenvector
10	.026	.989
30	7.867	16.686
50	31.368	69.221

To further illustrate how fast the amount of computation grows with system size, Table (4.1) lists the excution time for a CDC 6400 computer to compute the eigenvectors and/or eigenvalues for selected systems with various orders. A standard library subroutine has been used for the eigenvalue/eigenvector computations. This subroutine uses the QR double-step and Householder methods. These times demonstrate the fact that the amount of computation grows rapidly with the increase of the system order.

On the other hand, the only time required for the "tracking" approach, compared to eigenvalue repetition, is that involved in computing second-order sensitivities, LU-factorization of an ns^{th}-order matrix and the time to solve

iteratively an ns^{th}-order linear matrix equation. The number of arithmetic operations required to compute the second-order sensitivity of an eigenvalue with respect to a specific parameter is $(3\ ns^2 + ns)$. The number of arithmetic operations needed for factorizing a real matrix of order ns is $ns^3/3$ [108], and those required for solving the ns^{th}-order matrix equation are ns^2. Thus, for very large systems the number of arithmetic operations required for the tracking algorithm is approximately proportional to ns^3.

In order to compare the actual computational times of the proposed tracking approach to the repeated eigenvalue approach the following expressions are developed for the computation time of one base case and N additional evaluations in order to form a set of (N + 1) values. The expressions are given for both methods in terms of the computation time required for each step.

At the base condition the eigenvalues and the normal and transposed eigenvectors are needed as base data for eigenvalue sensitivity calculations. If the normal and transposed eigenvectors are normalized so that

$$\underset{\sim}{z}_i^t \underset{\sim}{v}_i = 1 \qquad (4.17)$$

and considering the fact:

$$\underset{\sim}{z}_i^t \underset{\sim}{v}_j = 0 \qquad \text{for all } i \neq j \qquad (4.18)$$

then, it follows that:

$$[\underset{\sim}{z}_1 \quad \underset{\sim}{z}_2 \quad \cdots \quad \underset{\sim}{z}_n]^{-1} = [\underset{\sim}{v}_1 \quad \underset{\sim}{v}_2 \quad \cdots \quad \underset{\sim}{v}_n]^t \qquad (4.19)$$

hence, the computation of the whole set of transposed eigenvectors involves the inversion of a complex matrix of order ns.

For repeated eigenvalue calculations the total computational time in seconds can be expressed as:

$$T_R = IV + 2 \times INV \times E \times p + IV \times N \times p \qquad (4.20)$$

where:

IV ≡ time to compute the complete eigenvalue set (sec.)

INV ≡ time to compute a normal or a transposed eigenvector by inverse iteration (sec.)

E ≡ number of eigenvalues whose movement we are specifically interested in

p ≡ number of parameters that we wish to study for eigenvalue movement.

If the time required to compute the base values for the repeated eigenvalue approach (normal and transposed eigenvectors corresponding to eigenvalues of interest) using the inverse iteration technique is greater than the time to obtain the complete set, the expression for T_R becomes:

$$T_R = IVC + IVT + IV \times N \times p \qquad (4.21)$$

where:

IVC ≡ time to compute the complete eigenvalue/eigenvector set (sec.)

IVT ≡ time to compute the whole set of transposed eigenvectors (sec.)

The corresponding expression for the computation time (T_T) using the tracking algorithm is:

$$T_T = IVC + IVT + I2 \times E \times p + INV \times N \times E \times p \quad (4.22)$$

where I2 is the time to compute each eigenvalue second-order sensitivity with respect to a specific parameter in seconds.

The expressions developed in equations (4.20)-(4.22) are used in Chapter 6 to compare the computation times for a simulated power system of order 50. It has been concluded that the fewer the number of eigenvalues of interest, compared to the total number of system eigenvalues, the greater the efficiency of the "tracking" method over the use of repeated eigenvalues. The time saving aslo depends on the number of parameters of interest; the greater their number the better the saving. In practical situations, one only needs to compute the sensitivities and track a small subset of the whole eigenvalue pattern (<10%). In this case the tracking method comprises about 20% of the time of the repeated eigenvalue computation method.

4.5 Practical Limitations

The approach presented for eigenvalue estimation and tracking is essentially based on the use of eigenvalue sensitivities to approximate the movements of selected eigenvalues under the variation of specific system parameters. Hence, the kind of practical limitations that have been discussed in Section 3.5 for the employment of eigenvalue sensitivities in power system studies are actually applied to the use of the proposed tracking method.

Second-order approximation is acceptable in practice for a parameter change of about one per unit (.5 p.u. change on each side of the base value) [116], [117], [119]. Consequently, the inverse iteration is only needed to be performed for, in general, less than 40% of the total points used to track eigenvalue movement over the practical range [119]. The computational efficiency of the proposed approach over the repeated eigenvalue approach can be easily predicted in cases where the effect of many parameters need to be studied. However, it should be mentioned that the tracking approach is particularly advantagous if the number of the critical eigenvalues is small (<20% of the total number of system eigenvalues). If it is required to study the movement of more than 50% of the total number of the eigenvalues, one would favour the use of the repeated eigenvalue method.

4.6 Summary

Eigenvalue tracking is a useful tool available to power engineers who wish to examine trends in system dynamic stability as some parameters of the system are changed. In this Chapter, an algorithm has been presented to track a small number of the total system eigenvalues. The use of this technique enhances the speed of computation in cases where the other eigenvalues are known to be insensitive to the changes being examined.

The use of the method in cases of real and complex eigenvalues has been described with a detailed discussion of the convergence properties of the method. The computational efficiency of the proposed method compared to the repeated eigenvalue method has been discussed and expressions given for the computation time for each of the two methods.

It has been concluded that the same practical limitations associated with the use of eigenvalue sensitivity techniques apply in the use of the tracking method in the analysis of power system dynamics.

Chapter 5

EFFECT OF LOAD CHARACTERISTICS ON POWER SYSTEM DYNAMIC STABILITY

5.1 Introduction

The effect of load characteristics is a significant part of the current interest in power system stability studies. This general interest has developed in recent years as stability margins have been reduced due to economic and environmental pressures. As developments have occurred in the representation and analysis of generation and transmission systems, attention is now being focused on the adequacy of load representation in the analysis programs. The incorporation of realistic load models is specifically important with the representation of generation controls which has made it essential to evaluate the contribution of all elements (including the loads) to system damping in order to obtain reasonable results [4].

In general, there are two aspects to the load problem. One is the examination of system data to determine the most appropriate model to use in subsequent studies. The other, the main concern in this Chapter, is the examination of possible interactions between the loads and generation controls and hence the investigation of the effect of a range of load models on system stability

evaluation. In the present analysis emphasis will be placed on the usual static representation of composite loads as function of bus voltage, but cases where dynamic representation is necessary will be briefly discussed. The family of load models considered in this study have been recommended by the IEEE Computer Analysis of Power Systems Working Group (CAPS) [2].

In order to apply this range of models, unlike the method presented in reference [43], the conceptual block diagram approach of deMello and Concordia [6] is extended to include the effect of static loads with different characteristics. Consequently, their effect on system stability is analysed through the evaluation of damping and synchronizing torques. The general conclusions reached in using the simplified block diagram model are then justified by considering a more detailed and accurate machine model.

In Section 5.2 the available information on load modeling in stability studies is briefly reviewed. The method of analysis is described in Section 5.3 and the effect of the range of models on system dynamic stability is investigated under the consideration of machine excitation and stabilization controls in Section 5.4.

Section 5.5 extends the analysis to include situations where composite loads are remote from the generation bus.

Finally, the important aspects relating the effect of loads and machine controls interaction on system dynamic stability are summarized in Section 5.6.

5.2 System Load Representation

The importance of load behaviour as a function of voltage in stability studies of power systems has been recognized long ago [33]. Even though, due to the lack of knowledge about the actual load behaviour, it was traditional to represent loads in stability studies as constant power, constant current or constant impedance elements. Recently, power system engineers have devoted much effort to the problem of realistic load modeling by performing and analysing actual field measurements [2], [3], [34]. The analytical approach of constructing accurate load models by analysing and combining the characteristics of each of the individual components of the load has also been considered [35]-[37].

The following is a review of the available information on load characteristics, mainly as a function of load bus voltage.

5.2.1 Dynamic Representation

Large industrial loads can, generally, include synchronous and asynchronous motors. These motors might

have significant inertial time constants compared to system generators. Hence, in some stability studies, it may be necessary to represent these loads with detailed dynamic modeling to the same extent that generation is modeled.

It has been mentioned in Chapter 2 that a synchronous motor can be represented by a generator model except that governor effects are neglected and the shaft system is modified to account for mechanical load dynamics.

The modeling of induction motor loads in dynamic and transient stability studies is the subject of many papers [39]-[42]. Induction motor loads are usually numerous and scattered throughout the distribution network. Consequently, different approaches have been presented to construct dynamical equivalents for asynchronous motor groups in stability studies [41], [42].

The mathematical equations describing the performance of a single induction motor can be arranged with reference to a synchronously rotating frame (D, Q) as:

$$\underset{\sim}{v} = [R]\ \underset{\sim}{i} + \frac{1}{\omega_o}\ [X]\ \dot{\underset{\sim}{i}} + [G]\ \underset{\sim}{i} \tag{5.1}$$

$$\frac{2Hm}{\omega_o}\ \dot{\omega}_r + D\ \omega_r + T_m = T_e \tag{5.2}$$

$$T_e = X_{sr}\ (i_{rD}\ i_{sQ} - i_{rQ}\ i_{sD}) \tag{5.3}$$

where the stator-rotor voltage component vector is:

$$\underset{\sim}{v} \triangleq [v_{sD},\ v_{sQ},\ v_{rD},\ v_{rQ}]^t,$$

the stator-rotor current component vector is:

$$\underset{\sim}{i} \triangleq [i_{sD},\ i_{sQ},\ i_{rD},\ i_{rQ}]^t,$$

the stator-rotor resistance matrix is:

$$[R] \triangleq \text{diag}\ [r_s,\ r_s,\ r_r,\ r_r],$$

the motor reactance matrix is:

$$[X] = \begin{bmatrix} X_s & 0 & X_{sr} & 0 \\ 0 & X_s & 0 & X_{sr} \\ X_{sr} & 0 & X_r & 0 \\ 0 & X_{sr} & 0 & X_r \end{bmatrix}$$

and

$$[G] = \begin{bmatrix} 0 & -X_s & 0 & -X_{sr} \\ X_s & 0 & X_{sr} & 0 \\ 0 & -X_{sr}(\omega_o-\omega_r) & 0 & -X_r(\omega_o-\omega_r) \\ X_{sr}(\omega_o-\omega_r) & 0 & X_r(\omega_o-\omega_r) & 0 \end{bmatrix}$$

T_e is the electrical torque and T_m is the mechanical shaft torque, ω_o is the synchronous angular frequency and ω_r is the motor rotor speed (elec. rad/sec.). All the motor parameters in equations (5.1)-(5.3) are in per unit based on the induction motor ratings.

It has been stated in reference [39] that induction motor stator transients usually have negligible effects in

power system stability studies and these transients can be disregarded by setting the derivatives of the stator flux terms to zero, i.e.

$$X_s \dot{i}_{sD} + X_{sr} \dot{i}_{rD} = 0$$
$$X_s \dot{i}_{sQ} + X_{sr} \dot{i}_{rQ} = 0 \qquad (5.4)$$

The above physical assumption results in a third-order model for an induction motor and can be used as in [41] to construct the dynamical equivalent of a group of induction motors.

5.2.2 Static Composite Load Representation

Searching through the available literature, one can find different static models that represent composite load characteristics as a function of load bus voltage. Some of these models have been developed based on actual field tests [2], [3] and others based on analytical methods [35]-[37]. The available models for composite loads, including dynamic load components with insignificant inertia, can be classified as follows:

1. Exponential Model: this model has been recommended by the IEEE working group [2]. The equations representing the relationship between load active and reactive power (P_ℓ, Q_ℓ) and load bus voltage v are:

$$P_\ell = C_1 v^{K_p}$$
$$Q_\ell = C_2 v^{K_q} \qquad (5.5)$$

where C_1 and C_2 are proportionality constants and K_p and K_q are the power-voltage sensitivity coefficients depending on the type of load. The coefficients K_p and K_q are usually obtained from approximating the curves representing the actual dynamic behaviour of the load.

The nonlinear load model given by equation (5.5) can represent the three load-voltage characteristics provided in most digital stability programs. The constant power model is obtained by setting the sensitivity coefficient to zero. If this coefficient is unity one obtains the constant current model, and the constant impedance model can be as easily obtained by setting $K_p=K_q=2$. Thus, the exponential load model is adequate in most transient and dynamic stability studies [11], [43], [44].

2. Polynomial Model: In this model the actual load power is expressed as a polynomial function in the load bus voltage as:

$$P_\ell = C_0 + C_1 v + C_2 v^2 + \ldots + C_n v^n \qquad (5.6)$$

with similar expression for Q_ℓ. This model has been suggested in reference [38] to account for the significant inertial effects in motor loads. A special case is the

quadratic function where only the first three terms in equation (5.6) are considered, the coefficients C_0, C_1 and C_2 are obtained from field tests. The quadratic function model as presented in reference [3] has been criticized due to the fact that it does not pass through a zero P_ℓ or Q_ℓ point for zero voltage. However, it is as acceptable as the exponential model for the range of voltages encountered during swings [2].

3. Incremental Model: This has been introduced by Berg et al [35], [36] and it offers both voltage and frequency dependence. The equations relating the incremental change in load power due to incremental changes in bus voltage and frequency (Δv, $\Delta \omega$) are:

$$\begin{bmatrix} \Delta P_\ell \\ \Delta Q_\ell \end{bmatrix} = \begin{bmatrix} \frac{\partial P_\ell}{\partial v} & \frac{\partial P_\ell}{\partial \omega} \\ \frac{\partial Q_\ell}{\partial v} & \frac{\partial Q_\ell}{\partial \omega} \end{bmatrix} \begin{bmatrix} \Delta v \\ \Delta \omega \end{bmatrix} \tag{5.7}$$

The incremental model is particularly suitable for dynamic stability studies. The sensitivity coefficient matrix in equation (5.7) can be obtained analytically for composite loads as in [35] and [37].

Throughout the analysis of possible interactions between system composite loads and machine excitation control, we will follow the recommendation of the IEEE working group [2] in utilizing a static model of the exponential form for composite load representation.

However, it should be noted that both the quadratic function and the incremental models (considering only voltage dependence) can just as easily be applied to the method of analysis if desired.

5.3 Method of Analysis

The analysis of load effects on synchronous machine dynamic stability and the investigation of possible interactions between system loads and machine excitation control can be achieved by either one of two methods. First is the use of the damping and synchronizing torque concepts. These are usually associated with the use of simplified, but sufficiently accurate, models. This method facilitates the derivation of simple expressions that can be used in turn to build up the basic concepts and to derive general conclusions concerning the interactions. Alternatively, eigenvalue and eigenvalue sensitivity techniques can be applied to study specific systems and hence the amount of detail desired can be incorporated in the system model. Consequently, this approach provides a good opportunity to justify the general conclusions that can be derived by using the simplified model.

Reference [43] details a state space system formulation incorporating a variety of load representations from dynamic induction motor models to static models of the

exponential form and constant impedance. The authors indicated that computational difficulties may arise in the calculation of the coefficient matrix with a "not very large" system. They also noted the difficulty in simplifying the order of their system.

The method presented here was developed in order to attempt such a simplification. In order to verify the suitability of the simplified block diagram model for this purpose, results have been compared by using a detailed generator model and the evaluation of system eigenvalue location and movement.

5.3.1 Block Diagram Representation

The investigation of load effects, through the evaluation of synchronizing and damping torque coefficients, is based on the well known block diagram approach of deMello and Concordia [6]. The system under study is shown in Figure (5.1). The generator is modeled with a constant prime mover power, no damper windings, no stator copper loss, and in addition, stator flux derivatives are neglected. The loads are modeled in the exponential form as indicated earlier. Under small perturbations, the system can be described by the block diagram in Figure (5.2). The

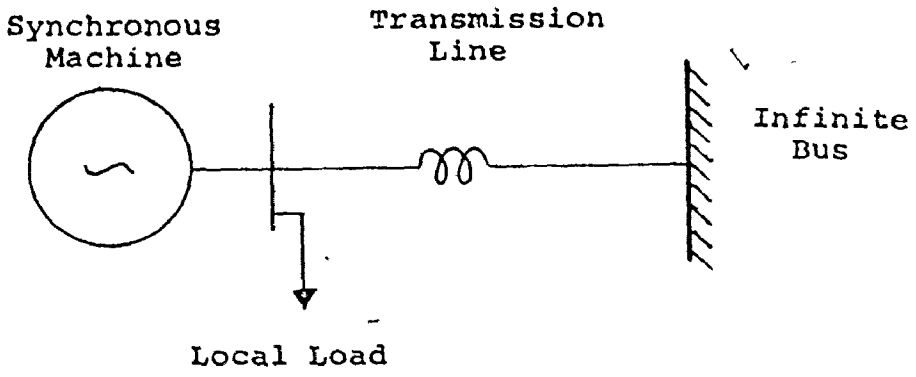

Figure 5.1 System Line Diagram

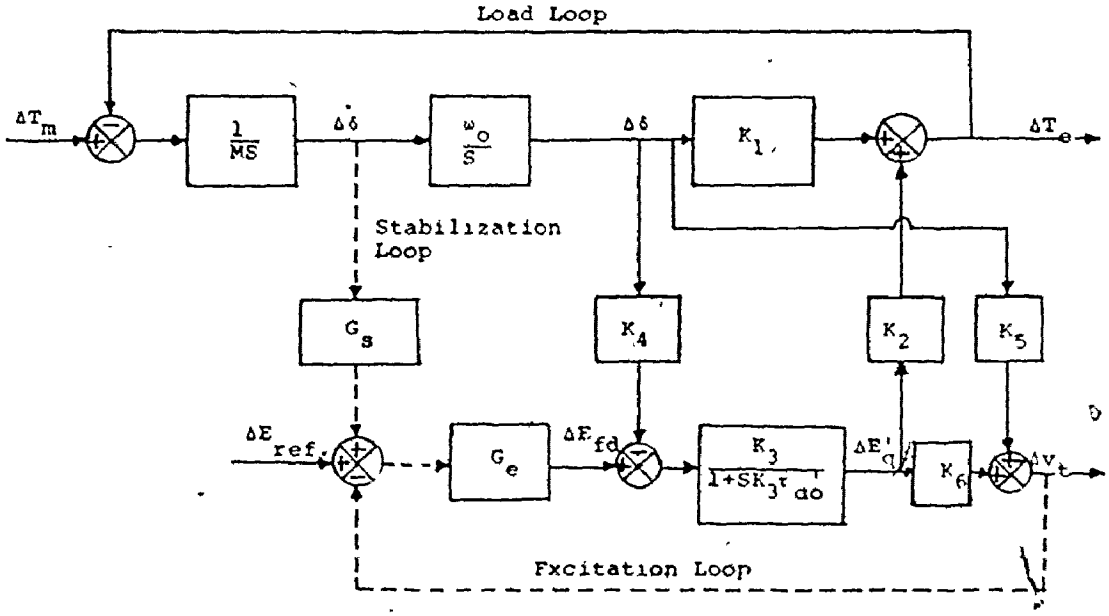

Figure 5.2 Simplified Block Diagram Model for System Under Study

coefficients K_1-K_6, which appear in the block diagram, relate the machine variables to each other at a particular operating condition. The dotted paths represent the additional signals coming through the machine static exciter and power system stabilizer. The block diagram coefficients are functions of the load point and system configuration as well as the load characteristics (K_p, K_q). For a constant impedance static load (K_p=K_q=2), the expressions for the coefficients K_1-K_6 are straight forward and well known [6]. If the load is nonlinear, this is no longer the case.

5.3.2 Derivation of Block Diagram Coefficients

Considering nonlinear static composite local loads, Figure (5.2) is unchanged but the expressions for the coefficients must be derived anew. The equations for the machine, network, and static load are given in Appendix C. The machine is represented with a third-order model as mentioned before. The linearized version of these equations as well as analytical expressions for K_5 and K_6 are also given. It may be seen that these expressions are cumbersome and complicated and do not permit the kind of simple interpretation that is the strength of the block diagram approach for linear load model. It is also noted that the other expressions have not been included because they are even more complicated and hence less useful.

The alternative approach is to obtain the coefficients numerically. The linearized equations are arranged in the PQR form as in equation (2.2) where:

the state vector is:

$$\underset{\sim}{x} = \Delta[E'_q,\ \omega,\ \delta]^t \tag{5.4}$$

the input vector is:

$$\underset{\sim}{u} = \Delta[E_{fd},\ T_m]^t \tag{5.5}$$

the output vector is:

$$\underset{\sim}{y} = \Delta[v_d, v_q, i_{dg}, i_{qg}, i_{fd}, E_q, T_e, v_t, i_{D\ell}, i_{Q\ell}, i_{DN}, i_{QN}, v_D, v_Q]^t \tag{5.6}$$

In a manner similar to that in Chapter 2, advantage is taken of the sparsity of the matrices [P], [Q] and [R]. The structure of these matrices is shown in Figure (5.3) using the notation: [////] is a matrix of non zero elements, and [ ] is a null matrix.

Using the procedure described in Chapter 2, the state space coefficient matrices can be obtained in a very straight forward manner. Again, the structure of these matrices is illustrated in Figure (5.4) using the same notation. Noting that:

$$\underset{\sim}{y} = [C]\ \underset{\sim}{x} \tag{5.7}$$

and

$$\Delta\delta \triangleq x(3) \quad , \quad \Delta T_e \triangleq y(7) \tag{5.8}$$

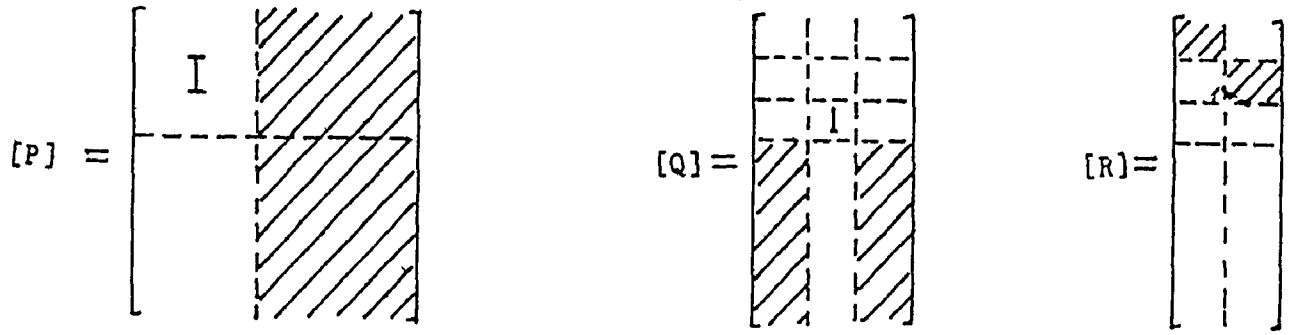

Figure 5.3 Structure of the P,Q,R Matrices

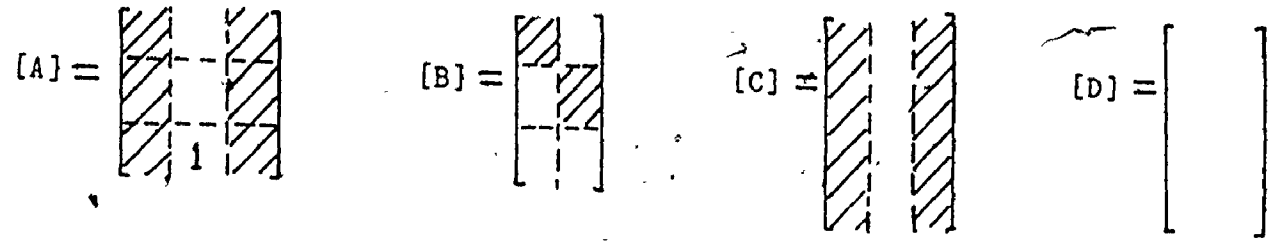

Figure 5.4 Structure of the A,B,C,D Matrices

and recalling the definition of $K_1 = \Delta T_e / \Delta \delta$ for E_q' constant yields the relationship:

$$K_1 = c\ (7,3) \tag{5.9}$$

In a similar manner one can obtain:

$$\begin{aligned} K_2 &= c\ (7,1) \\ K_3 &= -1\ /[T_{d0}'\ a(1,1)] \\ K_4 &= -T_{d0}'\ a(1,3) \\ K_5 &= c(8,3) \\ K_6 &= c(8,1) \end{aligned} \tag{5.10}$$

Thus, due to the independence of the output variables on machine rotor speed deviations, it is possible to obtain the coefficients in a very simple manner as indicated above. It is possible to check the algorithm by setting $K_p = K_q = 2$ and comparing with the original method of deMello and Concordia [6].

5.3.3 Effect of Load Characteristics on the Block Diagram Coefficients

The block diagram coefficients have been calculated for the system shown in Figure (5.1) and the variation of these coefficients with the change in load parameters (K_p, K_q), for a variety of generation and load conditions, have been plotted in Figures (5.5) and (5.6). Plots of those

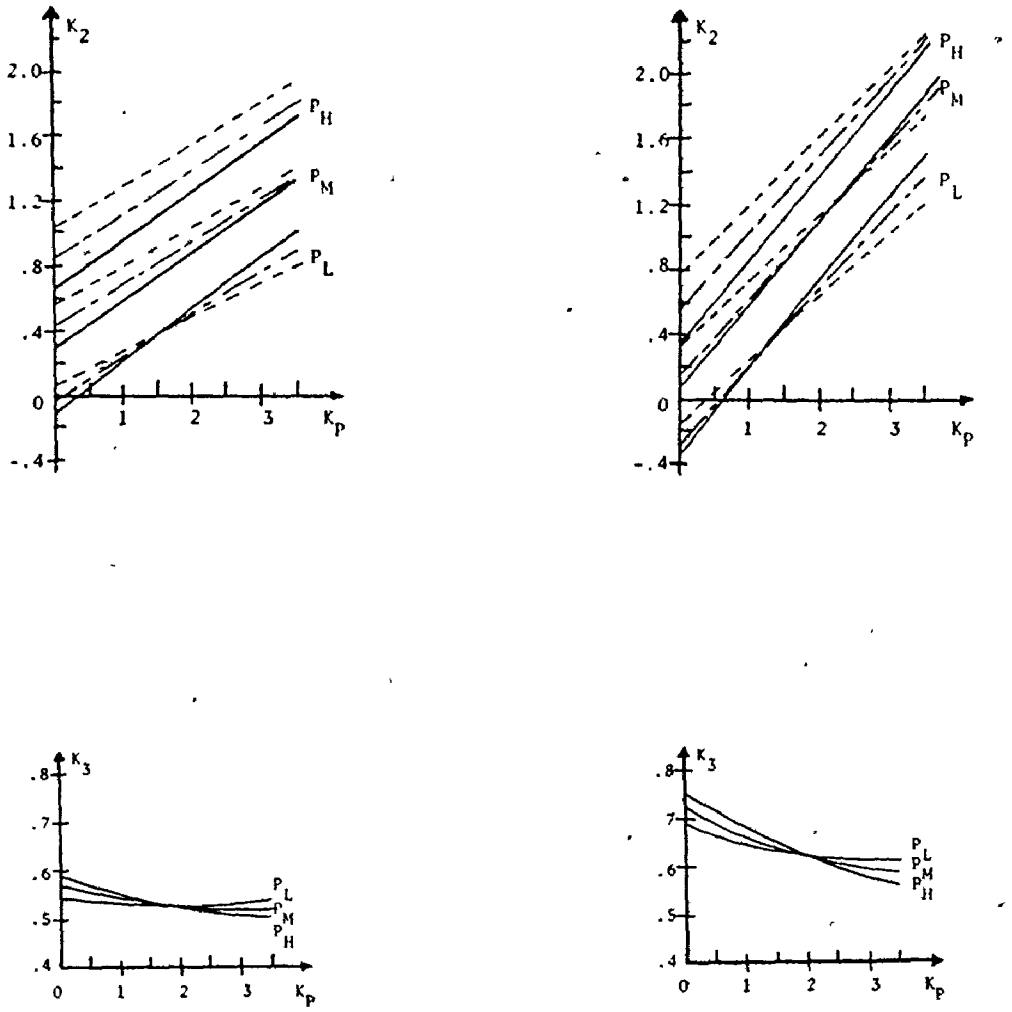

(a) Inductive Load (b) Capacitive Load

Figure 5.5 Coefficient Variation With K_p

Generation Levels In pu $P_H = 1$, $P_M = .6$, $P_L = .2$

Composite Load 1.25 pu, .8 pF

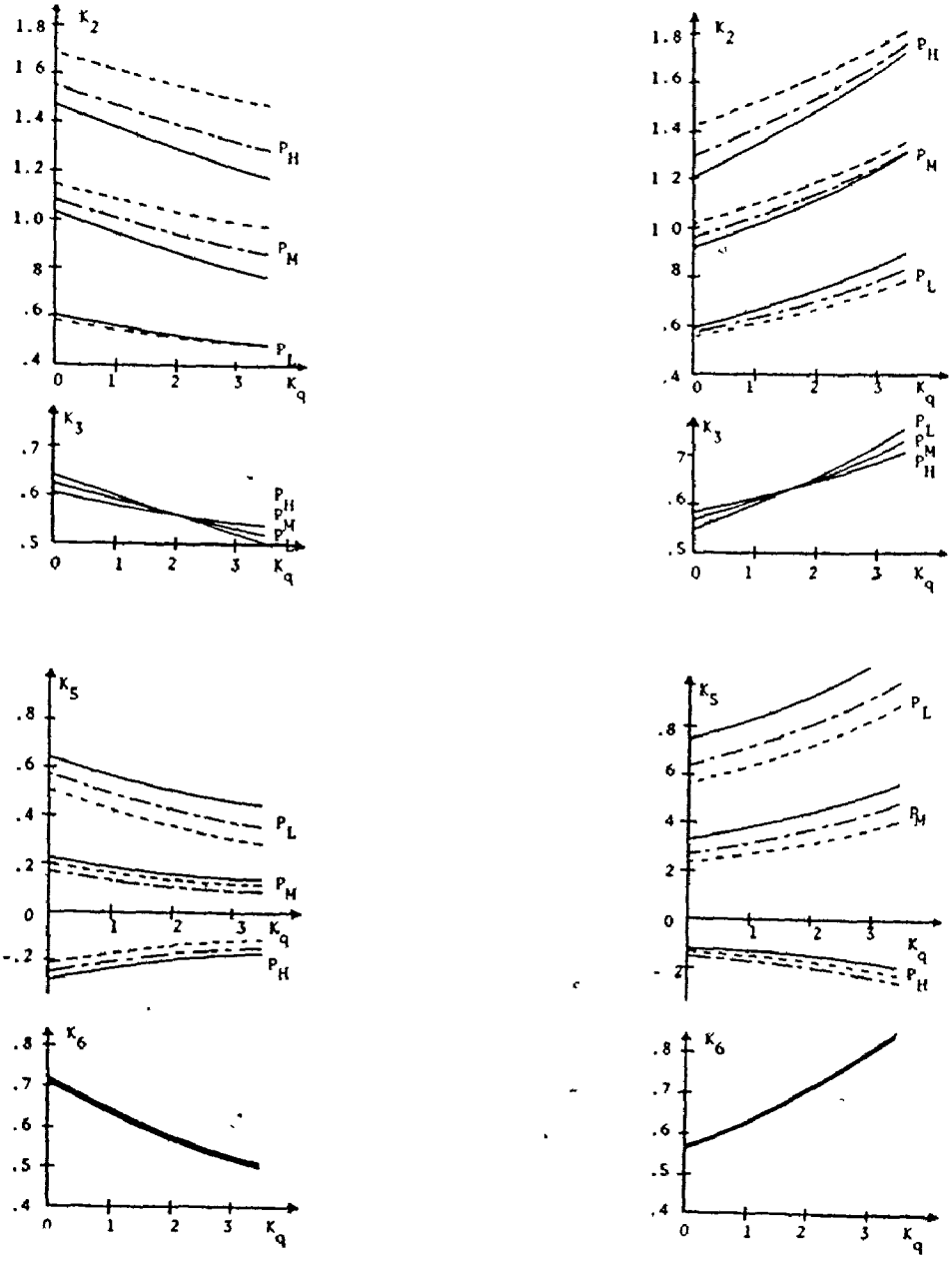

(a) Inductive Load

(b) Capacitive Load

Figure 5.6 Coefficient Variation With K_q

Generation and Load Conditions same as for Figure 5.5

coefficients which did not change more than 5% have been omitted.

Effect of MW-Sensitivity to voltage:

The variation of K_2 and K_3 versus the change in the load parameter K_p is illustrated in Figures (5.5.a) and (5.5.b) for a variety of generation and load. The other coefficients K_1 and K_4-K_6 do not change significantly with K_p. Typical values are noted in Appendix C.

Examining Figure (5.5.a), it can be noticed that the coefficient K_2 exibits large variation to changes in the load index K_p. This may be explained as follows.

In the system studied, the static composite load is supplied by two sources, the local hydro-electric machine connected directly to the load bus, and the remote infinite bus source which supplies the load through a transmission line reactance. If the load bus voltage varies, the load active power changes, the amount depending on the MW-voltage sensitivity (K_p). This change in demand power will be balanced by the two sources. If K_p is relatively large, the generator active power is required to change to a greater degree, causing larger electric torque variations which result in greater variation of K_2 with K_p.

Effect of MVAR-Sensitivity to Voltage:

The two important parameters changing with reactive power sensitivity (K_q) are K_5 and K_6. These represent,

respectively, the proportionality constants of the terminal voltage deviations due to changes in machine rotor angle and the voltage proportional to direct axis flux linkage. It can be seen from Figures (5.6.c) and (5.6.d) that there is quite a difference in the behaviour of these parameters with different local inductive or capacitive loads. These differences may be explained in the following way.

If, in the case of an inductive local load drawing reactive power, the sensitivity of this reactive power to voltage is high (K_q is high), and in the event that the terminal bus voltage decreases; the reactive power drawn by the load will also decrease. This has a damping effect on further voltage reduction due to the lower internal voltage drops caused by machine currents. This is illustrated by curve (a) in Figure (5.7). This means in turn that both K_5 and K_6 should decrease in magnitude with the increase in K_q.

If, we consider a reduction in the bus terminal voltage of a capacitive local load which delivers reactive power rather than absorbing it, the machine is required to supply additional reactive power, hence the internal voltage drops increase, causing a further decrease in terminal voltage as illustrated in curve (b). Curve (c) illustrates the effect with an inductive local load with zero sensitivity. In this case the damping effect on voltage swings is reduced and the variation is seen to be greater

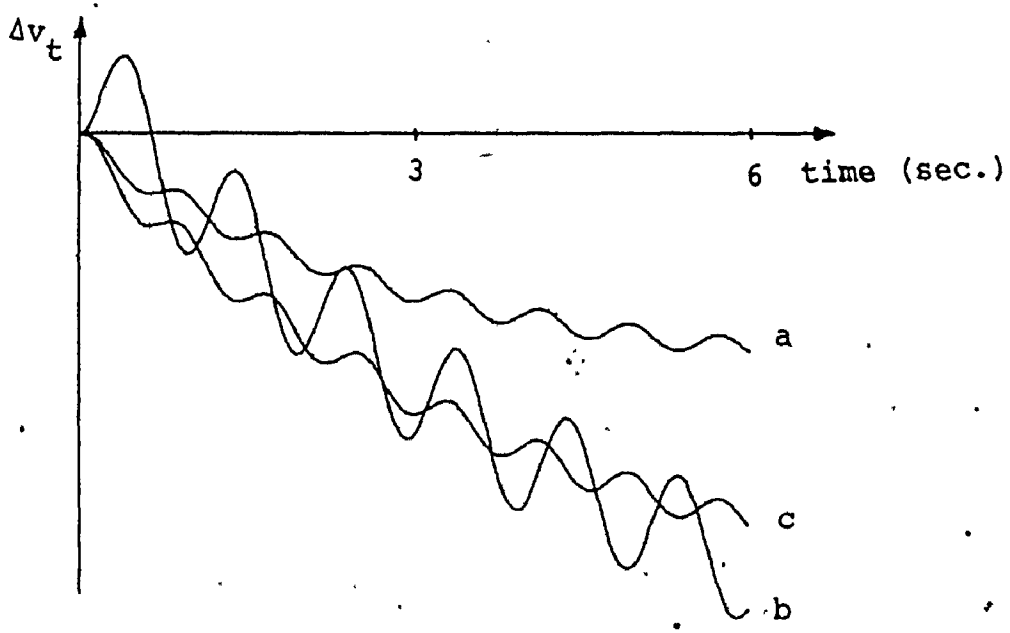

Figure 5.7 Voltage Swing Curves (Step Change in E_{fd})

than in curve (a).

To understand the behaviour of the coefficient K_2, we note that in the model chosen the machine is represented with a constant voltage behind a reactance. There is a cross-coupling between the generation of active and reactive power so that any increase in reactive power causes an increase in active power and hence torque and the coefficient K_2. Inductive and capacitive loads cause opposite effects in the internal voltage drop and thus it follows that K_2 increases with K_q for capacitive loads but decreases for inductive loads as shown in Figure (5.6.a).

5.4 Effect of Load Characteristics on System Stability

Dynamic stability prediction of the system under study is a function of the block diagram coefficients (K_1 - K_6). It has been shown in the previous section that some of these coefficients are highly dependent on the static load characteristics and hence it is of interest to evaluate their effect on the system stability.

Under small perturbations and at any oscillation frequency, the developed braking torque can be separated into two components [6]; one is in phase with rotor angle deviation called synchronizing torque, the other in phase with rotor speed deviation called damping torque. The condition for stability is that both of the respective co-

efficients are positive. The expressions of these coefficients are functions of the block diagram coefficients, and hence the load characteristics, and the excitation-stabilization loop parameters.

The salient advantage of the block diagram model is its good accuracy for many practical studies despite the simplifying assumptions inherent in the machine representation. To ensure that this simple model is valid for varying degrees of load sensitivity to voltage, a detailed model has been used to include the effects of damper windings, stator resistance, stator flux derivatives, and governor action. Thus, eigenvalue plots have been obtained to illustrate the validity of the general conclusions reached based on the simplified model using the synchronizing and damping torque concepts.

5.4.1 Machine Equipped With Static Exciter

Static exciters are used because of their fast response and hence ability to provide synchronizing torque under transient conditions. The concurrent disadvantage is the reduction of damping torque under dynamic conditions [6]. The transfer function of a static exciter is given below:

$$G_e = \Delta E_{fd}/\Delta e_t = - K_e/(1 + S\ T_e) \qquad (5.11)$$

where K_e is the exciter gain and T_e is the time constant which is usually very small compared to T'_{do}.

Simple expressions for the damping and synchronizing torque coefficients, for a machine equipped with a static exciter, have been derived in [19]. They are valid for the case where $T_e << T_{eq}$, $\omega^2 T_{eq} T_e << 1$, $K_e K_3 K_6 >> 1$. This is generally the case for a static exciter. These expressions are:

$$K_s(\omega) \approx K_1 - \frac{\frac{K_2}{K_6}\left[K_5 + \frac{K_4}{K_e}\right]}{1 + \omega^2 T_{eq}^2} \tag{5.12}$$

$$K_D(\omega) \approx \frac{\frac{K_e K_2}{K_6}\left[K_5 + \frac{K_4}{K_e}\right]}{1 + \omega^2 T_{eq}^2} \tag{5.13}$$

$$T_{eq} = T'_{do}/K_6 K_e \tag{5.14}$$

also the steady state synchronizing coefficient is given in [6] as:

$$K_s = K_1 - K_2 K_3 K_4 \tag{5.15}$$

In practical situations K_4/K_e is much smaller than K_5 and thus can be neglected in the above expressions.

Effect of MW-Sensitivity to Voltage:

Figure (5.8.a) shows the variation of the steady state synchronizing torque coefficient K_s with the change in

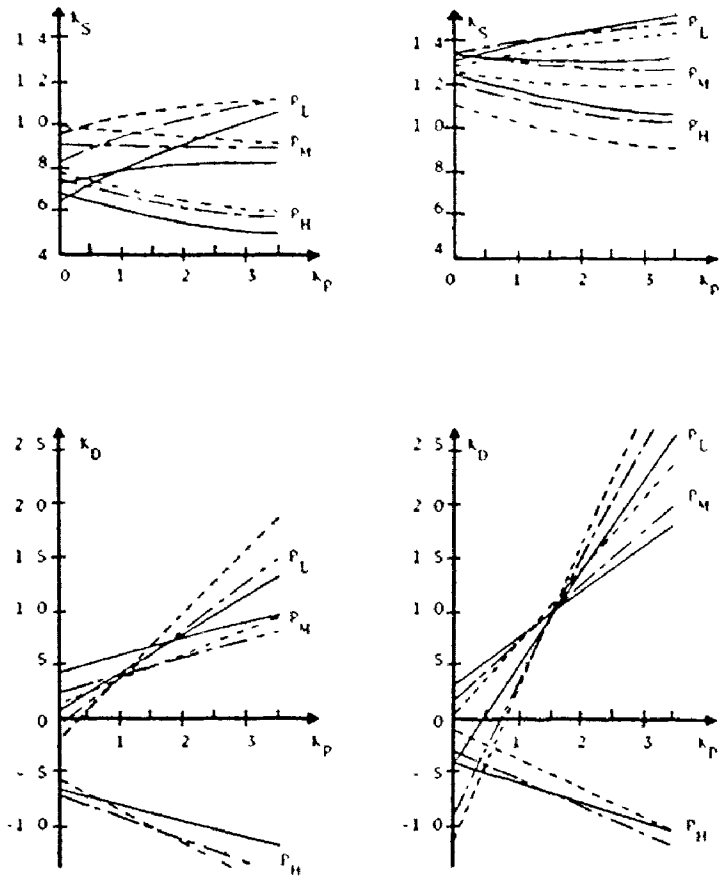

(a) Inductive Load (b) Capacitive Load

Figure 5.8 Variation of Braking Torque Coefficients With K_p

Generation and Load Conditions same as for Figure 5.5

K_p, using equation (5.15). This coefficient is seen to increase under light generation. This is due essentially to the fact that K_4, while independent of K_p, is negative for light generation, and the slight decrease in K_3 is overshadowed by the strong increase in K_2. Under heavy generation conditions, K_4 is positive and K_s decreases as the load sensitivity K_p increases.

The damping torque coefficient K_D, as obtained from equation (5.13), is normalized (per unit torque/per unit speed) and plotted against K_p at a frequency of oscillation of 7.0 rad/sec. which is an average value for the chosen machine under different generation conditions. It may be seen that in general for heavy generation K_5 is negative, thus the damping is negative; while K_5 reverses and thus both are positive for medium and light generation. The amount of damping whether positive or negative, increases significantly with load sensitivity, again the dominating factor is K_2.

For the system under study, positive synchronizing torque exists under all conditions. The decrease in synchronizing torque as generation increases has been noted and the effect of MW-Voltage sensitivity is seen to be minimal. The significance upon damping torque however is marked. In many systems using automatic voltage regulators there is a trade-off between an improvement in synchronizing

torque and a degradation in damping torque where the damping produced by voltage regulator action negates the inherent machine damping. This is demonstrated by examining equation (5.13). The natural machine damping (through K_4) is positive while at high levels of generation the voltage regulator caused damping (through K_5) is negative. It may also be seen from the equation that as the exciter gain increases, the relative effect of the natural damping is reduced. Under conditions of light generation where K_5 is positive, the voltage regulator aids the natural machine damping. Both conditions will be affected by K_2 which tends to be positive.

These effects are verified by the eigenvalue analysis of the more detailed model as indicated in Figure (5.9). The fact that the critical eigenvalue is a complex pair with varying real part implies that the instability is due to lack of damping.

Figure (5.10) demonstrates that there are some specific cases where the choice of local load model is critical. For example let us consider the case of light local generation with a heavy local load. Using a constant impedance model (K_p=2.0), K_2 is positive and sufficiently large that we would predict adequate damping and synchronizing torques for stable operation. However, if we choose another popular model for composite loads, that of

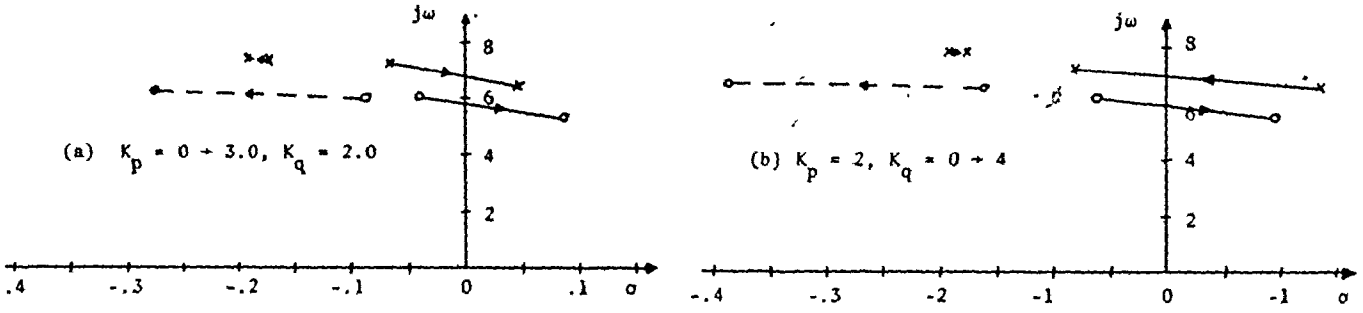

Figure 5.9 Critical Eigenvalue Plot

_____ Heavy Generation, ------ Medium Generation

x x Inductive local load, o o Capacitive local load

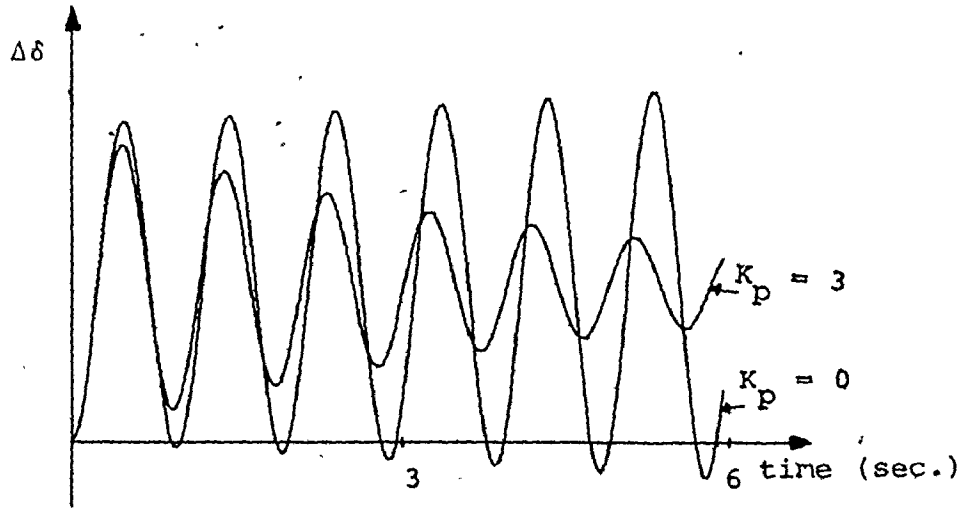

Figure 5.10 Rotor Angle Oscillations (Step Change in E_{fd})

$K_q = 2$, $K_e = 50$

$P_G = .2$, $\Omega_G = 0.0$

constant active power (K_p=0), we should predict instability due to negative damping. The difference in predicted performance is illustrated by the two rotor angle swings corresponding to light load and the two values of K_p that are given in Figure (5.10).

Effect of MVAR-Voltage Sensitivity to Voltage:

The variation of K_s and K_D versus the change in K_q under the same conditions of Figure (5.8) are plotted in Figure (5.11). The behaviour of the steady state synchronizing coefficient is consistent with the variation of K_2 and K_3, K_1 and K_4 being practically constant. The variation of the normalized damping coefficient is also consistent. The variations in K_2 and K_6 tend to cancel so that the major effect is determined by K_5 for large values of exciter gain which is true for static exciters.

The system performance is quite different under the effect of inductive and capacitive local loads. Near the dynamic stability limit, where higher values of K_q increase stability with an inductive local load, they have an unstabilizing effect with local capacitive loads. This can be explained with reference to the behaviour of K_2 and K_5 with the change in K_q as shown in Figures (5.6.a) and (5.6.c).

In the case of the inductive load, both K_2 and K_5 decrease in magnitude with the increase in K_q. This in turn

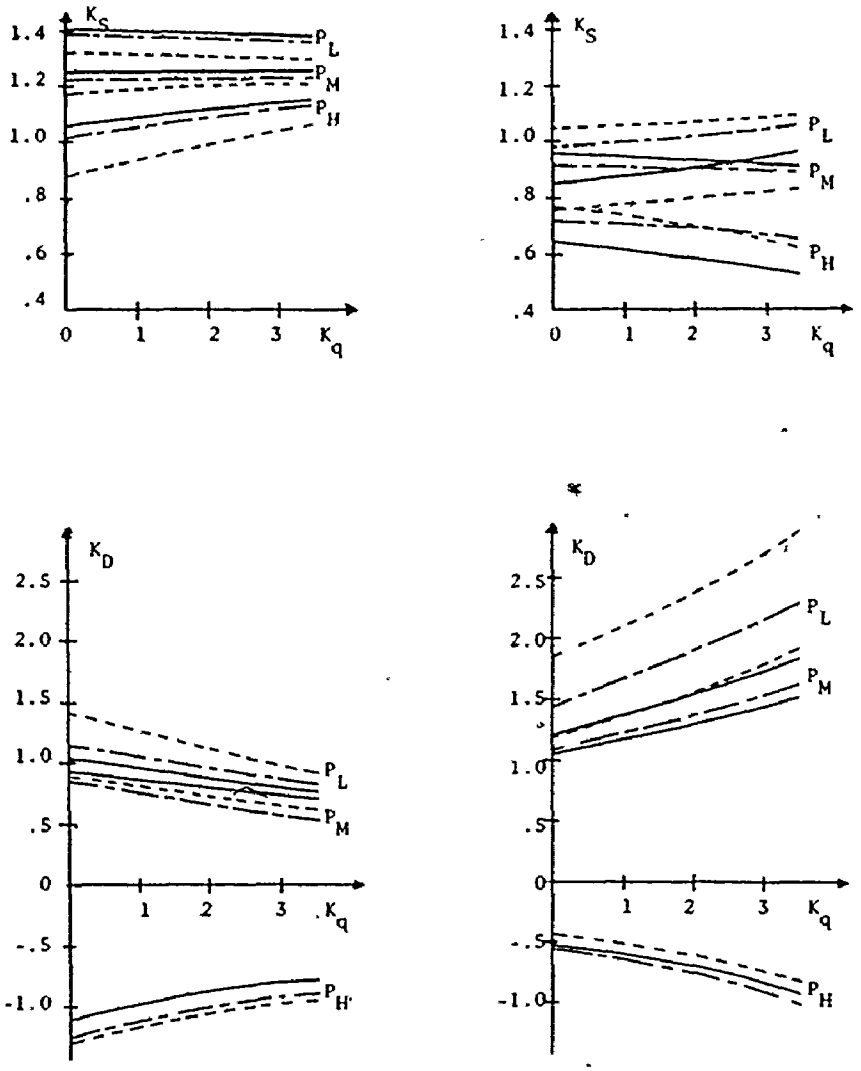

(a) Inductive Load (b) Capacitive Load

Figure 5.11 Variation of Braking Torque Coefficients With K_q Generation and Load Conditions same as for Figure 5.5

reduces the magnitude of the damping torque component through the static exciter, equation (5.13). For negative values of K_5 (near the stability boundary) the amount of negative damping introduced by the static exciter becomes smaller with larger vallues of K_q (Figure 5.11.a) and the net damping torque can become positive due to the natural damping of the machine. This is illustrated and confirmed by the movement of the complex eigenvalue for the more detailed model in Figure (5.9). The opposite is true in cases where K_5 is positive (light and moderate generation levels) and still decreases with the increase in K_q which results in a smaller positive damping torque component. This again is confirmed by the eigenvalue analysis.

In the case of the local capacitive load where both K_2 and K_5 increase in magnitude as K_q increases, the effect is opposite to the inductive case for both the high and moderate generation levels and this again is born out by examining the movement of the dominant eigenvalue in the more detailed model.

5.4.3 Machine Equipped With Stabilizer

In the present analysis a stabilizing signal derived from machine speed deviations is considered. The machine stabilizer is represented by the transfer function G_s in the block diagram of Figure (5.12). The output signal from the

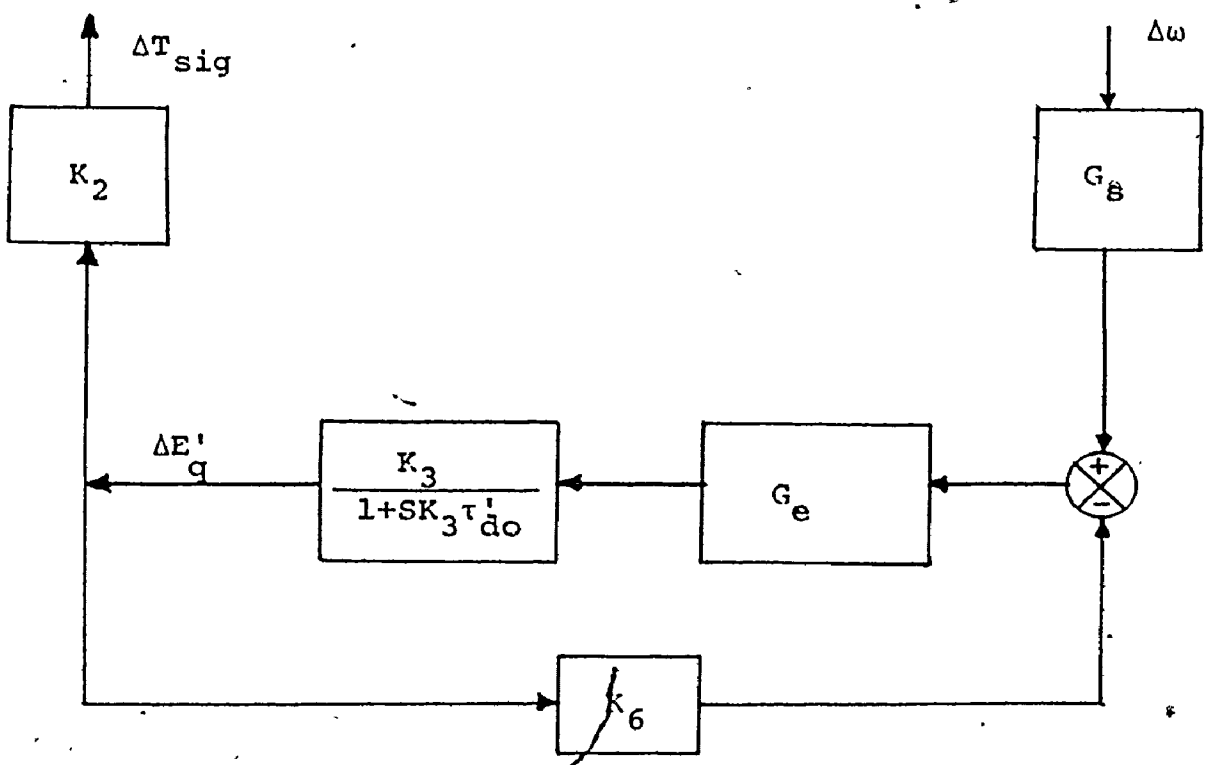

Figure 5.12 Component of Torque Produced by Voltage Regulator Action in Response to a Speed Derived Signal

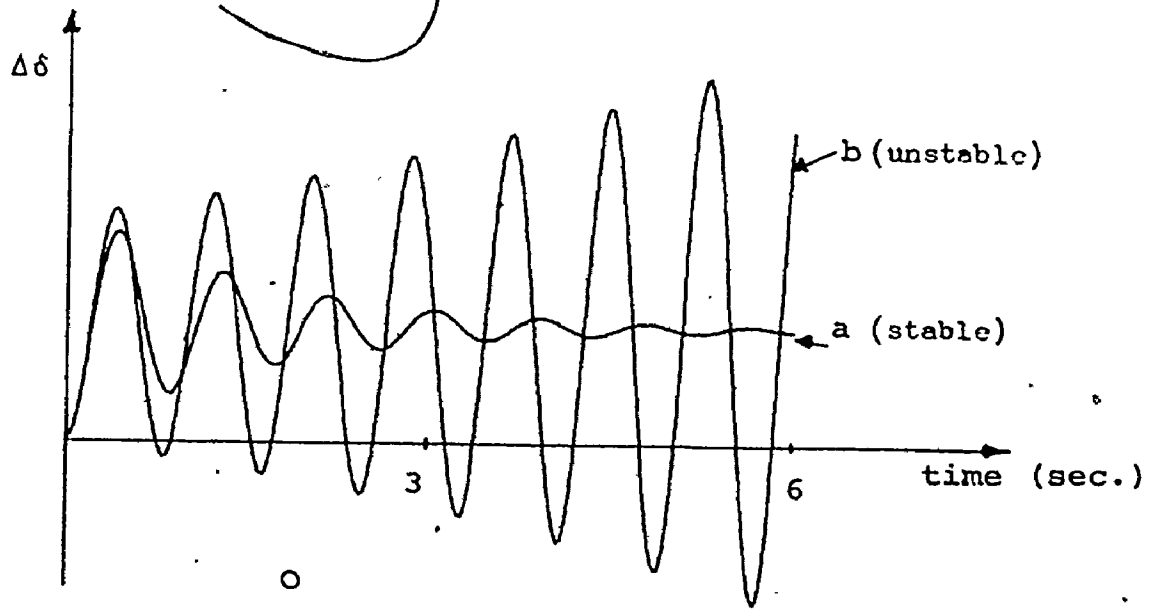

Figure 5.13 Rotor Angle Oscillations For Machine Equipped With Stabilizer (Step Change in T_m)

stabilizer is a function of the oscillating frequency and it is usually designed in such a fashion as to provide adequate damping over the spectrum of expected frequency of oscillation, i.e., G_s should have enough phase lead to compensate a significant part of the phase lag contributed by the machine and regulator [21]. Figure (5.12) is taken directly from reference [6]. This shows the elements of the system in question relating the effect of speed through the stabilizing function G_s through the voltage regulator loops affecting $\Delta E'_q$ which produces a component of torque ΔT_{sig}.

Inspecting Figure (5.12) it can be seen that the stabilizing torque signal ΔT_{sig} is in phase of $\Delta E'_q$ with the proportionality constant K_2. It can also be realized that if the stabilizer is idealy designed ($\Delta E'_q$ is in phase with $\Delta\omega$) the pure damping torque component supplied by the stabilizer will be directly proportional to the block diagram coefficient K_2. On the other hand, it was shown in Section 5.3 that the coefficient K_p is highly dependent on the MW-voltage sensitivity coefficient K'_p. Moreover, the sign of K_2 changes under light generation conditions from the case of constant active power load model (K_p=0) to constant impedance load model (K_p=2). Consequently, the choice of the stabilizer parameters, in this case, is very sensitive to the actual system load characteristics under light generation conditions.

In order to further illustrate the interaction between system loads with different characteristics, and the stabilizer action; the machine rotor angle oscillations were computed using the simplified model with a stabilizer. The stabilizer was designed to provide an adequate damping torque component under the classical assumption of constant impedance load model. This is illustrated by curve (a) in Figure (5.13). Curve (b) demonstrates the unstabilizing action of the power system stabilizer, with the same transfer function as before, under the consideration of constant active power load model (K_p=0, K_q=2). The negative damping is attributed, in this case, to the use of the stabilizer due to the negative value of K_2 while it was assumed positive in the design procedure.

This phenomenon will be discussed in more detail in the next Chapter using the same system structure but with a detailed model for the generating unit. The eigenvalue and eigenvalue sensitivity techniques will be used in the analysis.

5.5 System with Remote Composite Load

The analysis presented so far, considers a system with a local load supplied in part with local hydro generation, the balance coming from a remote infinite source. It is of interest to extend the previously

presented investigations to the case where the load is remote from the hydro generation and for dispatch conditions which result in rotor angles of that generation to lead the infinite bus. This case has been considered in this section. Figure (5.14) shows a single line diagram of the system.

The block diagram coefficients (K_1-K_6) have been obtained using the same method as in Section 2.3, then the steady state synchronizing coefficient K_s and the damping coefficient K_D have been calculated. The variation of these coefficients (K_s and K_D) versus the change in the load indices (K_p and K_q) are illustrated in Figures (5.15) and (5.16) under a variety of operating conditions.

Examining the behaviour of the damping and synchronizing torque coefficients in this case, it can be noticed that the synchronous machine stability is affected by loads with different characteristics. The effect is consistent with the previously analysed case utilizing a local load. It can also be seen that the coefficients K_s and K_D exhibit smaller changes in the practical range of load index varition. Consequently, it can be inferred that under the situation of remote composite load, synchronous machine stability is less dependent on the choice of the load model. This is essentially due to the fact that the amount of interaction between system load and machine excitation

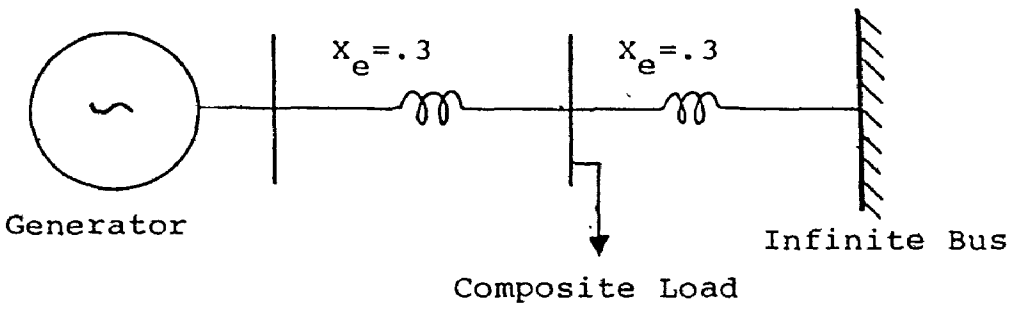

Figure 5.14 System Configuration (Remote Load Case)

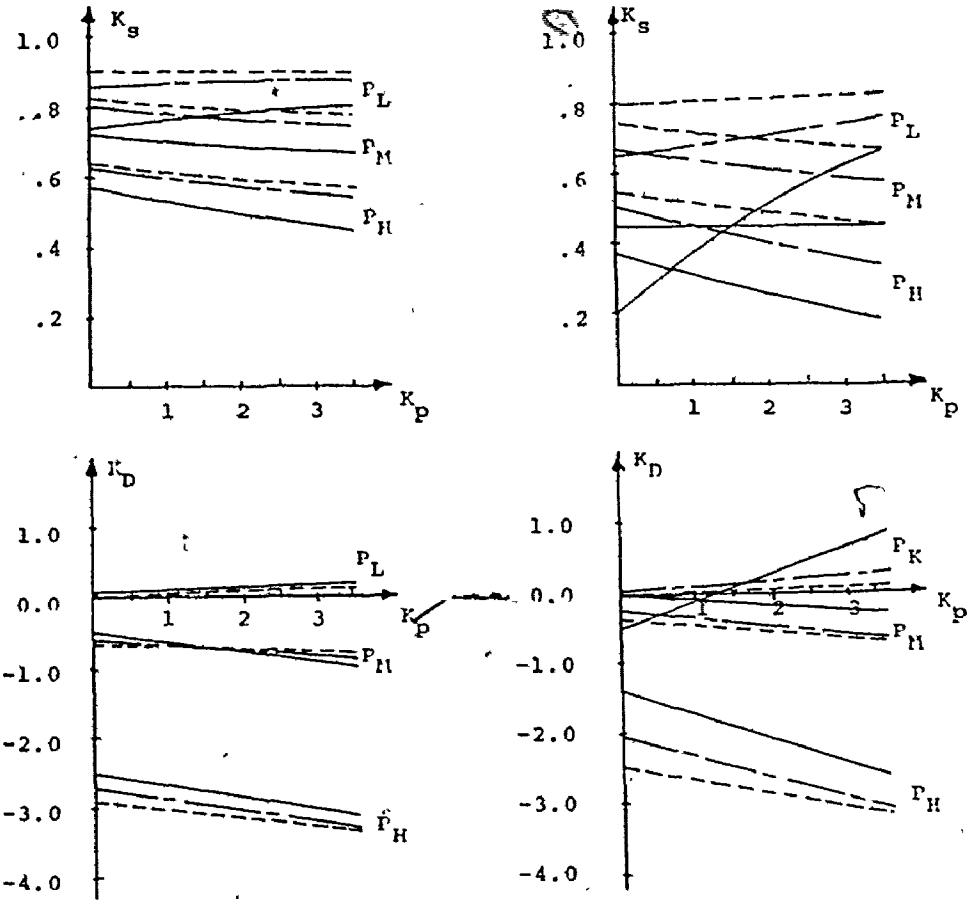

Figure 5.15 Variation of Braking Torque Coefficients With K_p

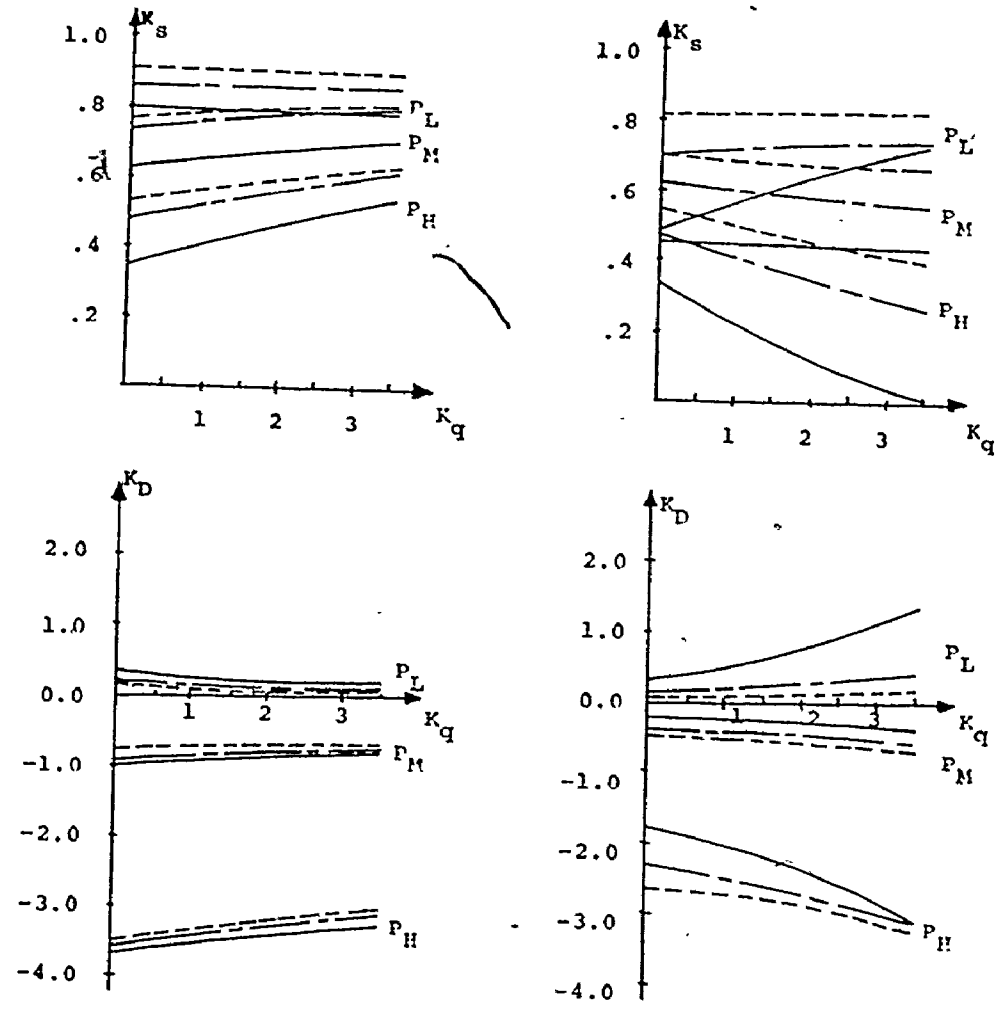

(a) Inductive Load

(b) Capacitive Load

Figure 5.16 Variation of Braking Torque Coefficients With K_q Generation and Load Conditions same as for Figure 5.5

control is reduced.

5.6 Summary

The simple block diagram approach has been extended to include the effect of composite loads modeled as static nonlinear functions of system bus voltage. The behaviour of the block diagram coefficients has been presented for a variety of generation levels and load characteristics. Consequently, the possible interactions between system loads and machine excitation control have been investigated. Hence, the effect of these interactions on synchronous machine dynamic stability has been analysed using the concepts of damping and synchronizing torque.

The analysis based on the simple block diagram model has been verified by using a more detailed model for the synchronous machine (13^{th} order compared to 4^{th}) to plot the movement of the critical eigenvalue pair with different load parameters.

The study has predicted that the choice of constant power or constant impedance load model is critical for stability predictions where the local generation is light relative to the load requirements. A constant impedance model results in a prediction of stable operation whereas a constant power model can result in a prediction of instability due to negative damping. This negative damping

is attributable to the use of a static exciter and is expected to be worsened by the presence of a supplementary stabilizing signal.

This type of analysis and the results obtained reinforce the need for field test data in order to select an adequate load model in stability studies. This is particularly important in situations where the choice of load model can make the difference between correct and incorrect prediction relating to the stability of operation.

Chapter 6

APPLICATION TO PRACTICAL SYSTEMS

6.1 Introduction

In Chapters 2 through 4 an approach has been developed to model and analyse interconnected power systems subject to small perturbations. The overall approach is divided into two sections. The first describes a technique to formulate the system equations in state-space form. The second describes a technique to track the critical eigenvalues over the practical range of control and design parameters. The tracking technique is based on the use of eigenvalue sensitivities in estimating the possible eigenvalue movement.

In Chapter 5 a simplified approach has been presented to build up the basic concepts related to composite load effects on system dynamic stability.

In this Chapter the application of these approaches are considered for three specific cases:

1. Employment of eigenvalue sensitivities to predict the interaction between static loads with different characteristics and excitation control loop parameters. This leads to recommendations concerning light generation operation, in particular the use of

stabilizing signals. This is reported in Section 6.2.

2. Prediction of the dependency of subsynchronous modes on system parameters for a thermal generating unit with a large induction motor load. The machine is connected to a large external system via a compensated transmission line. Eigenvalue sensitivities are used to determine which parameters have a linear, and which have a nonlinear, effect on subsynchronous resonance instability. Section 6.3 gives a detailed analysis of this situation.

3. Dynamic stability evaluation of a 3-generator, 5-bus system. The eigenvalue tracking approach is used to re-evaluate system stability as some parameters of the system are changed. The computational efficiency of the tracking approach over the repeated eigenvalue approach is demonstrated using the expressions developed in Section 4.4. The overall study is presented in Section 6.4.

General concluding comments are made in Section 6.5.

6.2 Lightly Loaded Hydro Generator With Local Composite Load

This section demonstrates the use of second-order eigenvalue sensitivities in clarifying the interaction between machine excitation control and composite local loads with different characteristics and hence the effect on damping the synchronous machine slow oscillations. It will be shown that this is particularly significant under light generation operation where a static excited generator is equipped with a power system stabilizer. The stabilizing signal is derived from the generator speed and it is designed to improve the steady state stability under heavy generation conditions.

Figure (6.1) is a single line diagram of a hydro generator connected to a large interconnected system (represented by an infinite bus) through a transmission line (reactance). The generator is equipped with a static exciter and a supplementary stabilizing signal, governor effects are also included. The terminal bus is feeding a composite load with its power consumption represented as an exponential function of bus voltage as in equation (5.5). The system data are given in Figure (6.1).

In the simulation of the system, network electrical transients have been neglected since they do not have a significant effect on the stability of the synchronous

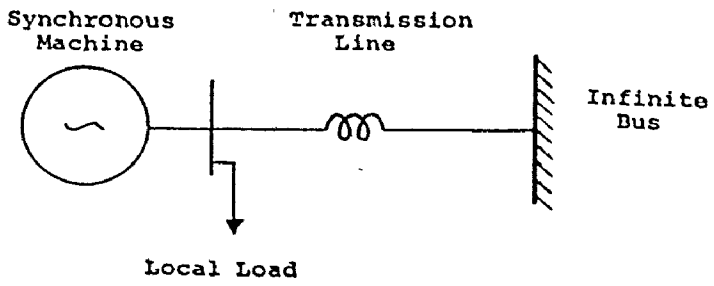

Figure 6.1 Hydro System

Data for Figure 6.1

Machine 66 MVA, 13.8 KV Rating

In pu based on machine rating:

$X_{ad} = .567$, $X_f = .14$, $X_{rd} = .087$, $X_{aq} = .33$, $X_{kq} = .163$,

$r_a = .002$, $r_f = .00035$, $r_{rd} = .02$, $r_{rq} = .04$, $H = 4.29$ sec.

$P_G = .2$, $Q_G = .7$

Exciter-Stablizer

$K_e = 200$, $K_Q = 20$

$\tau_e = .002$, $\tau_Q = 1.4$, $\tau_a = .121$, $\tau_x = .033$, $\tau_v = .03$ sec.

Table 6.1 Normalized First and Second-Order Sensitivities

$K_p = K_q = 2$

System Eigenvalues		Load Real Power Index C_p		Load Reactive Power Index C_q		Stabilizer Gain K_Q		Exciter Gain K_e	
	λ	λ_n	$\ddot{\lambda}_n$	λ_n	$\ddot{\lambda}_n$	λ_n	$\ddot{\lambda}_n$	λ_n	$\ddot{\lambda}_n$
1	-127.±j738	-81.9∓j60.0	14.20±j3.42	46.3±j65.3	-19.4±j23.2	-.172±j.342		.353±j.899	.001∓j.002
2	-508.0	-.76	-.033	2.60	-.843	-1.39	.007	-8.04	.230
3	- 81.6	-1.74	-.288	-1.67	.190	-1.39	.145	13.42	-6.93
4	- 69.1	1.36	-.250	- .461	.114	.633	- .100	1.70	.776
5	-25.7±j27.0	4.48±j5.00	-1.49∓j.420	1.59∓j7.20	.287±j1.45	5.33±j5.84	-1.77∓j.389	-7.53±j28.8	6.68∓j5.00
6	- 40.5	-4.86	2.36	-2.80	-.145	-6.38	2.95	7.15	-7.45
7	-1.27±j6.69	-.974∓j1.13	.312±j.007	0.11±j.015	-.004±j.005	-.874∓j1.01	.267±j.000	.053∓j.276	.001±j.304
8	-3.15±j1.78	-.022±j.095	-.004±j.016			-.020±j.084	-.003±j.008	.001±j.011	-.002∓j.015
9	- 1.44	.028	.002			.026		.003	- .002
10	- .73	- .022	-.002			-.020			
11	-.175±j7.55	-.043±j.004		-.002±j.003		no stabilizer $K_Q = 0$			

machine torque-angle loop which is of concern in this study.

The set of equations describing the dynamic performance of the system has been arranged in state space form as proposed in Chapter 2. The eigenvalues of the system coefficient matrix [A] have been examined for stability including and neglecting power system stabilizer action.

6.2.1 Generator With Stabilizer

Before examining the eigenvalue sensitivities, it should be mentioned that the characteristic of the local load present in this system is significant in evaluating the steady state stability. If the load approximates constant active power combined with constant reactance ($K_p = 0.0$, $K_q = 2.0$), then the system is expected to be unstable. The eigenvalue pair corresponding to the synchronous machine torque angle mode is $+.053 \pm j7.74$. If the load approximates constant impedance ($K_p = K_q = 2.0$), then the system is expected to be stable (the eigenvalue pair is $-1.27 \pm j6.69$). Thus we know that for this system the damping of the machine rotor slow oscillations is related to the value of K_p that describes the load characteristic.

Table (6.1) lists both first and second-order normalized eigenvalue sensitivities with respect to load indices and the stabilizer and exciter gains. The relevant

system eigenvalues are listed at the left. The eigenvalues corresponding to the stator and rotor modes (rows 1-4) and governor modes (rows 8-10) are included for comparison as are the sensitivities to the reactive power index of the load.

Examining the entries of the table it can be noted that the second-order sensitivities are relatively large in rows 5, 6 and 7. The eigenvalues in these rows correspond to the AVR, exciter and the main torque angle modes respectively. The real part of the second-order sensitivity is approximately one third to one half of the first-order term for each of these eigenvalues for both the active power load index (K_p) and the stabilizer gain (K_Q). The sensitivities of the imaginary parts tend to be much smaller implying that the major effect will be related to the damping in these modes and not to the frequency of oscillation. Both the AVR and the exciter modes are affected by the static exciter gain (K_e), the second-order term being approximately equal to the first-order real part.

Of the three modes, the one corresponding to the torque-angle (row #7) is of most importance because the sensitivity terms indicate significant movement of the real part of the eigenvalue with moderate parameter changes; i.e., the damping present in this mode will be significantly affected if either the load characteristic (the index K_p) or

the stabilizer gain changes. In rows #5 and #6 the second-order term will affect the accuracy of prediction but this prediction is less critical.

Figure (6.2) illustrates the improved accuracy in the eigenvalue movement prediction obtainable by including the second-order terms. An eigenvalue plot obtained by repeated eigenvalue computation is shown corresponding to the main torque-angle mode for a practical range of values of K_p. Using a starting point of $K_p = 2$ where the eigenvalue is computed, the other values are estimated by using the first and second-order sensitivity calculations. It can be seen that the use of second-order terms allows one to explore the complete range of values for K_p with only one eigenvalue computation whereas the use of first-order terms only would necessitate additional eigenvalue computations of the complete set, particularly at the low end of K_p which is critical in this case. The error is seen to be almost completely in the real part of the eigenvalue corresponding to the degree of damping present.

This is further demonstrated in Figure (6.3) where the real part of the eigenvalue is shown plotted against the parameter K_p to illustrate the nonlinear relationship.

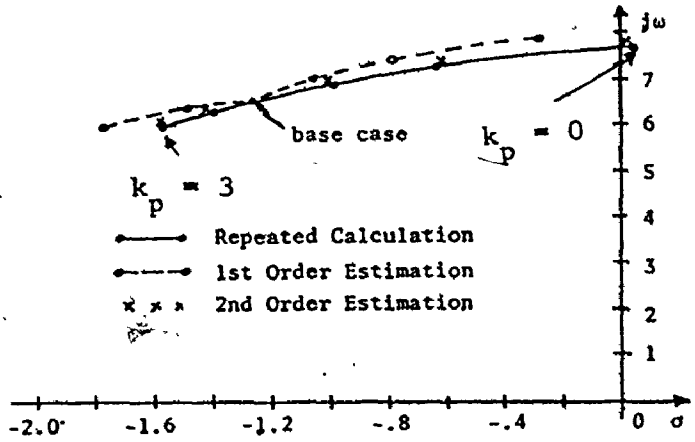

Figure 6.2 Calculated and Estimated Eigenvalues

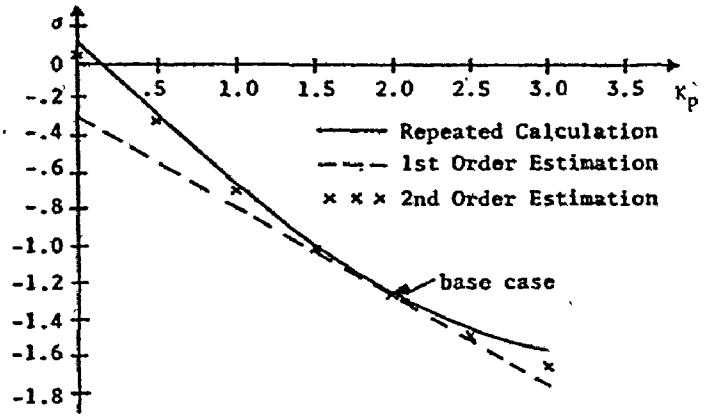

Figure 6.3 Calculated and Estimated Values of σ

6.6.2 Removal of The Stabilizer

The use of a static exciter can be detrimental to the damping of the machine rotor slow oscillations especially under full load conditions [6]. Consequently, a stabilizing signal may be included to improve the damping of this mode and thereby to extend the steady state stability limit.

However, under light generation conditions, the presence of the stabilizing signal may have the reverse effect. In particular, Figures (6.2) and (6.3) illustrate that the system is expected to be unstable if the load is characterized by a constant power model but stable if it is closer to a constant impedance. Removal of the stabilizer signal at light generation level worsens the damping for a constant impedance load model but improves it for constant power by removing the negative damping that previously existed. This reduced sensitivity to the load characteristic is noted in row #11 of Table (6.1).

This instability phenomenon has two practical implications. One is the need for system measurement to determine load representation for adequate system control, the other is the need to know the range of possible load characteristics for stabilizer design.

The results obtained in this study confirm the general conclusions reached in the previous Chapter.

6.3 Subsynchronous Resonance Effects

This section demonstrates the effect of different system parameters on the subsynchronous modes for a thermal generator with a long compensated transmission network.

Figure (6.4) is a single line diagram representing a large thermal generating unit feeding an induction motor load through a compensated transmission line. This subsystem is connected to an infinite bus through a relatively shorter transmission line. The synchronous machine is represented with one damper circuit in each axis as in Appendix A. The generator mechanical shaft is represented as a five mass system, these represent one equivalent rotating mass corresponding to each turbine stage and one equivalent mass representing the generator rotor. The parameters of the synchronous machine, shaft system, static exciter-stabilizer, and the governor system are taken directly from reference [13] and are given with block diagram illustrations in Figures (6.4) and (6.5). Network and stator electrical transients are included in order to obtain correct subsynchronous resonance effects. The induction motor load is represented by an equivalent fifth-order model as described in Section (5.2), the load parameters are given in Figure (6.4).

The system coefficient matrix [A] is obtained as described in Chapter 2. Then, the system eigenvalues and

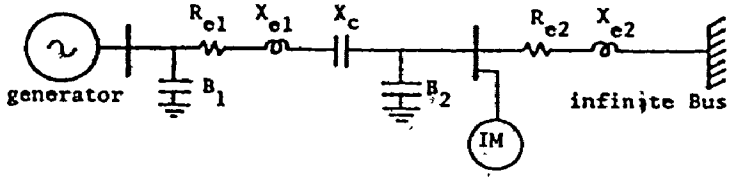

Figure 6.4 Thermal System Configuration

DATA: Machine

555 MVA, 24 KV Rating

In pu based on machine rating:

$X_{ad} = 1.138$, $X_f = .0781$, $X_{rd} = .088$

$X_{aq} = 1.038$, $X_{Kq} = .227$, $r_a = .00153$

$r_f = .000748$, $r_{Kd} = .00805$, $r_{Kq} = .00253$, $H = 3.38$ sec.

$P_G = .9$, $Q_G = .44$

Network

$R_{e1} = .04$, $X_{e1} = .5$, $X_c = .2$, $R_{e2} = .015$

$X_{e2} = .15$, $B_1 = .10$, $B_2 = .12$

Induction Motor

$X_s = X_r = 29.0$, $X_{sr} = 28.5$, $r_s = r_r = .019$ pu

$S = .0072$, $H_m = .44$ sec.

Exciter-Stabilizer

$K_e = 200.$, $\tau_e = .002$, $\tau_a = .09$, $\tau_Q = 1.41$

$\tau_x = .033$ sec., $K_Q = 7.$; $z = .5$ pu.

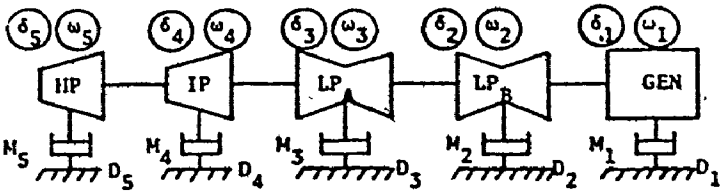

(a) Mechanical System Model

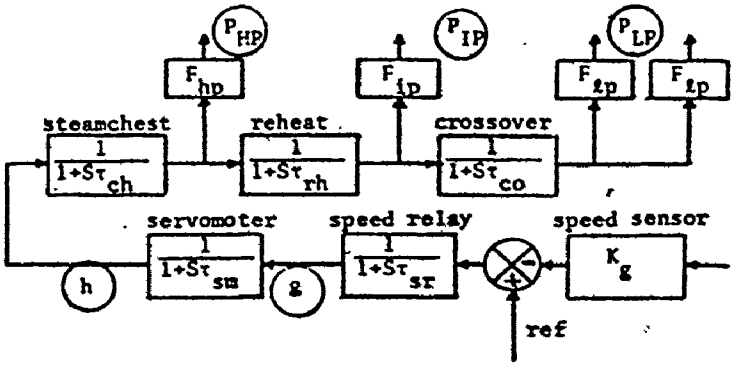

(b) Governor and Turbine Model

Figure 6.5 Mechanical Shaft and Turbine Governor Models

DATA: Shaft

$M_1 = 1.71$, $M_2 = 2.38$, $M_3 = 2.31$, $M_4 = .464$

$M_5 = .248$, $D_1 = 0$, $D_2 = .249$, $D_3 = .259$

$D_4 = .255$, $D_5 = .237$, $S_{12} = 62.3$

$S_{23} = 75.6$, $S_{34} = 48.4$, $S_{45} = 21.8$

Turbine-Governor

$\tau_{ch} = .3$, $\tau_{rh} = 7.$, $\tau_{co} = .2$, $\tau_{sr} = .2$

$\tau_{sm} = .3$ sec., $K_g = 25.$, $F_{HP} = .4$,

$F_{IP} = .3$, $F_{LP} = .15$

eigenvalue sensitivities are calculated at a generating level of 1.0 per unit at .9 power factor lagging.

6.3.1 Effect of Network Parameters

The set of eigenvalues corresponding to different system modes is listed in column 1 of Table (6.2). These reflect the instability of three oscillatory modes corresponding to the three shaft frequencies of 103.5, 151, and 190 rad/sec. Applying sensitivity analysis, it can be determined that the shaft instabilities are due to the interaction of the network mode at 173.5 rad/sec. (#6) and the shaft modes corresponding to the first three eigenvalues.

In columns 2 and 3 are shown the normalized first and second-order sensitivities with respect to the network parameters X_c and X_{el}. Considering first-order sensitivities, the conclusions which can be drawn from the results shown are in general agreement with these presented in [69]. A relatively small increase in the tie line reactance X_{el} is seen to reinforce the shaft instability mode at 190 rad/sec. (#2) and cures shaft instabilities at 151 and 103.5 rad/sec. (#1 and #3). This is reasonable since a small increase in X_{el} increases the frequency of the interacting electrical mode at 173.5 rad/sec. (#6) and hence moves it towards the mechanical mode at 190 rad/sec. (#2) and away from the other

Table 6.2 Normalized First and Second-Order Sensitivities

		1	2 X_c		3 X_{el}		4 R_r		5 H_m	
		λ	$\dot{\lambda}_n$	$\ddot{\lambda}_n$	$\dot{\lambda}_n$	$\ddot{\lambda}_n$	$\dot{\lambda}_n$	$\ddot{\lambda}_n$	$\dot{\lambda}_n$	$\ddot{\lambda}_n$
Shaft	1	.197±j151.	2.58∓j.087	+8.23±j6.00	-.864∓j.075	1.38∓j.526				
	2	.044±j190.	-1.58±j.754	8.74±j1.88	.350∓j.166	.289±j.178				
	3	.021±j103.5	.547±j1.46	1.00±j1.62	.226∓j.893	.309±j.885	-.025±j.003			
	4	-.300∓j276								
Stator/ Network	5	-8.00±j2065			.270∓j45.3	-.136±j21.7	-.575±j.000			
	6	-13.3±j173.5	.097∓j104.5	-17.5±j27.6	3.58±j28.6	-3.68∓j17.6	.458∓j.036			
	7	-14.2±j2932	-.103±j5.74		9.67∓j362.7	-10.9±j335.6	-.40±j.00			
	8	-14.4±j580.	-.058±j101.	.064∓j25.8	3.91∓j26.9	-2.65±j16.3	-.127∓j.010			
	9	-18.6±j3742	-.069±j8.51		12.4∓j681.	-13.5±j626.	-.172±j.000			
	10	-55.5∓j10241			-.235±j152.	-.213∓j153.8				
Machine/Excit.- Stabilizer	11	- .768	- .020	-.01	.018	- .015	- .016	.020		
	12	- .930	.033	.013	- .030	.023	.029	- .039		
	13	-2.17∓j11.6	-1.07∓j2.10	-.446∓j.705	1.02±j1.92	-.831∓j1.37	-.092±j.482	.174∓j.060	.252±j.749	-.152±j.386
	14	-10.5±j14.1	1.01∓j1.79	.610∓j.776	-1.08±j1.64	1.04∓j1.34	-.043±j.187	-.231±j.112	.046∓j.620	.472±j.207
	15	-30.1		-.014						
	16	-91.8	-1.32	-.030	1.59	-1.03				
	17	-500.5			- .067	.042				
Ind. Motor	18	-3.54±j18.2	-.243±j.915	-.414±j.463	.204∓j.871	-.40±j.783	-2.89∓j.463	.159∓j.300	-.380∓j7.46	-.314±j6.76
	19	- 5.51	- .864	-.529	.779	- .741	-6.06	-4.24	.138	
	20	-9.57±j376.8					.000∓j.132			
Turbine- Governor	21	- .142								
	22	- 2.90	- .263	-.104	.237	- .179	- .091	.209		
	23	-3.89±j.901	.131∓j.194	.046∓j.066	-.119±j.174	.084±j.123	-.163∓j.231	.868±j.332		
	24	- 4.96	- .032	.01	.029		- .201	2.11		

Table 6.3 Normalized First and Second-Order Sensitivities

		1	2 K_Q		3 Z		4 τ_{co}		5 τ_{sr}	
		λ	$\dot{\lambda}_n$	$\ddot{\lambda}_n$	$\dot{\lambda}_n$	$\ddot{\lambda}_n$	$\dot{\lambda}_n$	$\ddot{\lambda}_n$	$\dot{\lambda}_n$	$\ddot{\lambda}_n$
Shaft	1	.197±j151.	.100∓j.614							
	2	.044±j190.	-.120∓j.025		-.507∓j.136					
	3	.021±j103.5	.055∓j.217		-.124±j.432					
	4	-.300∓j276								
Stator/ Network	5	-8.00±j2065								
	6	-13.3±j173.5	.061±j.328		.590∓j.174	.012∓j.010				
	7	-14.2±j2932								
	8	-14.4±j580.								
	9	-18.6±j3742								
	10	-55.5∓j10241								
Machine/Excit.- Stabilizer	11	- .768	- .102	-.103						
	12	- .930	.164	.103					.016	
	13	-2.17∓j11.6	-3.43±j.537	-.850±j.085	.012±j.01				-.017∓j.017	.023±j.000
	14	-10.5±j14.1	4.29±j.321	1.86∓j.498						
	15	-30.1	.152	-.015						
	16	-91.8	- .081		- .018					
	17	-500.5	- .011		- .01					
Ind. Motor	18	-3.54±j18.2	-1.11±j1.23	-1.02±j.519	.020∓j.000					
	19	- 5.51	.121				.095	-.964	.227	-.704
	20	-9.57±j376.8								
Turbine- Governor	21	- .142								
	22	- 2.90							.358	.508
	23	-3.89±j.901	.024±j.037				-.088∓j.015	-.196±j.178	2.29±j.118	-2.68∓j3.46
	24	- 4.96	.0110				5.08	-3.65	-.151	.511

two modes.

The above analysis is only true under the assumption of small changes in X_{el}. Using the complementary frequency concept [23], the resonating frequency in a stationary network is proportional to the reciprocal of the square root of the total inductive reactance in the resonating loop. This explains the relatively high second-order sensitivities, due to changes in X_{el} for both the corresponding network modes (especially #6 and #8) and the first three unstable shaft modes. Sensitivities to changes in X_c indicate opposite effects compared to corresponding changes in X_{el}.

Eigenvalues #13 and #14 are seen to be sensitive to variations in X_c and X_{el}, this is expected since these eigenvalues correspond respectively to the main torque-angle loop and the AVR oscillatory modes. Again the relatively high second-order sensitivities demonstrate the fact that these eigenvalues are not simple linear functions of network parameters.

6.3.2 Effect of Induction Motor Loads

The sensitivities of eigenvalues #6 and #3 to an increase in the induction motor rotor resistance (r_r) show the effect of negative damping on the mode at 173.5 rad/sec. and the positive damping effect on the mode at 103.5 rad/sec. This is in agreement with the results presented in

[69] and the analysis in [29]. At subsynchronous frequencies, currents at that frequency flow in the motor stator causing the equivalent induction motor rotor resistance to be negative (induction generator action); hence, the increase in the magnitude of the equivalent rotor resistance causes an opposite effect compared to the increase in the positive tie line resistance.

Sensitivity of eigenvalues #18 and #19 to changes in r_r demonstrates the effect of rotor resistance in damping induction motor rotor oscillations. The increase in the inertia constant of the induction motor load (H_m) is seen to increase the damping and decrease the frequency of induction motor rotor oscillation (#18). This reflects back an unstabilizing effect on the main torque-angle loop of the synchronous machine (#13). This is reasonable since the induction motor load is frequency dependent.

6.3.3 Stabilizer Effects

Examining column 2 of Table (6.3) yields the fact that the increase in the stabilizer gain (K_Q) adds a positive damping component at 11.6 rad/sec. (#13) and the amount of damping is seen to be practically proportional to K_Q which is to be expected if the stabilizer is appropriately designed. It follows that the damping effect on the dominant oscillations at 11.6 rad/sec. due to the

increase in K_Q causes in turn additional damping to the induction motor rotor oscillations at 18.2 rad/sec. (#18).

Examining the sensitivities of the first three eigenvalues to changes in K_Q illustrates the interaction between machine stabilizer and shaft instabilities [15]. Increasing K_Q is seen to provide positive damping at 190 rad/sec. (#2). However, it contributes negative damping at 151 and 103.5 rad/sec. (#1 and #3). The insignificant second-order sensitivities at the above three frequencies in this case can be explained by examining the stabilizer produced damping for the shaft oscillatory modes. These damping torques can be positive or negative depending on the mode frequency [15]. Since the frequency of the shaft modes are changing insignificantly, the amount of damping torque is proportional to changes in K_Q.

The sensitivities listed in column 3 show the significant effect of the selection of the speed pick up point (Z) on the stability of shaft modes (#2 an #3).

6.3.4 Governor Effects

In the last two columns of Table (6.3), are listed the sensitivities with respect to two of the governor time constants. These are presented to demonstrate the importance of second-order sensitivities. For example, relying on the first-order sensitivity of eigenvalue #24 to

changes in τ_{co} (crossover time constant), a one per unit increase in τ_{co} is seen to cause instability to the mode corresponding to eigenvalue #24. Consideration of the second-order term demonstrates the nonlinear relationship between eigenvalue #24 and τ_{co} with the result that system stability is preserved even with relatively wide changes in τ_{co}.

6.4 Three Machine-Five Bus System

This Section demonstrates the application of the eigenvalue "tracking" approach to the dynamic stability analysis of a five-bus system. Figure (6.6) shows the structure and the operating conditions of the interconnected system. The system comprises three generating units at buses #1, #2 and #3; the first is fossil, the second is nuclear, and the third is a smaller hydro unit. Machines #1 and #2 are equipped with static exciters and stabilizing signals derived from each machine speed, machine #3 is equipped with a type 1 exciter. Governor effects are included in the simulation of the three machines. System loads are represented as linear static elements at buses #2, #3 and #4 in addition to two dynamical equivalents for induction motor loads at buses #1 and #4. The values given in Figure (6.6) are in per unit based on 600 MVA and 24 KV. The values of different subsystem parameters are also given.

DATA:

Machine #1

Same as the Machine of Figure 6.4

Exciter-Stabilizer

$K_e = 350.$, $K_Q = 6.0$, $\tau_v = .03$, $\tau_e = .002$

$\tau_Q = 1.4$, $\tau_a = .121$, $\tau_x = .033$ sec.

Turbine-Governor

$K_g = .04$, $\tau_3 = .1$, $\tau_4 = .3$ sec.

Machine #2

635 MVA, 24 KV Rating

In pu Based on Machine Rating:

$X_{ad} = .945$, $X_f = .0755$, $X_{Kd} = .085$

$X_{aq} = .945$, $X_{Kq} = .085$, $r_a = .00153$,

$r_f = .00039$, $r_{Kd} = .00805$, $r_{Kq} = .00253$

$H = 5.4$

Exciter-Stabilizer

$K_e = 200.$, $K_Q = 10$, $\tau_v = .03$, $\tau_e = .002$

$\tau_Q = 1.4$, $\tau_a = .12$, $\tau_x = .033$ sec.

Turbine-Governor

$K_g = .04$, $\tau_3 = .1$, $\tau_4 = .3$ sec.

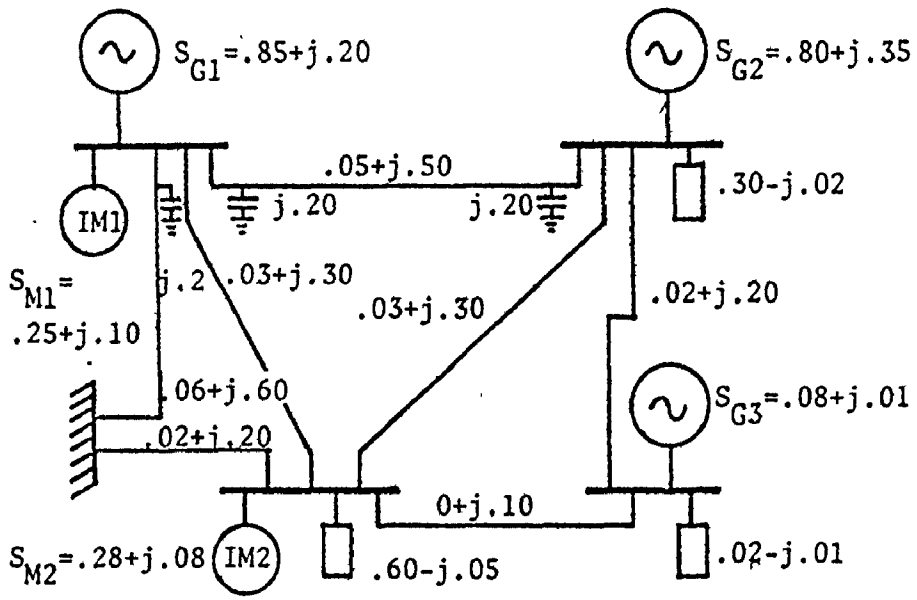

Figure 6.6 Multimachine System Configuration

Machine #3

Same as the Machine of Figure 6.1

Exciter

$K_A = 200$, $K_E = -.17$, $K_F = .04$, $S_E = .95$

$\tau_A = .05$, $\tau_E = .95$, $\tau_F = 1.$, $\tau_v = .03$ sec.

Turbine-Governor

$K_g = .04$, $\tau_1 = .4$, $\tau_3 = .4$, $\tau_5 = .35$ sec.

6.4.1 Eigenvalue Sensitivities

The system equations, linearized around the chosen operating point, were developed in the state space form using the technique described in Chapter 2 with programming on a CDC 6400 computer. The eigenvalues listed in Table (6.4) were obtained for the system using a standard library subroutine.

First and second-order sensitivities of the whole eigenvalue pattern were obtained with respect to a variety of control parameters. Using this information, the three complex pairs of eigenvalues corresponding to the main torque-angle loops of the multimachine system were identified. These are listed in Table (6.5) with the sensitivities normalized with respect to a small number of control parameters of interest. The three eigenvalues are seen to be significantly sensitive to the selected parameters and it would be of interest to track them over appropriate ranges of the chosen parameter variations.

6.4.2 Eigenvalue Tracking

Figures (6.7)-(6.10) show the first and second-order approximations to the different eigenvalue movements as compared to the exact values computed using the inverse iteration method. These results clearly demonstrate that the second-order estimation is sufficiently accurate for

Table 6.4 System Eigenvalues at Base Condition

N	Eigenvalue	N	Eigenvalue	N	Eigenvalue	N	Eigenvalue	N	Eigenvalue
1	-.542±j1.854	8	-2.823	15	-10.42	22	-19.96±j376.2	29	-49.95
2	-.628±j5.943	9	-2.975±j9.947	16	-10.46	23	-20.58	30	-52.21
3	-.691±j.121	10	-3.195	17	-12.21	24	-30.54	31	-152.6
4	-.750	11	-3.218±j2.004	18	-13.06±j18.13	25	-30.92	32	-167.8
5	-1.000	12	-7.576±j20.96	19	-13.58	26	-33.02	33	-239.5±j1365.
6	-1.334	13	-8.312±j21.23	20	-14.41±j376.5	27	-34.01	34	-500.6
7	-1.436±j6.242	14	-8.555±j27.10	21	-15.17±j430.3	28	-34.39±j560.9	35	-502.1

Table 6.5 Normalized First and Second-Order Sensitivities to System Parameters

N	1	2 K_{Q1}		3 Ke_1		4 K_{Q2}		5 K_A	
	λ	$\dot{\lambda}_n$	$\ddot{\lambda}_n$	$\dot{\lambda}_n$	$\ddot{\lambda}_n$	$\dot{\lambda}_n$	$\ddot{\lambda}_n$	$\dot{\lambda}_n$	$\ddot{\lambda}_n$
1	-2.975±j9.947	-1.279∓j1.757	.531±j.136	1.165∓j.246	-1.464±j.516	.252∓j.359	.137±j.226	... ...	... ...
2	-1.436±j6.242	-.076±j.124	.042±j.005	-.060∓j.067	.791±j.048	-.950∓j1.173	-.319±j.087	.158∓j.169	.011∓j.068
3	-.628±j5.943	-.034∓j.035	... ...	.017±j.009	-.018∓j.006	.025±j.374	.543∓j.280	-.108±j.144	-.014±j.065

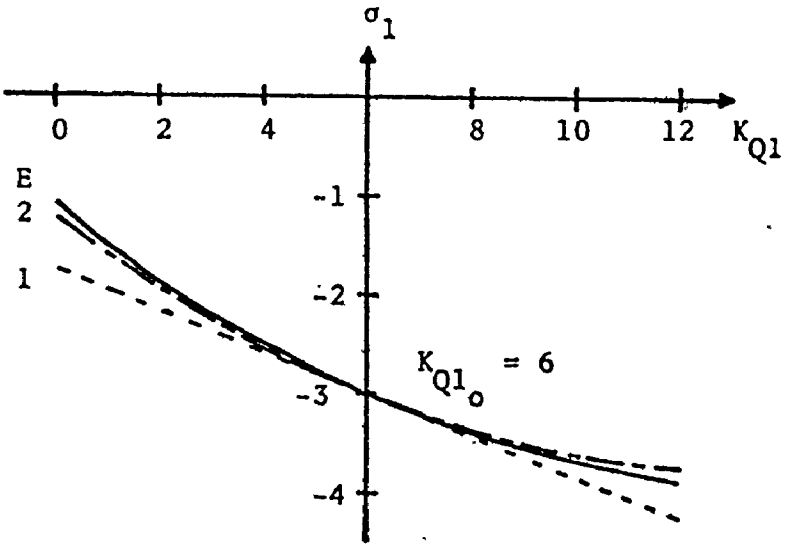

Figure 6.7 Re(λ_1) vs Gen. #1 Stabilizer Gain

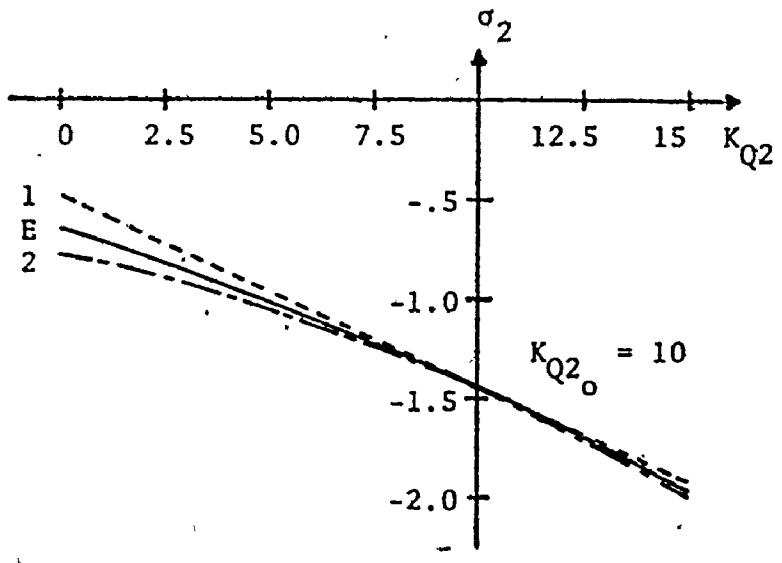

Figure 6.9 Re(λ_2) vs Gen. #2 Stabilizer Gain

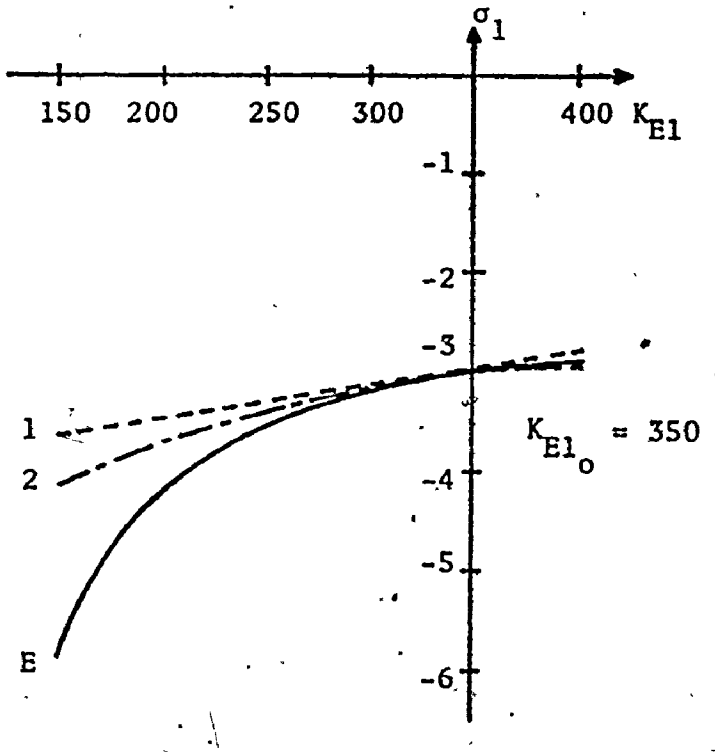

Figure 6.8 Re(λ_1) vs Gen. #1 Exciter Gain

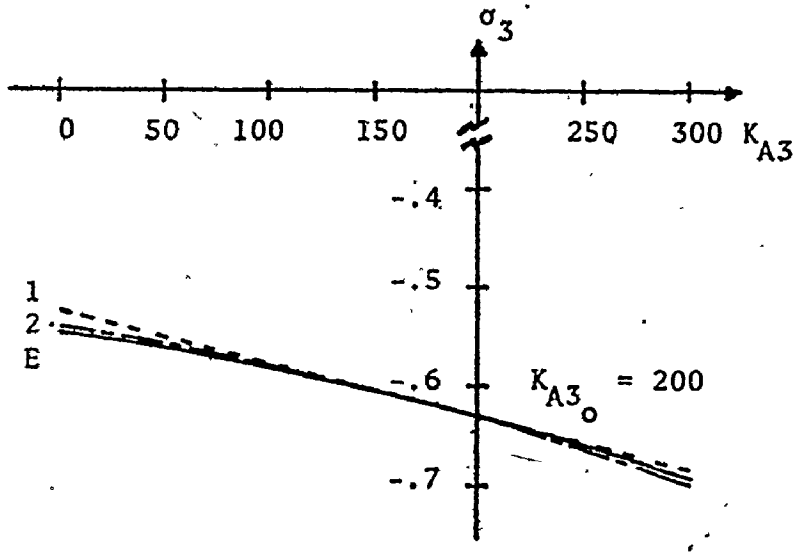

Figure 6.10 Re(λ_3) vs Gen. #3 Amplifier Gain

-------- 1st-Order Estimate

——— 2nd-Order Estimate

——————— Exact Value

changes in the control parameters up to ±.5 pu except for the case in Figure (6.8) which illustrates the change in the real part of the first eigenvalue versus the change in the gain of machine #1 static exciter (K_{e1}). In this case, the relation is shown to be highly nonlinear and it is beneficial to use the inverse iteration to find the exact movement. Results obtained using the inverse iteration technique were double checked using repeated eigenvalue computation at selected points. The results obtained by both methods are in complete agreement to six decimal places.

6.4.3 Time Comparison

The time to compute one base case and nine additional evaluations to form a set of ten values was obtained for both the repeated eigenvalue and the tracking approach using the expressions developed in Section 4. The time was compared on the CDC 6400 computer using a standard library subroutine for eigenvalue/eigenvector evaluation and the five-bus example of order 50.

Table 6.6: Computation Time Comparison

	One Eigenvalue			Fifteen Eigenvalues		
P	T_R	T_T	%	T_R	T_T	%
1	316	83.9	26.6	344	214.1	62.2
2	601	93.2	15.5	640.2	353.6	55.2
3	885	102.5	11.5	922.2	493.1	53.5

In the first method the eigenvalue computation is repeated 9 times whereas in the second method the second-order sensitivities are calculated for the Exp combinations followed by the 9 inverse iterations for each of the Exp cases. In Table (6.6) the time in seconds for each method is given along with the percentage of the time for the second method compared to that for the first. It can be seen that if only one eigenvalue of the fifty is of interest the computation time is reduced to approximately 18% depending on the number of parametets for which the eigenvalue movement is required, the greater the number the better the saving. If fifteen of the 50 eigenvalues need to be checked the saving is about 40%. This effectively means about half the total since a large portion of the eigenvalues occur as complex conjugate pairs. A more realistic case would be E = p = 3 for which the tracking method comprises about 20% of the time for the repeated eigenvalue computation method.

6.5 Summary

The techniques and concepts developed in Chapters 2 to 5 have been applied to three specific systems. The formulation described in Chapter 2 has been used to arrange the linearized system equations in state space form. Eigenvalue first and second-order sensitivities have been used to

reveal the interaction between system composite loads with different static characteristics and the excitation control parameters of a hydro unit. It has been demonstrated that, where a stabilizer is used based on a full load design, the stabilizer can cause instability at light generation levels if the load approximates a constant real power requirement. This analysis reinforces the need for accurate system data on load characteristics since the type of load rather than the amount may cause the instability.

Eigenvalue sensitivities have been also employed to study the complex interactions involved with subsynchronous resonance instability. These have been shown to give rise to certain second-order sensitivities as large as or larger than first-order ones. This re-emphasizes the advantage in using second-order terms in such sensitivity analysis where the relationship is significantly nonlinear. It is also useful to know which relationships are linear. In particular, the damping introduced by the stabilizer at shaft natural frequencies has been found to be linearly dependent on stabilizer gain and speed pickup point.

The tracking approach, as presented in Chapter 4, has been used to study the effect of control parameters on the dynamic stability of a five-bus system. Eigenvalue sensitivities have been used to identify the modes sensitive to parameter changes. Then, the eigenvalues corresponding to

these modes have been tracked over the practical range of control parameter variation. The computational efficiency of this approach over the repeated eigenvalue approach has been demonstrated. The repeated evaluation of only a few of the eigenvalues as described enhances the speed of computation in cases where the other eigenvalues are known to be insensitive to the changes being examined.

Chapter 7

CONCLUSIONS

An efficient approach for power system dynamic stability analysis has been presented. The development is divided into two sections. The first describes a technique to formulate the system equations in state-space form. The second section describes a technique to track the critical eigenvalues over the practical range of control and design parameters.

The formulation is based on grouping the states of each individual machine together. Then all the system states and variables are ordered in such a fashion as to reduce the computational expense in forming the state-space model. This approach has flexibility for different degrees of representation of generating systems and a variety of loads. The technique also allows the inclusion of network transients and machine shaft dynamics. The formulation has been shown to be particularly suitable for eigenvalue sensitivity applications and in subsequent studies that need system updating.

The tracking algorithm has been constructed for the purpose of computing the dominant or critical system eigenvalues over a wide range of system parameter settings.

This algorithm is essentially based on the use of the second-order sensitivity technique in obtaining a good estimate for the eigenvalue pattern shift due to parameter changes. It has been shown that this approach is more economical than the repeated eigenvalue approach, especially if the number of eigenvalues to be tracked is small and the number of parameters to be varied is large. The application of the tracking approach is limited to systems with nonrepeated eigenvalues which is usually the case in power systems.

The application of these techniques to the analysis of systems with practical data provided by Ontario Hydro has shown consistency with other results and conclusions reached by other researchers in the field. One of the important problems now receiving interest is the analysis of load effects on power system dynamics. An attempt has been made, in this thesis, to derive some general conclusions related to the interaction between system composite loads and machine static excitation and stabilization controls. These conclusions have been derived using a simplified system representation with the use of damping and synchronizing torque concepts. The general concepts developed using this method have resulted in a prediction of some specific situations where the choice of a load model can make a critical difference in describing system stability. These

predictions have been further illustrated by applying the eigenvalue tracking approach, considering these specific situations, to a system with a more detailed representation.

This computational approach has also been applied to other practical problems. The effects of different parameters and components of a system exhibiting subsynchronous resonance have been analysed. Also, the stability of modes corresponding to the performance of the main torque-angle loops of a multi-machine system has been investigated under a multiplicity of control parameters changes.

7.1 Contributions of the Thesis

The specific contributions of the overall study are considered to be as follows.

7.1.1 Theoretical Development

(1) Development of an efficient multimachine formulation technique. The formulation is flexible and accomodates system loads with different static and/or dynamic characteristics. It also allows the inclusion of network transients and machine shaft dynamics.

(2) Derivation and application of simple expressions for eigenvalue second-order sensitivities with respect to general system parameters.

(3) Development and use of an efficient eigenvalue tracking approach. This approach is specifically useful if it is required to track the movement of only a small number of system eigenvalues.

7.1.2 Application

These techniques have been employed to analyse various practical problems currently receiving interest in the electric utility industry. The system data have been provided by Ontario Hydro. These studies have contributed toward the following.

(1) Development of basic concepts related to the interaction between system composite loads and generation excitation control. These concepts have been developed using simplified models for system representation. However, the computational techniques developed have been applied to study a more accurately represented system to justify the stability predictions using the simple model.

(2) Prediction of linear and nonlinear dependence of subsynchronous resonance modes on different system parameters.

The use of these techniques and concepts in the studies performed in Chapter 6 demonstrate the applicability of these techniques in the analysis of power system

dynamics. These studies have contributed to a better understanding of the correspondence between system eigenvalues and eigenvectors and the different modes in the system. It has been demonstrated that the use of these techniques renders a simple way to interpret physical interactions involved in power system dynamics. This is considered as a further important contribution of the overall study.

7.2 Suggestions for Future Work

Specific topics which seem worthy of further study are:

(1) Second-order estimates for eigenvalue movement have been shown to be acceptable in practice for relatively wide parameter variation. These have been used under the situation of changing one parameter at a time. It would be of interest to apply the sensitivity analysis method in similar studies but with more than one parameter variation.

(2) The overall tracking approach has been developed for systems with nonrepeated eigenvalues. Fortunately, this is the case for large scale power systems. For other systems, it would seem useful to study the situation of identical or very close eigenvalues.

(3) The inverse iteration method has been used with

second-order estimates to track eigenvalue movement. Alternatively, this method can be used in a diakoptic approach [120] to calculate only the eigenvalues and eigenvectors of a particular subsystem without the need to compute the overall system eigenvalues. This can be achieved by using the overall system coefficient matrix with the eigenvalues of the isolated subsystem, as estimates, in the inverse iteration method.

(4) The effect of composite loads on system dynamic stability has been analysed considering a generator equipped with a static exciter and a supplementary stabilizing signal derived from the machine rotor speed. Investigation and comparison of load effects under the use of other types of exciters is desirable.

This Thesis has presented an efficient comprehensive approach to study the dynamics of large power systems. This approach has been applied to the analysis of various practical problems. The results obtained are encouraging since they have shown consistency with other results obtained in the literature. One of the systems studied in Chapter 6 is of order fifty which is of comparable size to systems being analysed by electric utilities. It would be of interest if this computational approach were to be

adopted by a utility where it can be applied to the analysis of existing systems of even larger sizes.

REFERENCES

[1] F.P. deMello, "Power System Dynamics - Overview", presented at Symposium on Adequacy and Philosophy of Modeling: Dynamic System Performance at 1975 Winter Power Meeting, IEEE Publication 75CH0790-4-PWR, Jan., 1975.

[2] IEEE Committee Report, "System Load Dynamics - Simulation Effects and Determination of Load Constants", IEEE Trans. Power Apparatus and Systems, Vol. PAS 92, pp. 600-609, March-April, 1973.

[3] M.H. Kent, W.R. Schmus, F.A. McCrackin, and L.M. Wheeler, "Dynamic Modeling of Load in Stability Studies", IEEE Trans. Power Apparatus and Systems, Vol. PAS 88, pp. 756-763, May, 1969.

[4] C. Concordia, "Representation of Loads", IEEE Special Publication 75-CHO-970-4-PWR, pp. 41-45, presented at the Power Engineering Society Winter Meeting, New York, Jan., 1975.

[5] P. Kundur and P.L. Dandeno, "Practical Application of Eigenvalue Techniques in the Analysis of Power System Dynamic Stability Problems", presented at 5th Power System Computation Conference, Cambridge, England, Sept., 1975.

[6] F.P. deMello and C. Concordia, "Concepts of Synchronous Machine Stability as Affected by Excitation Control", IEEE Trans. Power Apparatus and Systems, Vol. PAS 92, pp. 316-329, April, 1969.

[7] A.H. ElAbiad and K. Nagappan, "Transient Stability Regions of Multimachine Power Systems", IEEE Trans. Power Apparatus and Systems, Vol. PAS 85, pp. 169-179, Feb., 1966.

[8] K. Prabhashankar and W. Janischewskyj, "Digital Simulation of Multimachine Power Systems for Stability Studies", IEEE Trans. Power Apparatus and Systems, Vol. PAS 87, pp. 73-80, Jan., 1968.

[9] G.A. Luders, "Transient Stability of Multimachine Power Systems via the Direct Method of Liapunov",

IEEE Trans. Power Apparatus and Systems, Vol. PAS 90, pp. 23-36, Jan.-Feb., 1971.

[10] H.W. Dommel and N. Sato, "Fast Transient Stability Solutions", IEEE Trans. Power Apparatus and Systems, Vol. PAS 91, pp. 1643-1650, July-Aug., 1972.

[11] P.L. Dandeno and P. Kundur, "A non-iterative Transient Stability Program Including the Effects of Variable Load-Voltage Characteristics", IEEE Trans. Power Apparatus and Systems, Vol. PAS 92, pp. 1478-1484, Sept.-Oct., 1973.

[12] H. Yee and B.D. Spalding, "Transient Stability Analysis of Multimachine Power Systems by the Method of Hyperplanes", IEEE Trans. Power Apparatus and Systems, Vol. PAS 96, pp. 276-284, Jan.-Feb., 1977.

[13] R.T.H. Alden and P.J. Nolan, "Evaluating Alternative Models for Power System Dynamic Stability Studies", IEEE Trans. Power Apparatus and Systems, Vol. PAS 95, pp. 443-440, March-April, 1976.

[14] M.C. Hall, "Experience with 500 kV Subsynchronous Resonance and Resulting Turbine Generator Shaft Damage at Mohave Generating Station", unnumbered conference paper presented at Subsynchronous Resonance symposium at IEEE Summer Power Meeting, San Francisco, California, July, 1975.

[15] W. Watson and M.E. Coultes, "Static Exciter Stabilizing Signals on Large Generators - Mechanical Problems", IEEE Trans. Power Apparatus and Systems, Vol. PAS 92, pp. 204-211, Jan.-Feb., 1973.

[16] V. Arcidiacono, E. Ferrari, and F. Saccomanno, "Studies on Damping of Electromechanical Oscillations in Multimachine Systems With Longitudinal Structure", IEEE Trans. Power Apparatus and Systems, Vol. PAS 95, pp. 450-460, March-April, 1976.

[17] C. Concordia, "Steady-State Stability of Synchronous Machines as Affected by Voltage Regulator Characteristics", AIEE Trans., Vol. 63, pp. 215-220, May, 1944.

[18] P.L. Dandeno, A.N. Karas, K.R. McClymont and W. Watson, "Effect of High Speed Rectifier Excitation Systems on Generator Stability Limits", IEEE Trans. Power Apparatus and Systems, Vol. PAS 87, pp.

190-201, 1968.

[19] M.K. El-Sherbiny and D.M. Mehta, "Dynamic System Stability, Part I - Investigation of Different Loading and Excitation Systems", IEEE Trans. Power Apparatus and Systems, Vol. PAS 92, pp. 1538-1546, Sept.-Oct., 1973.

[20] F.P. deMello and T.F. Laskowski, "Concepts of Power System Dynamic Stability", IEEE Trans. Power Apparatus and Systems, Vol. PAS 94, pp. 827-833, May-June, 1975.

[21] W. Watson and G. Manchur, "Experience with Supplementary Damping Signals for Generator Static Excitation Systems", IEEE Trans. Power Apparatus and Systems, Vol. PAS 92, pp. 199-203, Jan.-Feb., 1973.

[22] J.P. Bayne, P. Kundur, and W. Watson, "Static Exciter Control to Improve Transient Stability", IEEE Trans. Power Apparatus and Systems, Vol. PAS 94, pp. 1141-1146, July-August, 1975.

[23] C.E.J. Bowler, D.N. Ewart and C. Concordia, "Self Excited Torsional Frequency Oscillations with Series Capacitors", IEEE Trans. Power Apparatus and Systems, Vol. PAS 92, pp. 1688-1695, Sept.-Oct., 1973.

[24] J.W. Ballance and S. Goldberg, "Subsynchronous Resonance in Series Compensated Transmission Lines", IEEE Trans. Power Apparatus and Systems, Vol. PAS 92, pp. 1649-1658, Sept.-Oct., 1973.

[25] G. Jancke, N. Fahlen and O. Nerf, "Series Capacitors in Power Systems", IEEE Trans. Power Apparatus and Systems, Vol. PAS 94, pp. 915-925, May-June, 1975.

[26] L.A. Kilgore, L.C. Elliott and E.R. Taylor, "The Prediction and Control of self Excited Oscillations Due to Series Capacitors in Power Systems", IEEE Trans. Power Apparatus and Systems, Vol. PAS 90, pp. 1305-1311, May-June, 1971.

[27] C.E.J. Bowler, "Understanding Subsynchronous Resonance", unnumbered conference paper presented at Subsynchronous Resonance Symposium at IEEE Summer Power Meeting, San Francisco, California, July, 1975.

[28] O. Saito, H. Mukae and K. Murotani, "Suppression of Self-Excited Oscillations in Series-Compensated

Transmission Lines by Excitation Control of Synchronous Machines", IEEE Trans. Power Apparatus and Systems, Vol. PAS 94, pp. 1777-1788, Sept.-Oct., 1975.

[29] IEEE Special Publication, "Analysis and Control of Subsynchronous Resonance", No. 76-CH1066-0-PWR, presented at the Power Engineering Society Winter Meeting, New York, Jan., 1976.

[30] M.A. Badr and A.M. El-Serafi, "Effect of Synchronous Generator Regulation on the Subsynchronous Resonance Phenomenon in Power Systems", IEEE Trans. Power Apparatus and Systems, Vol. PAS 95, pp. 461-468, March-April, 1976.

[31] J.M. Undrill and F.P. deMello, "Subsynchronous Oscillations, Part II - Shaft-System Dynamic Interactions", IEEE Trans. Power Apparatus and Systems, Vol. PAS 95, pp. 1456-1464, July-Aug., 1976.

[32] R.T.H. Alden, P.J. Nolan and J.P. Bayne, "Shaft Dynamics in Closely Coupled Identical Generators", IEEE Trans. Power Apparatus and Systems, Vol. PAS 96, pp. 721-728, May/June, 1977.

[33] S.B. Crary, "Steady-State Stability of Composite Systems", AIEE Trans., Vol. 53, pp. 1809-1814, 1934.

[34] F. Iliceto, A. Ceyhan, and G. Ruckstuhl, "Behaviour of Loads During Voltage Dips Encountered in Stability Studies, Field and Laboratory Tests", IEEE Trans. Power Apparatus and Systems, Vol. PAS 91, pp. 2470-2479, Nov.-Dec., 1972.

[35] G.J. Berg and A.K. Aktar, "Model Representation of Power System Loads", Proceedings of the PICA Conference, 1971, pp. 153-162.

[36] G.J. Berg, "Power System Load Representation", Proc. IEE, Vol. 120, No. 3, 1973.

[37] G.R. Quan and M.Z. Tarnawecky, "Load Representation for Transient Stability Studies Digital Modeling", IEEE Paper A75-583-5, presented at the Power Engineering Society Summer Meeting, San Francisco, July, 1975.

[38] M.E. El-Hawary, Discussion to Reference [44].

[39] D.S. Brereton, D.G. Lewis, and C.C. Young, "Representation of Induction-Motor Loads During Power-System Stability Studies", AIEE Trans., Vol. 76, Part III, pp. 451-460, 1957.

[40] A.K. Desarkar and G.J. Berg, "Digital Simulation of Three-Phase Induction Motors", IEEE Trans. on Power Apparatus and Systems, Vol. PAS 89, pp. 1031-1037, July-Aug., 1970.

[41] F. Iliceto and A. Capasso, "Dynamic Equivalents of Asynchronous Motor Loads in System Stability Studies", IEEE Trans. Power Apparatus and Systems, Vol. PAS 93, pp. 1650-1659, Sept.-Oct., 1974.

[42] M.M.A. Hakim and G.J. Berg, "Dynamic Single-Unit Representation of Induction Motor Groups", IEEE Trans. Power Apparatus and Systems, Vol. PAS 95, pp. 155-165, Jan.-Feb., 1976.

[43] W. Mauricio and A. Semlyen, "Effect of Load Characteristics on the Dynamic Stability of Power Systems", IEEE Trans. Power Apparatus and Systems, Vol. PAS 91, pp. 2295-2304, Nov.-Dec., 1972.

[44] R.T.H. Alden and H.M. Zein El-Din, "Effect of Load Characteristics on Power System Dynamic Stability", Paper No. A76-363-2, presented at the IEEE Power Engineering Society Summer Meeting, Portland, July, 1976.

[45] M.Y. Akhtar, "Frequancy-dependent Dynamic Representation of Induction-motor Loads", Proc. IEE, Vol. 115, No. 6, pp. 802-812, June, 1968.

[46] C.B. Cooper, D.M. McLean, and K.G. Williams, "Application of Test Results to the Calculation of Short-Circuit Levels in Large Industrial Systems with Concentrated Induction-motor Loads", Proc. IEE, Vol. 116, No. 11, pp. 1900-1906, Nov., 1969.

[47] W.D. Humpage, K.E. Durrani, and V.F. Carvalho, "Dynamic-response Analysis of Interconnected Synchronous-asynchronous Machine Groups", Proc. IEE, Vol. 116, No. 12, pp. 2015-2027, Dec., 1969.

[48] W. Janischewskyj and D.H. Campbell, "Stabilization of a Synchronous Machine by Piecewise-Constant Feedback Control", Paper No. A75-475-4 presented at the Summer Power Meeting, San Francisco, California, July, 1975.

[49] K. Bollinger, A. Laha, R. Hamilton and T. Harras, "Power Stabilizer Using Root Locus Methods", IEEE Trans. Power Apparatus and Systems, Vol. PAS 94, pp. 1484-1488, Sept.-Oct., 1975.

[50] G.N. Yu, K. Vongsuriya and L.N. Wedman, "Application of an Optimal Control Theory to a Power system", IEEE Trans. Power Apparatus and Systems, Vol. PAS 89, pp. 55-62, Jan., 1970.

[51] S. Raman and S.C. Kapoor, "Synthesis of Optimal Regulator for Synchronous Machine", Proc. IEEE, Vol. 119, # 9, pp. 1383-1390, Sept., 1972.

[52] M. Ramamoorty and M. Arumugam, "Design of Optimal Regulators for Synchronous Machines", IEEE Trans. Power Apparatus and Systems, Vol. PAS 92, pp. 262-277, Jan.-Feb., 1973.

[53] V.H. Quintana, M.A. Zohdy, and J.H. Anderson, "On the Design of Output Feedback Excitation Controllers of Synchronous Machines", IEEE Trans. Power Apparatus and Systems, Vol. PAS 95, pp. 954-961, May-June, 1976.

[54] S. Elangovan and A. Kuppurajula, "Suboptimal Control of Power Systems Using Simplified Models", IEEE Trans. Power Apparatus and Systems, Vol. PAS 90, pp. 911-919, May-June, 1972.

[55] P.J. Nolan, N.K. Sinha and R.T.H. Alden, "Computer Control of Turbo-Alternators Using Optimal Low-Order Models", Proc. 8th Annual Princeton Conference on Information Sciences and Systems, Princeton, New Jersey, March, 1974.

[56] K.P. Daloke, "Suboptimal Linear Regulators with Incomplete State Feedback", IEEE Trans., Control, Vol. AC 15, pp. 88-95, Feb., 1970.

[57] P.J. Nolan, N.K. Sinha and R.T.H. Alden, "Optimization of Turbo-Alternator Dynamic Response Using State Feedback Decoupling", Int. J. Control, Vol. 19, # 6, pp. 1177-1186, 1974.

[58] M.K. El-Sherbiny and A.A. Fouad, "Digital Analysis of Excitation Control for Interconnected Power Systems", IEEE Trans. Power Apparatus and Systems, Vol. PAS 90, pp. 441-447, March-April, 1971.

[59] J.M. Undrill, "Structure in the Computation of Power-System Nonlinear Dynamical Response", IEEE Trans. Power Apparatus and Systems, Vol. PAS 88, pp. 1-6, Jan., 1969.

[60] J.H. Anderson, "Matrix Methods for the Study of a Regulated Synchronous Machine", Proc. IEEE, Vol. 57, pp. 2122-2139, 1969.

[61] P.J. Nolan, "Power System Stability Including Shaft and Network Dynamics", Ph.D. Thesis, McMaster University, 1976.

[62] C.T. Chen, "Introduction to Linear System Theory", Holt Renehart and Winston Inc., New York, N.Y., 1970.

[63] O.I. Elgerd, "Control Systems Theory", McGraw Hill, New York, 1967.

[64] P.L. Dandeno, R.L. Hauth and R.P. Schulz, "Effect of Synchronous Machine Modelling in Large Scale System Studies", IEEE Trans. Power Apparatus and Systems, Vol. PAS 92, pp. 574-582, March-April, 1973.

[65] M. Enns, J.E. Matheson, J.R. Greenwood and F.T. Thomson, "Practical Aspects of State Space Methods", Joint Automatic Control Conference, Stanford, California, pp. 494-513, 1964.

[66] M.A. Laughton, "Matrix Analysis of Dynamic Stability in Synchronous Multimachine Systems", Proc. IEEE, Vol. 113, # 2, pp. 325-336, Feb., 1966.

[67] J.H. Anderson, D.J. Leffen and V.M. Raina, "Dynamic Modelling of an Arbitrary Number of Interconnected Power Generating Units", Paper # C73-093-2 presented at the Winter Power Meeting, New York, N.Y., Jan., 1973.

[68] P.J. Nolan, N.K. Sinha and R.T.H. Alden, "Eigenvalue Sensitivities of a Power System Using the PQR Matrix Technique", IEEE Canadian Communication and Power Conference Digest, Cat. # 74-CHO-894-6, REG 7, Nov., 1974.

[69] P.J. Nolan, N.K. Sinha, and R.T.H. Alden, "Eigenvalue Sensitivities of Power Systems Including Network and Shaft Dynamics", IEEE Trans. Power Apparatus and Systems, Vol. PAS 95, pp. 1318-1324, July-Aug., 1976.

[70] J.M. Undrill, "Dynamic Stability Calculations for an Arbitrary Number of Interconnected Synchronous Machines", IEEE Trans. Power Apparatus and Systems, Vol. PAS 87, pp. 835-844, March, 1968.

[71] J.E. Van Ness and W.F. Goddard, "Formation of the Coefficient Matrix of a Large Dynamic System", IEEE Trans. Power Apparatus and Systems, Vol. PAS 86, pp. 80-83, Jan., 1968.

[72] R.T.H. Alden and H.M. Zein El-Din, "Multi-Machine Dynamic Stability Calculations", IEEE Trans. Power Apparatus and Systems, Vol. PAS 95, pp. 1529-1534, Sept.-Oct., 1976.

[73] H.M. Zein El-Din and R.T.H. Alden, "An Efficient Multimachine Formulation for Power System Dynamic Stability Studies Including Electrical Transients", Digest of the International Conference and Exposition, Toronto, Ont., Oct., 1975, Paper No. C75-242.

[74] B. Stott, "Review of Load-Flow Calculation Methods", IEEE Proc., Vol. 62, # 7, pp. 916-929, July, ,1974.

[75] E.V. Larson and W.W. Price, "Manstap/Possim Power System Dynamic Analysis Program - A New Approach Combining Nonlinear Simulation and Linearized State-Space/Frequency Domain Capabilities", Proceedings of the PICA Conference, May 1977, pp. 350-358.

[76] P.L. Dandeno, P. Kundur and R.P. Schulz, "Recent Trends and Progress in Synchronous Machine Modelling in Electric Utility Industry", Proc. IEEE, Vol. 62, pp. 941-950, July, 1974.

[77] P.L. Dandeno and P. Kundur, "Stability Performance of 555 MVA Turbo-Alternators - Digital Comparisons with System Operating Tests", IEEE Trans. Power Apparatus and Systems, Vol. PAS 93, pp. 767-776, May-June, 1974.

[78] W. Watson and G. Manchur, "Synchronous Machine Operational Impedances from Low Voltage Measurements at the Stator Terminals", IEEE Trans. Power Apparatus and Systems, Vol. PAS 93, pp. 777-784, May-June, 1974.

[79] C. Concordia, "Synchronous Machines", John Wiley and Sons, New York, 1951.

[80] J.P. Bayne, "Power System Modelling for Stability Studies", Ph.D. Thesis, Victoria University of Manchester, 1970.

[81] IEEE Committee Report, "Computer Representation of Excitation Systems", IEEE Trans. Power Apparatus and Systems, Vol. PAS 87, pp. 1460-1464, June, 1968.

[82] IEEE Committee Report, "Excitation System Dynamic Characteristics", IEEE Trans. Power Apparatus and Systems, Vol. PAS 92, pp. 64-75, Jan.-Feb., 1973.

[83] D.R. Fenwick and W.F. Wright, "Review of Trends in Excitation Systems and Possible Future Developments", Proc. IEE, Vol. 123, # 5, pp. 413-420, May, 1976.

[84] R.H. Park, "Fast Turbine Valving", IEEE Trans. Power Apparatus and Systems, Vol. PAS 92, pp. 1065-1073, May-June, 1973.

[85] IEEE Committee Report, "Dynamic Models for Steam and Hydro Turbines in Power System Studies", IEEE Trans. Power Apparatus and Systems, Vol. PAS 92, pp. 1904-1915, Nov.-Dec., 1973.

[86] P. Kundur and J.P. Bayne, "A Study of Early Valve Activation Using Detailed Prime Mover and Power System Simulation", IEEE Trans. Power Apparatus and Systems, Vol. PAS 94, pp. 1275-1287, July-Aug., 1975.

[87] IEEE Working Group Report, "MW Response of Fossil Fueled Steam Units", IEEE Trans. Power Apparatus and Systems, Vol. PAS 92, pp. 455-463, March-April, 1973.

[88] H. Nicholson, "Dynamic Optimization of a Boiler Turbo-Alternator Model", Proc. IEEE, Vol. 113, # 2, pp. 385-399, Feb., 1966.

[89] R.D. Dunlop, D.N. Ewart and R.P. Schulz, "Use of Digital Computer Simulation to Assess Long-Term Power System Dynamic Response", IEEE Trans. Power Apparatus and Systems, Vol. PAS 94, pp. 850-857, May-June, 1975.

[90] IEEE Committee Report, "A Bibliography for the Study of Subsynchronous Resonance Between Rotating Machines and Power Systems", Paper # F75-515-7 presented at the Summer Power Meeting, San Francisco, California, July, 1975.

[91] IEEE Subsynchronous Resonance Task Force, "Proposed Terms and Definitions for Subsynchronous Resonance", unnumbered conference paper presented at Subsynchronous Resonance Symposium at IEEE Summer Power Meeting, San Francisco, California, July, 1975.

[92] D.G. Taylor, "Analysis of Synchronous Machines Connected to Power System Networks", Proc. IEE, (London), Vol. 109, pt. C, pp. 606-610, 1962.

[93] G. Kron, "Tensor Analysis of Networks", MacDonald and Co., London, 1964.

[94] O.I. Elgerd, "Electric Energy Systems Theory", McGraw Hill, New York, 1971.

[95] M.M. Adibi, P.M. Hirsch and J.A. Jordan Jr., "Solution Methods for Transient and Dynamic Stability", Proc. IEEE, Vol. 62, # 7, pp. 951-959, July, 1974.

[96] G.W. Stagg and A.H. El-Abiad, "Computer Methods in Power System Analysis", McGraw Hill, New York, 1968.

[97] G. Gross and A.R. Bergen, "A Class of New Multistep Integration Algorithms for the Computation of Power System Dynamical Response", IEEE Trans. Power Apparatus and Systems, Vol. PAS 96, pp. 293-306, Jan.-Feb., 1977.

[98] D.N. Ewart and F.P. deMello, "A Digital Computer Program for the Automatic Determination of Dynamic Stability Limits", IEEE Trans. Power Apparatus and Systems, Vol. PAS 86, pp. 867-875, July 1967.

[99] A.S. Aldred and G. Shackshaft, "Frequency Response Analysis of the Stabilizing Effect of a Synchronous Machine Damper", Proc. IEEE, Vol. 107C, pp. 2-10, July, 1970.

[100] J.M. Undrill and T.E. Kostyniak, "Subsynchronous Oscillations, Part I - Comprehensive System Stability Analysis", IEEE Trans. Power Apparatus and Systems, Vol. PAS 95, pp. 1446-1455, July-Aug., 1976.

[101] C.A. Stapleton, "Root-Locus Study of Synchronous Machine Regulation", Proc. IEE, Vol. 111, pp. 761-768, 1964.

[102] C. Concordia, "Synchronous Machine Damping and Synchronizing Torques", AIEE Trans., Vol. 70, pp.

731-737, 1951.

[103] R.V. Shepherd, "Synchronizing and Damping Torque Coefficients of Synchronous Machines", AIEE Trans., Vol. 54, pp. 180-189, June, 1961.

[104] W.K. Marshall and W.J. Smolinski, "Dynamic Stability Determination by Synchronizing and Damping Torque Analysis", IEEE Trans. Power Apparatus and Systems, Vol. PAS 92, pp. 1239-1246, July-Aug., 1973.

[105] J.H. Anderson, "The Control of A Synchronous Machine Using Optical Control Theory", Proc. IEEE, Vol. 59, pp. 25-35, 1971.

[106] R.J. Kuhler and V.J. Watson, "Eigenvalue Analysis of Synchronous Machines", IEEE Trans. Power Apparatus and Systems, Vol. PAS 94, pp. 1629-1634, Sept.-Oct., 1975.

[107] R.T. Byerly, D.E. Sherman and D.K. McCain, "Normal Modes and Mode Shapes Applied to Dynamic Stability Analysis", IEEE Trans. Power Apparatus and Systems, Vol. PAS 94, pp. 224-229, March-April, 1975.

[108] J.H. Wilkinson, "The Algebraic Eigenvalue Problem", London: Oxford University Press, 1965.

[109] L. Fox, "An Introduction to Numerical Linear Algebra", Clarendon Press, Oxford, 1964.

[110] J.H. Wilkinson and C. Reinsch, "Linear Algebra", Spring-Verlag New York Heidelberg Berlin, 1971.

[111] J.E. Van Ness, "Inverse Iteration Method for Finding Eigenvectors", IEEE Trans. on Automatic Control, Vol. AC-14, pp. 63-66, Feb., 1969.

[112] J.E. Van Ness, J.M. Boyle and F.P. Imad, "Sensitivities of Large Multiple-Loop Control Systems", IEEE Trans. Automatic Control, Vol. AC 10, pp. 308-315, July, 1965.

[113] R. Kasturi and P. Doraju, "Sensitivity Analysis of a Power System", IEEE Trans. Power Apparatus and Systems, Vol. 33, pp. 1521-1529, Oct., 1969.

[114] D.K. Faddeev and V.N. Faddeeva, "Computational Methods of Linear Algebra", San Francisco, CA: Freeman, 1963.

[115] B. Porter and R. Crossley, "Model Control - Theory and Applications", Taylor and Francis Ltd., London, 1972, pp. 121-135.

[116] H.M. Zein El-Din, R.T.H. Alden and P.C. Chakravarti, "Second Order Eigenvalue Sensitivities Applied to Multivariable Control Systems", IEEE Proceedings, Vol. 65, No. 2, Feb., 1977, pp. 277-278 (Letter).

[117] H.M. Zein El-Din and R.T.H. Alden, "Second Order Eigenvalue Sensitivities Applied to Power System Dynamics", IEEE Trans. Power Apparatus and Systems, accepted for publication (paper No. F77-005-2).

[118] H.M. Zein El-Din and R.T.H. Alden, "First and Second-Order Eigenvalue Sensitivities of Large Multiple-Loop Systems", Department of Electrical Engineering, McMaster University, Hamilton, Ont., Internal Report No. SOC-129, April, 1976.

[119] H.M. Zein El-Din and R.T.H. Alden, "A Computer Based Eigenvalue Approach for Power System Dynamic Stability Evaluation", Proceedings of the PICA Conference, May, 1977, pp. 186-192.

[120] P.J. Nolan and W. Janischewskyj, "A Diakoptical Approach to the Eigenvalue Problem in Power System Dynamic Stability Studies", Proceedings of the PICA Conference, May, 1977, pp. 211-219.

[121] A.H. El-Abiad, O. Mansour, and A. Aguilar, "Optimal Parameter Selection of Linearized Dynamic Systems with Application to Synchronous Generators", Proceedings of the PICA Conference, June, 1975, pp. 335-344.

[122] O. Mansour, A discussion to reference [117].

APPENDIX A

SUBSYSTEM MODELS

It was mentioned in Section 1.4 that the development of subsystem models is outside the scope of this thesis. A number of appropriate references were given in Section 1.4 for each subsystem modeling. In this Appendix the equations describing the performance of each subsystem will be presented. The models are taken directly from the appropriate references but the equations representing them are rearranged in a matrix form which is compatible with the overall formulation presented in Chapter 2.

A1 Synchronous Machines

The modeling of a synchronous machine in state space form has been considered by many authors. Two different approaches have been adopted in choosing the states of the model. Anderson [60] used the stator and rotor currents (referred to the machine rotor frame) as states. Alternatively, Undrill [70] used the stator and rotor fluxes (referred to the machine rotor frame) as states. The choice of the machine fluxes as states has clearer physical significance over currents in stability studies. This approach is followed in this thesis.

$$\begin{bmatrix} \dot{\Delta\psi}_{fd} \\ \dot{\Delta\psi}_{d} \\ \dot{\Delta\psi}_{kd} \\ \dot{\Delta\psi}_{q} \\ \dot{\Delta\psi}_{kq} \end{bmatrix} - \begin{bmatrix} \omega_o r_{fd} & & & & \\ & -\omega_o r_s & & & \\ & & \omega_o r_{kd} & & \\ & & & -\omega_o r_s & \\ & & & & \omega_o r_{kq} \end{bmatrix} \begin{bmatrix} \Delta i_{fd} \\ \Delta i_{d} \\ \Delta i_{kd} \\ \Delta i_{q} \\ \Delta i_{kq} \end{bmatrix} - \begin{bmatrix} & \\ \omega_o & \\ & \\ & \omega_o \\ & \end{bmatrix} \begin{bmatrix} \Delta V_d \\ \Delta V_q \end{bmatrix}$$

$$= \begin{bmatrix} & \omega_o & & & \\ \omega_o & & & & \\ & & & \omega_o & \\ & & \omega_o & & \end{bmatrix} \begin{bmatrix} \Delta\psi_{fd} \\ \Delta\psi_{d} \\ \Delta\psi_{kd} \\ \Delta\psi_{q} \\ \Delta\psi_{kq} \end{bmatrix} + \begin{bmatrix} & \frac{\omega_o r_{fd}}{X_{afd}} \\ \psi_{qo} & \\ & \\ -\psi_{do} & \\ & \end{bmatrix} \begin{bmatrix} \Delta\omega \\ \Delta e_{fd} \end{bmatrix}$$

or symbolically:

$$\dot{\Delta\psi} - \omega_o[R]\Delta i_M = \omega_o[IF]\Delta\psi_i + [IC]\begin{bmatrix} \Delta\omega \\ \Delta e_{fd} \end{bmatrix}$$

Figure A.1 The Linearized State Equations for a Synchronous Machine

$$\begin{bmatrix} \Delta\psi_{fd} \\ \Delta\psi_{d} \\ \Delta\psi_{kd} \\ \Delta\psi_{q} \\ \Delta\psi_{kq} \end{bmatrix} = \begin{bmatrix} X_{fd} & -X_{ad} & X_{ad} & & \\ X_{ad} & -X_{d} & X_{ad} & & \\ X_{ad} & -X_{ad} & X_{kd} & & \\ & & & -X_{q} & X_{aq} \\ & & & -X_{aq} & X_{kq} \end{bmatrix} \begin{bmatrix} \Delta i_{fd} \\ \Delta i_{d} \\ \Delta i_{kd} \\ \Delta i_{q} \\ \Delta i_{kq} \end{bmatrix}$$

or

$$\Delta\underset{\sim}{\psi} = [X]\ \Delta\underset{\sim}{i}_{M}$$

$$V_t = \left[\frac{V_{do}}{V_{to}} \mid \frac{V_{qo}}{V_{to}}\right] \begin{bmatrix} \Delta V_d \\ \Delta V_q \end{bmatrix}$$

or

$$\Delta V_t = [VC]\ \Delta\underset{\sim}{V}_m$$

$$\Delta P_o = \left[i_{do} \mid i_{qo}\right] \begin{bmatrix} \Delta V_d \\ \Delta V_q \end{bmatrix} + \left[V_{do} \mid V_{qo}\right] \begin{bmatrix} \Delta i_d \\ \Delta i_q \end{bmatrix}$$

or

$$\Delta P_o = [CI]\ \Delta\underset{\sim}{V}_m + [VI]\ \Delta\underset{\sim}{i}_m$$

$$T_e = \left[i_{qo} \mid -i_{do}\right] \begin{bmatrix} \Delta\psi_d \\ \Delta\psi_q \end{bmatrix} + \left[-\psi_{qo} \mid \psi_{do}\right] \begin{bmatrix} \Delta i_d \\ \Delta i_q \end{bmatrix}$$

or

$$T_e = [CI]\ \Delta\underset{\sim}{\psi}_m + [SI]\ \Delta\underset{\sim}{i}_m$$

Figure A.2 Linearized Algebraic Equations for a Synchronous Machine

The equations of a model based on linear approximation around appropriate operating condition, for a synchronous machine, are taken directly from reference [70]. These equations are presented in matrix form in Figures (A.1) and (A.2).

A2 Excitation Systems

Throughout this thesis two types of exciters are used. These are a modern static exciter and a type 1 rotating exciter [81]. Machines equipped with static exciters are likely to be provided with a supplementary stabilizing signal.

The block diagram describing a static exciter and a power system stabilizer, using a signal derived from machine rotor speed, is shown in figure (A.3a). This model has been developed for the exciter-stabilizer being used by Ontario Hydro [15]. A state space representation of this model is given in reference [61]. The exciter is represented by a single time constant transfer function. The inputs are the stabilizing signal (e_s) and the difference between the reference voltage ($e_{ref.}$) and a signal corresponding to the machine terminal voltage (e_v). The function of the washout circuit is to eliminate any steady state offset of the speed signal into the exciter input. The phase lead compensator is used to cancel out the phase lag contributed by the

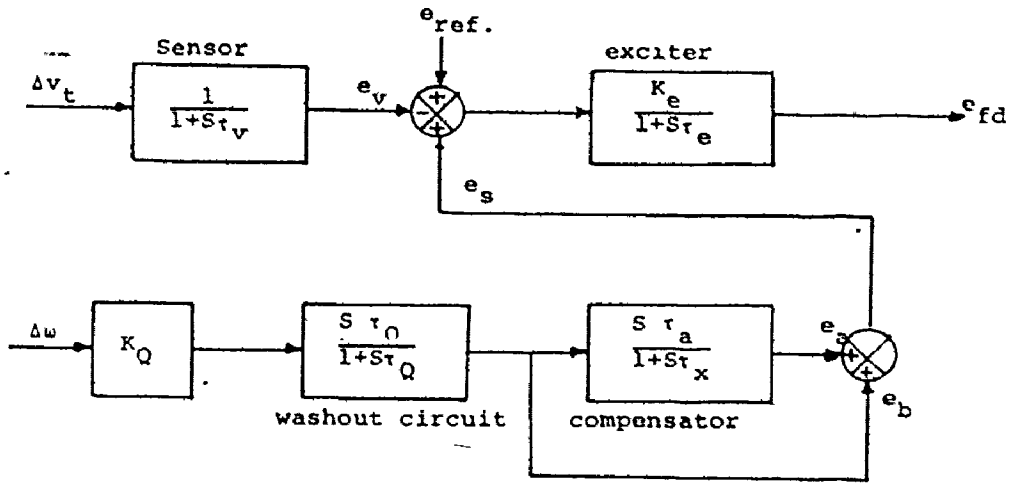

(a) Block Diagram Description

$$\begin{bmatrix} e_v \\ e_{fd} \\ e_x \\ e_y \end{bmatrix} = \begin{bmatrix} \frac{-1}{\tau_v} & & & \\ \frac{-K_e}{\tau_e} & \frac{-1}{\tau_e} & \frac{(1+\tau_a)K_e}{\tau_x \tau_e} & \frac{K_e}{\tau_e} \\ & & \frac{-1}{\tau_Q} & \\ & & \frac{-\tau_a}{\tau_x^2} & \frac{-1}{\tau_x} \end{bmatrix} \begin{bmatrix} e_v \\ e_{fd} \\ e_x \\ e_y \end{bmatrix} + \begin{bmatrix} \frac{1}{\tau_v} \\ \\ \\ \end{bmatrix} \Delta v_t + \begin{bmatrix} \\ \frac{(1+\tau_a)K_Q K_e}{\tau_x \tau_e} \\ \frac{K_Q}{\tau_Q} \\ \frac{-\tau_a K_Q}{\tau_x} \end{bmatrix} \Delta\omega + \begin{bmatrix} \\ \frac{K_e}{\tau_e} \\ \\ \end{bmatrix} e_{ref}$$

or symbolically:

$$\dot{x}_e - [TV]\,\Delta v_t = [Q_e]\,x_e + [B_e]\,u_e$$

(b) State-Space Equations

Figure A.3 Static Exciter-Stabilizer Model

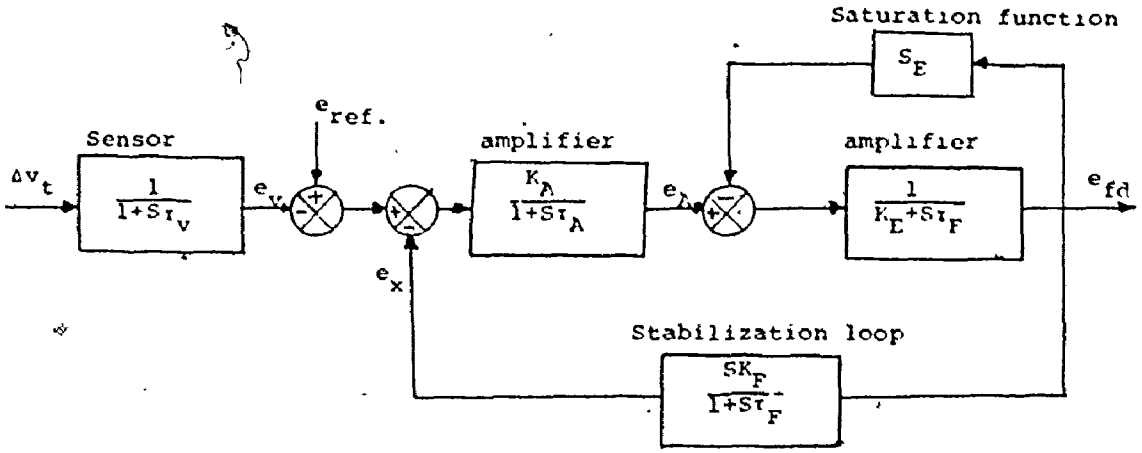

(a) Block Diagram Description

$$\begin{bmatrix} e_v \\ e_{fd} \\ e_A \\ e_x \end{bmatrix} = \begin{bmatrix} \frac{-1}{\tau_v} & & & \\ & \frac{-(K_E+S_E)}{\tau_E} & \frac{1}{\tau_E} & \\ \frac{-K_A}{\tau_A} & & \frac{-1}{\tau_A} & \frac{-K_A}{\tau_A} \\ & \frac{-K_F(K_E+S_E)}{\tau_F\tau_E} & \frac{K_F}{\tau_E\tau_F} & \frac{-1}{\tau_F} \end{bmatrix} \begin{bmatrix} e_v \\ e_{fd} \\ e_A \\ e_x \end{bmatrix} + \begin{bmatrix} \frac{1}{\tau_v} \\ \\ \\ \end{bmatrix} \begin{bmatrix} \Delta v_t \end{bmatrix} + \begin{bmatrix} \\ \\ \frac{K_A}{\tau_A} \\ \\ \end{bmatrix} \begin{bmatrix} e_{ref} \end{bmatrix}$$

or symbolically

$$\dot{x}_e - [TV]\,\Delta v_t = [Q_e]\,x_e + [B_e]\,e_{ref.}$$

(b) State-Space Equations

Figure A.4 Type 1 Exciter Model

machine and exciter.

The equations describing the performance of the exciter-stabilizer subsystem are arranged in state space form and are given in Figure (A.3b).

The block diagram representing a type 1 (rotating) exciter, is taken directly from reference [81]. This is depicted in Figure (A.4a). The first summing point compares the regulator reference with the output of the voltage sensor to determine the voltage error input to the regulator amplifier. The second summing point combines voltage error with the excitation major damping loop signal. The next summing point subtracts a signal which represents the saturation function of the exciter.

The equations describing the performance of a type 1 exciter are arranged in state space form and are given in Figure (A.4b).

Although only two exciter models have been considered throughout this thesis, the application of the technique in Chapter 2 is not restricted to the use of these models. Other exciter models can be as easily incorporated in the overall formulation.

A3 Turbine-Governor

In this Section two simplified models for turbine-governors are described. The models are taken directly from

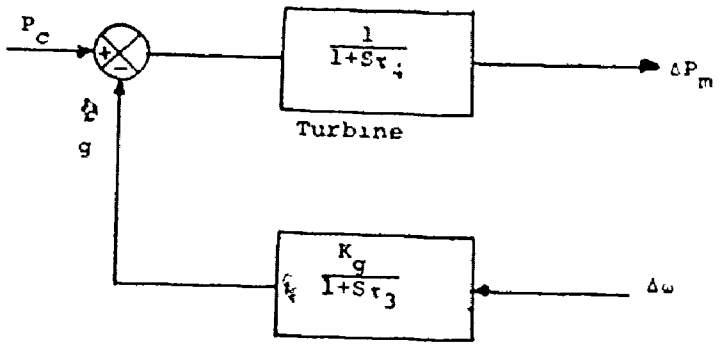

(a) Block Diagram Description

$$\begin{bmatrix} \Delta P_m \\ g \end{bmatrix} = \begin{bmatrix} -\frac{1}{\tau_4} & -\frac{1}{\tau_4} \\ & -\frac{1}{\tau_3} \end{bmatrix} \begin{bmatrix} \Delta P_m \\ g \end{bmatrix} + \begin{bmatrix} \frac{1}{\tau_4} \\ \end{bmatrix} \begin{bmatrix} P_c \end{bmatrix} + \begin{bmatrix} \\ \frac{1}{\tau_3} \end{bmatrix} \Delta\omega$$

or symbolically:

$$\dot{x}_g - [CN]\,\Delta\omega = [Q_g]\,x_g + [B_g]\,u_g$$

(b) State-Space Equations

Figure A.5 Turbine-Governor Model for Steam Unit

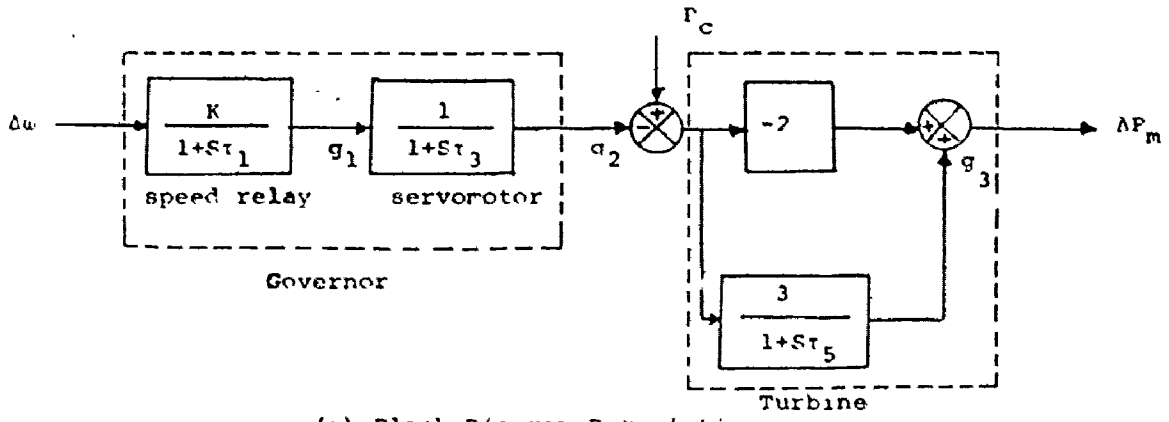

(a) Block Diagram Description

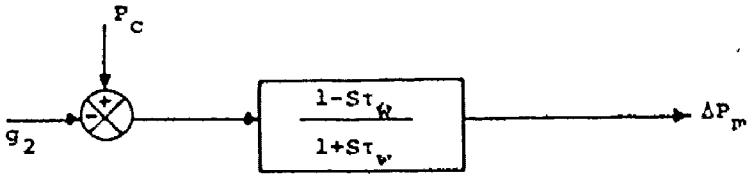

$$T_5 = T_w/2$$

(b) Turbine Transfer Function

$$\begin{bmatrix} \dot{g}_1 \\ \dot{g}_2 \\ \dot{g}_3 \end{bmatrix} = \begin{bmatrix} \frac{-1}{T_1} & & \\ & \frac{-1}{T_3} & \\ & \frac{-3}{T_5} & \frac{-1}{T_5} \end{bmatrix} \begin{bmatrix} g_1 \\ g_2 \\ g_3 \end{bmatrix} + \begin{bmatrix} \\ \\ \frac{3}{T_5} \end{bmatrix} \begin{bmatrix} P_c \\ \\ \end{bmatrix} + \begin{bmatrix} \\ \\ \end{bmatrix} \begin{bmatrix} \frac{K}{T_1} \\ \\ \end{bmatrix} \begin{bmatrix} \Delta\omega \\ \\ \end{bmatrix}$$

$$\Delta P_m = g_3 - 2(P_c - g_2)$$

or symbolically:

$$\dot{\underline{x}}_g - [C']\Delta\omega = [Q_g]\,\underline{x}_g + [B_g]U_g$$

(c) State-space Equations

Figure A.6 Turbine-Governor Model for Hydro Unit

reference [85] where the two models have been recommended for steam and nuclear units and hydroelectric units.

The turbine-governor model for steam and nuclear units is shown in Figure (A.5a). The turbine is modeled by a single time constant transfer function. The input is the difference between the control power (P_c) and the feedback signal through the governor (g). The governor is also described by a single time constant transfer function. The state space representation of the model is given in Figure (A.5b).

The dynamic model for a hydro turbine-governor subsystem is shown in Figure (A.6a). The governor model includes two single time constant transfer functions representing the speed relay and servomotor. The turbine representation in Figure (A.6a) is an equivalent for the block diagram description in Figure (A.6b). The state space representation is given in Figure (A.6c).

APPENDIX B

FORMULATION OF THE NETWORK ADMITTANCE MATRIX

A YBUS matrix relates the network bus currents to bus voltages, including non-generator load buses. This matrix can, generally, be arranged in the form:

$$\begin{bmatrix} \underset{\sim}{I}_N \\ \hline \underset{\sim}{I}_L \end{bmatrix} = \left[\begin{array}{c|c} Y_{11} & Y_{12} \\ \hline Y_{21} & Y_{22} \end{array}\right] \begin{bmatrix} \underset{\sim}{V}_N \\ \hline \underset{\sim}{V}_L \end{bmatrix} \qquad \text{(B.1)}$$

where $\underset{\sim}{I}_N$ and $\underset{\sim}{V}_N$ are the currents and voltages of all the generator buses. $\underset{\sim}{I}_L$ and $\underset{\sim}{V}_L$ are the currents and voltages of all non-generator load buses.

The network admittance matrix, [Y], relates the generator bus currents to the generator bus voltages. The construction of this matrix from the YBUS matrix can be achieved by eliminating all the non-generator load buses. This can, generally, be performed by two methods.

B1 Partitioning Method

Expanding equation (B.1) yields:

$$\underset{\sim}{I}_N = [Y_{11}]\ \underset{\sim}{V}_N + [Y_{12}]\ \underset{\sim}{V}_L$$

$$\underset{\sim}{I}_L = [Y_{21}]\ \underset{\sim}{V}_N + [Y_{22}]\ \underset{\sim}{V}_L \qquad \text{(B.2)}$$

If all system loads are represented by constant

admittances, the current-voltage relationship at all non-generator load buses can be described as:

$$\underset{\sim}{I}_L = - [Y_{LL}] \underset{\sim}{V}_L \qquad (B.3)$$

where $[Y_{LL}]$ is a diagonal complex matrix with each element representing the load admittance at the corresponding load bus. Combining equations (B.2) and (B.3) and upon reduction one obtains:

$$\underset{\sim}{I}_N = [Y] \underset{\sim}{V}_N \qquad (B.4)$$

where

$$[Y] = \{[Y_{11}] - [Y_{22}] ([Y_{LL}] + [Y_{22}])^{-1} [Y_{21}]\} \qquad (B.5)$$

Thus, the construction of the [Y] matrix from the YBUS matrix, using this method, requires a complex matrix inversion of an order equal to the number of all non-generator load buses in the system.

B2 Elimination Method

This method is a modification of the partitioning method in order to avoid the inversion of a complex matrix which can be of high order. In this method the load buses are eliminated one by one. Consequently, if we start with the last load bus arranged in equation (B.1), $[Y_{12}]$ will be a column vector, $[Y_{21}]$ a row vector, and hence, Y_{22} and Y_{LL} will become complex elements. Repeating the process in equation (B.3) we finally obtain the [Y] matrix.

APPENDIX C

BLOCK DIAGRAM MODEL-INCLUDING LOAD EFFECTS

In this Appendix the equations describing the block diagram model considered in Chapter 5 are presented. The reader is referred to reference [6] for definitions of the block diagram coefficients.

C1 Nonlinear Equations

C1.1 Generator

The performance equations of a synchronous generator, Figure (5.1), neglecting damper winding effects, armature resistance copper loss, and armature flux derivatives, as documented in reference [6], are:

$$v_d = x_q\, i_{qg}$$

$$v_q = E_q' - x_d'\, i_{dg}$$

$$E_q = E_q' + (x_q - x_d')\, i_{dg}$$

$$v_t^2 = v_d^2 + v_q^2$$

$$E_q' = x_{ad}\, i_{fd} - (x_d - x_d')\, i_{dg}$$

$$p\, E_q' = 1/\tau_{do}'\, e_{fd} - x_{ad}/\tau_{do}'\, i_{fd}$$

$$T_e = E_q\, i_{qg}$$

$$T_m - T_e = (2\,H/\omega_o)\;P\;\omega$$

$$p\,\delta = \omega$$

C1.2 Load

$$P_\ell = v_D\, i_{D\ell} + v_Q\, i_{Q\ell}$$

$$Q_\ell = v_Q\, i_{D\ell} - v_D\, i_{Q\ell}$$

C1.3 Network

The voltage-current relationship between the terminal and infinite buses, neglecting network transients, is:

$$\begin{bmatrix} v_D \\ v_Q - E_0 \end{bmatrix} = \begin{bmatrix} 0 & -x_e \\ x_e & 0 \end{bmatrix} \begin{bmatrix} i_{DN} \\ i_{QN} \end{bmatrix}$$

The interframe transformation at the terminal bus is:

$$\begin{bmatrix} i_{Dg} \\ i_{Qg} \end{bmatrix} = \begin{bmatrix} \cos\delta & -\sin\delta \\ \sin\delta & \cos\delta \end{bmatrix} \begin{bmatrix} i_{dg} \\ i_{qg} \end{bmatrix}$$

C2 Linearized Equations

Small perturbations of the system around any operating point results in the following linearized equations.

C2.1 Generator

$$\Delta v_d = x_q \, \Delta i_{qg}$$

$$\Delta v_q = \Delta E'_q - x'_d \, \Delta i_{dg}$$

$$\Delta E_q = \Delta E'_q + (x_q - x'_d) \, \Delta i_{dg}$$

$$\Delta v_t = \frac{v_{do}}{v_{to}} \Delta v_d + \frac{v_{qo}}{v_{to}} \Delta v_q$$

$$\Delta E'_q = x_{ad} \, \Delta i_{fd} - (x_d - x'_d) \, \Delta i_{dg}$$

$$p \, \Delta E''_q = 1/\tau_{do}' \, \Delta e_{fd} - x_{ad}/\tau_{do}' \, \Delta i_{fd}$$

$$\Delta T_e = E_{qo} \, \Delta i_{qg} + i_{qgo} \, \Delta E_q$$

$$\frac{2H}{\omega_o} p \, \Delta\omega = \Delta T_m - \Delta T_e$$

$$p \, \Delta\delta = \Delta\delta$$

C2.2 Load

$$\Delta P_\ell = \frac{P_{\ell o} \cdot K_p}{v_{to}} \Delta v_t = v_{DO} \Delta i_{D\ell} + i_{D\ell o} \Delta v_D + v_{Qo} \Delta i_{Q\ell} + i_{Q\ell o} \Delta v_Q$$

$$\Delta Q_\ell = \frac{Q_{\ell o} \cdot K_q}{v_{to}} \Delta v_t = v_{Qo} \Delta i_{D\ell} + i_{D\ell o} \Delta v_Q - v_{Do} \Delta i_{Q\ell} - i_{Q\ell o} \Delta v_D$$

C2.3 Network

$$\begin{bmatrix} \Delta v_D \\ \Delta v_Q \end{bmatrix} = \begin{bmatrix} 0 & -x_e \\ x_e & 0 \end{bmatrix} \begin{bmatrix} \Delta i_{DN} \\ \Delta i_{QN} \end{bmatrix}$$

$$\begin{bmatrix} \cos\delta_o & -\sin\delta_o \\ \sin\delta_o & \cos\delta_o \end{bmatrix} \begin{bmatrix} \Delta i_{dg} \\ \Delta i_{qg} \end{bmatrix} = \begin{bmatrix} \Delta i_{D\ell} \\ \Delta i_{Q\ell} \end{bmatrix} + \begin{bmatrix} \Delta i_{DN} \\ \Delta i_{QN} \end{bmatrix} + \begin{bmatrix} i_{Qgo} \\ -i_{Dgo} \end{bmatrix} \Delta\delta$$

$$\begin{bmatrix} \Delta v_d \\ \Delta v_q \end{bmatrix} = \begin{bmatrix} \cos\delta_o & \sin\delta_o \\ -\sin\delta_o & \cos\delta_o \end{bmatrix} \begin{bmatrix} \Delta v_D \\ \Delta v_Q \end{bmatrix} + \begin{bmatrix} v_{qo} \\ -v_{do} \end{bmatrix} \Delta\delta$$

The subscript "0" refers to steady state quantities.

C3 Analytic Expressions for K_5 and K_6

Using the linearized equations for the system in Figure (5.1), the following expressions are derived for the block diagram coefficients K_5 and K_6:

$$K_5 = \frac{E_o}{x_e\, v_{to}(A-B)} \{(a_1 v_{qo} - a_2 v_{do})\cos\delta_o - (a_1 v_{do} + a_3 v_{qo})\sin\delta\}$$

$$K_6 = \frac{1}{x'_d\, v_{to}(A-B)} \{a_1 v_{do} + a_3 v_{qo}\}, \text{ where}$$

$$a_1 = (v_{do}\, i_{d\ell o} - v_{qo}\, i_{q\ell o})/v_{to}^2$$

$$a_2 = (v_{do}\, i_{q\ell o} + v_{qo}\, i_{d\ell o} - \frac{v_{to}^2}{x_e} - \frac{v_{to}^2}{x'_d})/v_{to}^2$$

$$a_3 = (v_{do}\, i_{q\ell o} + v_{qo}\, i_{d\ell o} + \frac{v_{to}^2}{x_e} + \frac{v_{to}^2}{x_q})/v_{to}^2$$

$$A = -a_1^2 - a_2\, a_3$$

$$B = \frac{1}{v_{to}^2} \{K_p P_{\ell o}(a_1 v_{qo}^2 - a_1 v_{do}^2 - a_2 v_{do} v_{qo} - a_3 v_{do} v_{qo})$$

$$+ K_q Q_{\ell o}(a_2 v_{do}^2 - 2a_1 v_{do} v_{qo} - a_3 v_{qo}^2)$$

C4 Block Diagram Coefficients

In this Section representative values of block diagram coefficients that do not change significantly with the parameters K_p and K_q are listed in Tables (C.1) to (C.3). These values have not been included in Figures (5.5) and (5.6) in Chapter 5.

Table C.1 Block Diagram Coefficients

Fig. 5: K_q = 2, K_p = 0→3.5, 1.25 PU LOAD 0.8 PF INDUCTIVE												
	K_1			K_4			K_5			K_6		
Q_G =	0	.4	.8	0	.4	.8	0	.4	.8	0	.4	.8
P_G = .2	1.33	1.39	1.38	.024	-.013	-.045	.041	.047	.053	.56	.56	.56
P_G = .6	1.37	1.40	1.37	.265	.195	.136	.016	.016	.017	.56	.56	.56
P_G = 1.0	1.41	1.41	1.36	.475	.381	.305	-.018	-.022	-.023	.54	.55	.56

Table C.2 Block Diagram Coefficient

Fig. 8: K_q = 2.0, K_p = 0→3.5, 1.25 PU LOAD 0.8 PF CAPACITIVE												
	K_1			K_4			K_5			K_6		
Q_G =	0	.4	.8	0	.4	.8	0	.4	.8	0	.4	.8
P_G = .2	1.02	.96	.82	-.062	-.109	-.148	.070	.083	.095	.69	.71	.71
P_G = .6	1.03	.93	.77	.162	.081	.015	.032	.035	.042	.71	.71	.71
P_G = 1.0	1.02	.89	.71	.348	.248	.164	-.016	-.017	-.015	.69	.69	.69

Table C.3 Block Diagram Coefficients

Fig. 6: K_p = 2.0, K_q = 0→3.5 1.25 PU LOAD												
	.8PF INDUCTIVE						.8 PF CAPACITIVE					
	K_1			K_4			K_1			K_4		
Q_G =	0	.4	.8	0	.4	.8	0	.4	.8	0	.4	.8
P_G = .2	1.34	1.39	1.39	.026	-.016	-.045	1.03	.96	.82	-.048	-.105	-.149
P_G = .6	1.37	1.40	1.38	.267	.195	.136	1.03	.94	.78	.166	.086	.019
P_G = 1.0	1.41	1.40	1.35	.475	.382	.308	1.01	.89	.71	.345	.248	.163

Machine Data

66 MVA, 13.8 KV Hydro unit ratings (PU base)

X_{ad} = .567, X_f = .14, X_{Kd} = .087, X_{aq} = .33

X_{Kq} = .165, r_a = .00279, r_f = .00035, r_{Kd} = .02

r_{Kq} = .02, H = 4.29, X_L = .4